Comparative Analysis of Soil Erosion Using Large-, Intermediate-, and Small-Scale Test Plots of Bare Soil and Different Hydromulch Products under Large-Scale Rainfall Simulator

by

Matthew Dale Ricks

A dissertation submitted to the Graduate Faculty of
Auburn University
In partial fulfillment of the
Requirements for the Degree of
Doctor of Philosophy

Auburn, Alabama
December 12, 2020

Keywords: large-scale, intermediate-scale, small-scale test plots, rainfall simulation, erosion, erosion control, hydromulch

Approved by

Xing Fang, Chair, Professor of Civil Engineering
Wesley C. Zech, Co-Chair, Professor of Civil Engineering
Wesley N. Donald, Research Fellow IV Civil Engineering
Michael A. Perez, Assistant Professor of Civil Engineering

ABSTRACT

A study was conducted to compare the test results of three different size erosion-control plots under rainfall simulation to determine if there is a direct relationship to the size of a tested erosion-control plot and the experimental results of soil erosion. The plots were tested under the same rainfall simulator to minimize the impacts of spatial variability found with different simulators. Three plot sizes (2 ft by 4 ft, 4 ft by 8 ft, and 8 ft by 40 ft for plot width and flow length, which are small-, intermediate-, and large-scale, respectively) were tested for a loam bare soil control condition; and two plot sizes (small- and large-scale) were tested for three different hydromulch products. The large-scale bare soil plots had an average soil loss of 2,333 lb. (7.29 lb./ft^2). The intermediate-scale bare soil plots had an average soil loss of 62.8 lb. (1.96 lb./ft^2). The small-scale bare soil plots had an average soil loss of 2.58 lb. (0.323 lb./ft^2). The large-scale plots experienced significant rill erosion and the early signs of gully erosion; whereas the small-scale plots experienced very limited rill erosion. The flow length of the small-scale plots is inadequate to allow for the transportation of the dislodged sediment caused by splash erosion. However, it was determined that the soil loss for the various plot sizes was related to the horizontal projection of the soil slope length, λ, by the power law function. The experimental soil loss results were comparable to the theoretical results determined from Revised Universal Soil Loss Equation (RUSLE). The theoretical soil erodibility *K*-factor as determined in RUSLE was calculated to be 0.32 for the loam soil. The experimental *K*-factor was determined to be 0.28 and 0.24 for the large-scale and intermediate-scale simulations, respectively. However, the *K*-factor for the small-scale plots was estimated at only 0.06 due to limited rill erosion.

For the analysis of the hydromulch (HM) products, the large-scale tests resulted in the cover-management *C*-factors of 0.44, 0.50 and 0.55 for EcoFibre HM, SoilCover HM, and Terrawood HM, respectively. The small-scale tests however, resulted in *C*-factors of 0.15, 0.24 and 0.58 for EcoFibre HM, SoilCover HM, and Terrawood HM, respectively.

The hydromulch products were tested on small-scale plots for both loam and topsoil. The soil loss from the topsoil plots varied significantly when compared to the loam soil. The average soil loss for the topsoil plots when compared to the loam plots ranged from 30% to 146%.

The data gathered over the tested plot sizes indicate the opportunity to utilize flow length and plot area as useful factors to scale up soil loss results, but the plot length needs to be long enough for all soil erosion mechanism to be fully developed. This could provide additional justification for testing on a smaller scale at a reduced cost and scaling the data up to estimate soil losses on a larger area.

ACKNOWLEDGEMENTS

I would like to extend my gratitude to Dr. Xing Fang for his support and guidance throughout my time at Auburn University. Additionally, I would like to thank Dr. Wesley C. Zech, Dr. Wesley Donald, Dr. Michael Perez, and Dr. Mark Dougherty for their time and guidance throughout this research effort. I would also like to thank Mr. Guy Savage and all the students who assisted with our research effort. In addition, I would like to thank the Alabama Department of Transportation for their financial support of this research project.

I would like to thank my wife, Lacey, and my children for their unconditional love and support throughout this journey. Their understanding and accommodation throughout this process has been unparalleled. Most importantly, I would thank our Savior for the many blessings and opportunities that have been given to my family.

TABLE OF CONTENTS

LIST OF TABLES

LIST OF FIGURES

1 INTRODUCTION

1.1 BACKGROUND

The construction industry within the United States is responsible for creating as much as 80 million tons (72.6 million metric tons) of sediment which is washed into surface water bodies (Novotny 2003). The United States Environmental Protection Agency (USEPA) as well as other state and local authorities continue to revise and update the stormwater Best Management Practices (BMPs) across the country. In 1990, the USEPA created a stormwater program under the authority of the Clean Water Act. The first phase of this act required a National Pollutant Discharge Elimination System (NPDES) permit to discharge stormwater from certain municipal separate storm sewer systems (MS4s) which generally served over 100,000 residents; construction activity disturbing over five acres of land; and certain industrial discharges. In 2005, the USEPA revised the NPDES permit through the Phase II Final Rule to include additional MS4 operators as well as construction sites which disturb greater than one acre of land or are part of a larger development which disturbs greater than one acre (USEPA 2005b). To comply with the guidance of the permits, the erosion control industry has developed numerous BMPs. If sediment is allowed to be uncontrolled, it can be suspended in runoff generated from rainfall events and be transported downstream. This sediment-laden runoff has been shown to result in the degradation of downstream aquatic habitats which can negatively impact fisheries, drinking water intakes, and stream navigability USEPA 2005b).

Figure 1-1 Construction Site Stormwater Runoff (Keeper 2017)

The discharge of sediment-laden stormwater from active construction sites, such as highway construction projects, is a growing concern in the construction industry (Zech et al. 2007). The USEPA labels such discharge as nonpoint source (NPS) pollution, which is defined as land runoff, precipitation, atmospheric deposition, seepage, or hydrologic modification that does not meet the legal definition of 'point source' in section 502(14) of the Clean Water Act (USEPA n.d.).

Soil erosion is considered the largest contributor to NPS pollution in the U.S. (USEPA 1997). Construction sites are known to be a significant contributor to soil erosion by exhibiting soil loss rates that are 20 times greater from construction sites than agricultural lands, and 1,000 to 2,000 times greater than forest lands (Scholl et al. 2013; USEPA 2005b). Studies have shown that erosion rates on cut slopes of roadways have varied from 0.09 in./ac to 1.12 in./ac (5.93 mm/ha up to 70 mm/ha) (Megahan et al. 2001). When soil is eroded from construction sites, other harmful particulates such as fertilizers, pesticides, metals, and fuels attach to the soil and are transported into MS4s (Risse and Faucette 2001; USEPA 2005a). Polluted MS4s transport construction site

runoff directly to surface waters, ultimately causing sedimentation. In the U.S. alone, "sedimentation impairs 84,503 river and stream miles (12% of the assessed river and stream miles and 31% of the impaired river and stream miles)" (USEPA 2000). Sedimentation of surface water can lead to deterioration of aquatic habitats, the rapid loss of storage capacity of reservoirs, eroded streambanks, and increased turbidity of the waters thereby reducing photosynthesis, and clogging fish gills (Novotny 2003). An annual estimate of $17 billion is spent in the United States alone in an effort to control onsite sedimentation, bringing the national total to nearly $60 billion in erosion and sediment control activities (Brady and Weil 2014). Thus, the combination of environmental and economic downfalls related to erosion and sedimentation in the construction industry has developed a need for scientific research to be performed to understand the overall performance of erosion and sediment control (ESC) practices used at the federal, state, and local levels.

Construction projects typically create large areas of exposed soil due to clearing, grubbing, and land grading activities. Lack of vegetative cover leaves these areas susceptible to erosion during rain events. Highly concentrated sediment-laden stormwater runoff degrades existing ecosystems and water quality through the process of sedimentation and by increasing turbidity, making it difficult for aquatic organisms to survive.

There are several physical processes that contribute to the erosive potential of a particular soil. The first physical process that occurs in relation to water-based erosion is soil detachment. Detachment is caused by the kinetic energy of falling rainfall as it impacts the ground surface. The process of detachment is also referred to as interrill erosion, which is commonly mistaken as sheet erosion; however, sheet erosion does not include the concept of rain-splash (University 2010). Once soil particles are detached, the excess rainfall begins to flow over the particles and subsequently begins to transport the particles. This transport of particles initially begins to occur

as sheet flow. As the velocity and depth of water classified as sheet flow increases, the erosion transitions into rill erosion. Rill erosion is typically exhibited by areas of concentrated flow in small rivulets (University 2010). According to the National Resources Conservation Service (NRCS) rills may be any size but are typically considered to be less than four inches in total depth. Rills can also generally be repaired by tillage with standard implements (Service n.d.). Once rills reach a certain depth, the erosion is then referred to as gully erosion. Gully erosion typically forms a dendritic pattern and generally occurs in defined drainageways. Gullies may extend to the full depth of the soil profile. During the gully erosion process, the head cut (advancement of eroding channel upstream) is often observed.

In addition, several key factors contribute to the erosive potential of a particular project site, including soil properties, topography, local climate (i.e., rainfall intensity, frequency, and duration), and vegetative cover. The focus of this study is on the testing and evaluation of erosion control practices and products used on earthen slopes to minimize interrill and rill erosion.

With the increasing usage of erosion control practices and products, it is important for researchers, practitioners, contractors, inspectors, and regulatory agencies to understand their in-field performance along with suitable applications. Rainfall simulation testing has been conducted in the past to accomplish these objectives; however, there has been inconsistency in the size of the test plots used for simulation.

1.2 RAINFALL SIMULATION

As part of the ongoing research related to erosion processes, additional research is needed to evaluate the effectiveness of different erosion controls and their impact on the amount of soil displaced and subsequently transported. The intensity of natural rainstorms can vary widely and is extremely dynamic. With this phenomenon, a large portion of the total rainfall for a specific storm

can occur in a relatively short time period (Lascano et al. 1997). Detailed soil erosion data are needed to effectively control and minimize the detrimental effects on the environment caused by sediment transport and deposition. This data can be obtained and evaluated in some instances through simulated rainfall in lieu of natural rainfall events (Meyer and Harmon 1979). This study focuses on two separate scales of rainfall simulator as shown in Figure 1-2: (a) large-scale and (b) small-scale.

(a) Typical Large-Scale Rainfall Simulator (Company n.d.)

(b) Typical Small-Scale Rainfall Simulator (Grismer 2012)

Figure 1-2 Typical Rainfall Simulators

1.3 RESEARCH OBJECTIVES

The overall goal of this research is to compare the test results of several erosion control products through large-scale testing and small-scale testing. This will require the development of a rainfall simulator apparatus for the large-scale simulator as well as a comparable intermediate-scale apparatus, which will deliver similar rainfall depths over time. These goals will be accomplished through the following objectives:

(1) To review and publish the previous research conducted on small-scale rainfall simulation;

(2) To develop a large-scale rainfall simulator (8 ft width by 40 ft length) (2.4 m by 12.2 m) in accordance with ASTM 6459-19 (ASTM International 2019) which is capable of

modeling a rainfall event with intensities of 2, 4, and 6 in./hr (50.8, 101.6, and 152.4 mm/hr);

(3) To review, integrate, and publish the research conducted on large-scale rainfall simulation;

(4) To test and calibrate the small-scale (i.e., 2 ft by 4 ft or 0.6 m by 1.2 m) and the intermediate-scale (i.e., 4 ft by 8 ft or 1.2 m by 2.4 m) test plots that are placed under the large-scale rainfall simulator to ensure consistent rainfall intensities;

(5) To compare and contrast the results (e.g., soil loss and turbidity) for bare soil on the large-, intermediate-, and small-scale test plots and three hydromulch products on the large- and small-scale test plots (all 3:1 slopes).

(6) To compare and contrast the results (e.g., soil loss and turbidity) of bare soil and hydromulch products on topsoil and loam for the small-scale test plots.

The project was divided into the following tasks to satisfy the defined research objectives as follows:

(1) Review previous small-scale research conducted at AU-ESCTF, update, and publish findings;

(2) Design and construct a large-scale rainfall simulator capable of delivering the required rainfall intensities of 2, 4, and 6 in./hr (50.8, 101.6, and 152.4 mm/hr);

(3) Review previous large-scale rainfall simulator research conducted at AU-ESCTF, update, and publish findings;

(4) Calibrate small- and intermediate-scale erosion test plots under large-scale rainfall simulator and perform tests of bare soil over loam (control tests), hydromulch products over loam, and hydromulch products over the topsoil.

(5) Compare and analyze experimental results from various scales of plot testing.

1.4 EXPECTED OUTCOMES

The expected outcomes of this study are to provide ALDOT and the ESC industry with the knowledge and resources to understand the relationship between the scale of erosion control modeling under rainfall simulation. Scientifically backed results from this study will provide designers and manufacturers of erosion control products a better understanding of the effects of large-scale, intermediate-scale, and small-scale modeling and the expected correlation with field practice. Additional research efforts should emanate from this study allowing further opportunities for increasing knowledge on the scale of testing of erosion control practices to be implemented on construction projects.

1.5 ORGANIZATION OF DISSERTATION

This dissertation is divided into six chapters that organize, illustrate, and describe the steps taken to meet the defined research objectives. Following this chapter, Chapter Two: *Literature Review*, provides an overview of historical rainfall simulation, large-scale rainfall simulation, small- and intermediate-scale rainfall simulation, comparisons of various scales of rainfall simulation, a summary of raindrop velocity measurement techniques, and a review of previous research of small-scale simulations completed through AU-ESCTF. Results from this chapter have been published in *Water* journal (Ricks et al. 2020). Chapter 3: *Methodology,* outlines the testing apparatus, experimental design, testing methods, and procedures utilized for preparing and conduction large-, intermediate-, and small-scale rainfall simulation. Results from this chapter have been published in *Water* journal (Ricks et al. 2019). Chapter Four: *Results and Discussion,* details the various experimental data collected through all three scales of bare soil control testing, in addition to the hydromulch product testing on both large- and small -scale test plots. Chapter

Five: *Comparison of Data,* provides several analyses of experimental results collected from erosion control test plots and determines the correlation between various factors and the scale of the rainfall simulation. Chapter Six: *Conclusions and Recommendations,* provides a summary of the tasks accomplished through this study and identifies areas in which improvements can be made to the AU-ESCTF rainfall simulators and areas where further research can be conducted to advance this body of knowledge.

2 LITERATURE REVIEW

2.1 INTRODUCTION

This chapter provides a literature review of rainfall simulation and the various size and relationships between small-, intermediate-, and large-scale simulators. The design of the testing apparatus and methodology used in this study are based on the current industry testing methods and a review of current, available literature. The literature review focuses on relevant studies and current available data. The literature review also reviews current methodologies for evaluation of raindrop velocity measurement techniques to provide a foundation for future research and total storm kinetic energy calculations.

2.2 RAINFALL SIMULATION

Rainfall simulation has a long history of use as a means to evaluate BMPs for areas disturbed by construction (Birt et al. 2007). In the field of soil erosion in particular, rainfall simulators are used to investigate the interactions between soils and the various factors that contribute to sediment movement (Elbasit et al. 2015). Meyer (1988) describes the goal of rainfall simulation as the following: “Researchers should avoid becoming so involved in developing and improving rainfall simulators that little time is left for their use. The goal of rainfall simulator research should be the collection of accurate and useful data, not perfection of a rainfall simulator.” In years past, erosion studies utilizing natural rainfall could potentially take upwards of ten to twenty years to complete (Meyer 1965). Rainfall simulation enables researchers to test and evaluate specific technologies and products over a significantly shorter time period. Rainfall simulators have also been shown capable of evaluating the threshold for rainfall intensity that will generate erosion and test the effectiveness of various stabilization techniques on hillslopes (Covert and Jordan 2009).

Properly designed and operated rainfall simulators have several distinct advantages over field modeling rainfall events. Rainfall simulators can simulate rainfall more rapidly, efficiently and are more controlled and adaptable than natural rainfall modeling (Meyer 1988). Rainfall simulation also provides for rapid accumulation of data as it relates to rainfall intensity, duration, and kinetic energy when compared to natural rainfall simulation (Moore et al. 1983; Thomas and El Swaify 1989). Meyer (1988), Moore et al. (1983), and Bubenzer (1979) suggest similar key characteristics of effective rainfall simulators. These characteristics include: (1) similar drop size distribution to natural rainfall, (2) impact velocities near those of natural rainfall (i.e., at terminal velocity), (3) similar rainfall intensities to natural storms, (4) sufficient size of research area to evaluate conditions, (5) uniformity of intensity and drop characteristics, (6) continuous raindrop application, (7) repeatability, (8) near vertical drops, (9) outside environmental factors similar to natural characteristics, and (10) portability. In order to closely approximate natural rainfall, simulators must closely approximate criteria 1, 2, and 6 (Moore et al. 1983). Moore et al. (1983) also identifies the need for rainfall simulators to be practical for both large-scale and small (intermediate) scale testing of plots.

A variety of rainfall simulators have been developed over the years, but they can be broken down into two general categories: drop-forming and pressurized nozzles.

Drop forming simulators have evolved over time to use various drop creation methods to simulate rainfall. Early studies utilized yarn to form drops, while more recent studies have used hypodermic needles, capillary tubes, and other types of tubing to create drops (Bubuenzer n.d.). Most drop forming simulators are capable of producing constant size water droplets for a given simulation. While the consistency of the simulator is a desirable trait, natural rainfall does have a distribution of different drop sizes for varying intensities (Laws and Parsons 1943). Pall et al.

(1983) describes the limitation of drop forming simulators to produce rain drops of various size distributions. This characteristic can be improved; however, it is at the expense of the uniformity distribution of the simulator. There is concern that the results of a simulation from a single drop size simulator will not be valid due to the changing characteristics of natural rainfall (Elbasit et al. 2015). Drop forming simulators are typically utilized for experiments studying soil behavior and infiltration on small plots (Moore et al. 1983). The limitations of drop forming simulators are further clarified as "limitations on flow performance due to the frictional and capillary forces; difficulties maintaining uniformity at low intensities; and restrictions on screen suspension distance affects drop size distribution" (Regmi and Thompson 2000). There is also concern for the application of drop forming simulators due to the delivery of the rainfall. By nature of design, drop forming simulators deliver droplets of rainfall from consistent locations, therefore they impact the soil in the same location, unlike natural rainfall where the splash erosion varies in time and space due to mass and velocity variations (Angulo-Martinez et al. 2012). Drop forming simulators may also require heights as much as thirty meters in order for the drops to reach near terminal velocity (Birt et al. 2007).

In recent years, pressurized rainfall simulators have been utilized to conduct large-scale experiments (McLauglin and Brown 2006; Moore et al. 1983; Paige et al. 2003; Sharpley and Kleinman 2003; Swanson 1965). Through the use of pressurized systems, raindrops can reach terminal velocity rather quickly, which in turn allows for shorter, more portable systems. Pall et al. (1983) determined that nozzle pressure has the most significant effect on the uniformity of rainfall during simulation. In Shelton et al. (1985), it was discovered that by increasing the nozzle size and decreasing the pressure at which the rainfall simulator was applied to the plot allowed for a significant increase in the drop diameter. However, by increasing the nozzle size, the rainfall

intensity was significantly increased. The inverse was found to be true for decreasing nozzle size and increasing pressure. For several types of pressurized nozzle simulators, the required nozzle size to simulate natural rainfall typically has an excessive discharge rate. This discharge rate can be adjusted by several different methods: (1) spraying the water upwards over a large area, (2) moving the nozzle back and forth across the plot, and (3) physically obstructing the flow to intercept a significant portion of the spray (Pall et al. 1983). Shelton et al. (1985) also utilized air injected into the discharge supply lines to reduce the volume of discharge from the simulator. Pressurized nozzle simulators are best used to duplicate the natural drop distribution of rainfall and subsequently are best used in large-scale erosion plot studies (Mutchler and Hermsmeier 1965). Researchers have also increased drop size to more accurately represent natural rainfall by causing the spray to be intermittent in nature (Meyer and Harmon 1979). For pressurized simulators, maintaining the same nozzle size for the entirety of the test and varying the time the test plot is exposed to the nozzle creates a limitation as most natural rainfall has variable intensity and energy (Laws and Parsons 1943).

According to Covert and Jordan (2009), "studying soil erodibility properties in nature can be extremely difficult because of the natural variability of rainfall intensity, location, frequency, and duration, as well as variable slope and soil conditions. On a small spatial scale, rainfall simulators can be useful tools to help quantify the amount of infiltration, excess runoff, and erosion generated by different rainfall intensities, considering factors such as slope, soil type, burn severity condition, and the type of forest floor." The information gained from these small scale spatial experiments can provide important data that can be utilized for erosion process modeling (Covert and Jordan 2009). Bubenzer and Meyer (1965) recommended that laboratory scale experiments be

conducted to address the limitations of environmental conditions (i.e.. wind, temperature, relative humidity, etc.) on field testing experiments.

2.3 LARGE-SCALE RAINFALL SIMULATION

Rainfall simulation has long been used to study the effects of rainfall-induced erosion (Foltz and Dooley 2003; McLauglin and Brown 2006; Ming-Han et al. 2003; Shoemaker 2009; Xiao et al. 2010). The need for rainfall simulators arose when researchers determined that simulated rainfall provided more uniform control over experiments in comparison to natural rainfall. While natural rainfall is most desirable for testing of erosion control practices, simulated rainfall allows for expedited data collection and reproducible testing (McLauglin et al. 2001; Moore et al. 1983; Thomas and El Swaify 1989).

The earliest rainfall simulators used drop forming mechanisms (i.e., hypodermic needles and string) to form droplets (Mutchler and Hermsmeier 1965). Unpressurized systems need to release raindrops from heights of up to 9.1 m (30 ft) to ensure they reach terminal velocity, representative of natural rainfall. Furthermore, these systems are highly susceptible to environmental conditions (i.e., wind), leading to these type of simulators being employed almost exclusively in enclosed laboratory settings.

Beginning in the mid-20th century, pressurized rainfall simulation systems became more desirable to conduct large-scale, outdoor experiments (McLauglin and Brown 2006; Moore et al. 1983; Paige et al. 2003; Sharpley and Kleinman 2003; Swanson 1965). Pressurized rainfall simulators rely on nozzles or sprinkler heads to produce rain-like droplets. With a pressurized system, raindrops have the ability to reach terminal velocity quickly, thereby allowing for shorter, more portable simulators. Furthermore, pressurized rainfall simulators provide some resistance to environmental conditions, allowing researchers to conduct evaluations outdoors.

Moore et al. (1983) designed, what is referred to as a Kentucky rainfall simulator, using the following four criteria to generate conditions similar to natural rainfall: (1) uniform distribution, (2) rainfall intensities, (3) drop size distributions, and (4) raindrop velocities that create kinetic energy. Furthermore, a plot size large enough to effectively simulate field-like conditions is required. In addition to the above criteria, Meyer (1965) identified five supplementary design criteria that must be satisfied to adequately simulate natural rainfall: (1) intensities similar to storms producing medium to high rates of runoff and erosion, (2) near-continuous rainfall application, (3) near vertical impact of most drops, (4) satisfactory performance in windy conditions, and (5) portability of the system. A summary of the reviewed large-scale rainfall simulators is provided below in Table 2-1.

Table 2-1 Summary of Large-Scale Rainfall Simulators and Testing

Study	Drop Size Distribution, in. (mm)	Uniformity	Simulator Height (ft)	Rainfall Intensity (in./hr)	Plot Sizes, ft^2	Slopes, %
ASTM[a] D6459-19	Less than 10% > 0.24 (6) Less than 10% < 0.04 (1)	> 80%	14	2, 4, 6	29.7 (320)	33
Moore et al. 1983	D50 = 0.089 (2.25)	80.2 to 83.7	9.84	0.138 to 7.28	1,065	
Benik et al. 2003			8	2.36	252 and 126	35.7
Gascho et al. 1998	0.06 (1.52)		9.84	0.98	622	4.5
Pearce et al. 1998				2.36	322	3 to 5
Prats et al. 2016	natural				107	46
Robichaud et al. 2013	natural				377	69

Note: [a] ASTM International

2.4 SMALL-SCALE AND INTERMEDIATE-SCALE RAINFALL SIMULATION

Pressurized rainfall simulators differ between studies due to varying research objectives and plot sizes. Shoemaker et al. (2012) developed a laboratory-scale rainfall simulator to conduct

studies on the effectiveness of anionic polyacrylamide as an erosion control measure. The simulator consisted of a single solenoid operated nozzle. The nozzle was installed at a height of 10 ft. (3.05 m) and used a pressure regulator to control flow. Two 3H:1V sloped plots, each with a surface area of 8.0 ft^2 (0.74 m^2), were constructed and placed under the simulator. The nozzle was capable of producing a rainfall intensity of 4.4 in./hr (11.2 cm/hr). Tests consisted of four, 15-minute rainfall events separated by 15-minute intervals of no rainfall to allow for data collection. Using Christiansen's Uniformity Coefficient (CUC), Shoemaker et al. (2012) calculated an average uniformity of rainfall distribution of 83 to 87% on the test plots.

Kim et al. (2001) conducted a study examining the effectiveness of flocculant treatments on steep vegetable fields in South Korea. Six test plots were constructed on slopes ranging from 29% to 30% with surface areas of 2.4 m^2 (26 ft^2). Kim et al. (2001) constructed a rainfall simulator with steel angle iron and sprinklers set at a height of 2.4 m (8.0 ft). The simulator was capable of generating rainfall intensities from 2.8 to 3.3 in./hr (70 to 85 mm/hr).

McLaughlin and Brown (2006) conducted a rainfall simulation study with the objective of determining if application of flocculant to mulches provided erosion control improvements. For their study, 3.3 ft (1 m) wide by 6.6 ft (2 m) long test plots were constructed on slopes of 10 and 20%. A rainfall simulator based on a similar design to that of Miller's (1987) was constructed for their experiment. A 1/2HH-SS50WSQ Fulljet nozzle (Spraying Systems Co.®, Wheaton, Illinois, USA) was installed 13.0 ft (3.96 m) above the test plots to produce rain drops. The nozzle was set at a pressure of 5.0 psi (34 kPa) and produced droplet sizes similar to natural rainfall. During tests, the simulator produced constant rainfall intensity of 2.6 in./hr (68 mm/hr). The intensity was reduced to a rate of 1.3 in./hr (33 mm/hr) by programming a solenoid valve to cycle off-and-on in

10 second intervals. Tests were performed until 5 minutes after runoff was observed from the test plots. A summary of the reviewed large-scale rainfall simulators is provided below in Table 2-2.

Table 2-2 Summary of Small-Scale and Intermediate-Scale Rainfall Simulators and Testing

Study	Drop Size Distribution, in. (mm)	Uniformity	Simulator Height, (ft)	Rainfall Intensity, (in./hr)	Plot Sizes, (ft^2)	Slopes, %
Moore et al. 1983	D50 = 0.089 (2.25)	80.2 to 83.7	9.84	0.138 to 7.28	48.4 or 1,065	
Shoemaker et al. 2012		83 to 87	10	4.4	8	33
Kim et al. 2001			8	2.8 to 3.3	86	29 to 30
Miller 1987	0.089 to 0.098 (2.25 to 2.5)	90 to 95	9.84	3.4	10.8 or 32.3	10 and 20
McLauglin and Brown 2006	0.089 to 0.098 (2.25 to 2.5)	85.7 to 93.2	13	1.3 and 2.6	21.8	10 and 20
Gascho et al. 1998	0.06 (1.52)		9.84	0.98	60	4.5
Pearce et al. 1998				2.36	12.9	3 to 5
Prats et al. 2016	natural				2.69	46

2.5 COMPARISON OF RAINFALL SIMULATION SCALE

In Gascho et al. (1998), a comparison study was done to evaluate the relationships between large and intermediate scale plots. It was found that the volume of runoff for each rainfall event was generally equal for the large-scale plots (measuring 47.6 by 140.7 feet (14.5 by 42.9 meters)) and intermediate scale plots (measuring 6.0 by 6.7 ft (1.83 by 2.05 meters)) based on runoff depth through a trapezoidal flume. The focus of the study detailed by Gascho was nutrient transport. There was a reduction noted for the mean concentration of and loss of soluble Phosphorous of the intermediate scale plots when compared to the large-scale plots. The authors surmised that this could be due to the reduced flow length and time of flow for the smaller plots. The determination was also made that intermediate scale plots were capable of producing representative data of the

large-scale plots. The cost for performing intermediate scale experiments is significantly reduced versus the cost of performing large-scale experiments (Gascho et al. 1998).

In Pearce et al. (1998), a study was conducted to evaluate the amount of runoff, sediment yield, cover type (natural growth) and variations in soil composition for micro-plots and macro-plots. The micro-plots were defined as 2 ft by 13 ft (0.6 m by 2 m) while the macro-plots were defined as 10 ft by 33 ft (3 m by 10 m). It was determined that the intermediate scale plots were found to have greater sediment output than large-scale plots under equal rainfall scenarios. This is contrary to other researchers (Mutchler et al. 1994) who have stated that intermediate scale plots model interrill erosion only, while larger scale plots model interrill as well as rill erosion. Intermediate scale plots were found to be more sensitive to ground treatments than larger plots. The researchers noted that the micro-plots experienced more runoff per unit area than the macro-plots most likely due to the antecedent moisture condition of the soil. Given that observation, it is possible that the greater sediment output could be related to this as well. The study also established that increased sediment yield was also observed on plots where a silica sediment was present (Pearce et al. 1998).

Upon review of the Pearce et al. (1998) data, limitations to the experimental process are evident: no detailed information related to the relative compaction of the test soil on the plots is referenced and limited information related to the antecedent moisture condition. Through this research proposal, several key processes are proposed to minimize the error related to these conditions in an effort to provide a more complete understanding of the difference in intermediate and large-scale rainfall simulation performance. The moisture content of the soil samples will be measured prior to experimentation. The compaction of the soil on both the large plots and intermediate plots will be tested prior to the rainfall simulation. This research study will also

provide a comparative analysis of the treatments on both compacted loam and topsoil (typically consisting of organic materials and finer grain soil). This will provide useful data for future reference when designers are specifying ground cover products in the field.

2.6 RAINDROP VELOCITY MEASUREMENT

The most important factor in sheet erosion has been identified by researchers as raindrop impact (Pitt et al. 2007). The impact of a raindrop is related to the size of the raindrop as well as the kinetic energy of the drop as it impacts the ground surface. The kinetic energy of a raindrop is directly related to the velocity of the drop. There are various methods in practice to measure the velocity of raindrops. One of the earliest methods employed is the flour pan method (Laws and Parsons 1943). This method involves exposing a pan of uncompacted flour to rainfall for a time period of approximately four seconds. The drops are subsequently dried and sorted by size to determine the diameter of the raindrops. One limitation of this method is the likelihood that even though the flour is uncompacted, there is a potential for the raindrops to be disrupted due to the impact.

Fernandez-Raga et al. (2019) compared several methods of measuring the splash erosion of rainfall events, including the splash cup, funnel, Morgan tray, Tubingen cup, tower, and the gutter. It was determined through the research that the Tubingen cup provided the best method to measure the kinetic energy of the rainfall. The Tubingen cup method utilizes a flask containing a known quantity of sand which is exposed to the rainfall. The sand is weighed prior to and following the rainfall event to determine the kinetic energy based on the specified characteristics of the sand in use.

Another method used to evaluate kinetic energy is a Laser Precipitation Monitor. Meshesha et al. (2016) utilized an infrared laser beam to measure drop diameter and velocity as the rainfall

passed through the beam. One advantage to this device is the speed at which the analysis is conducted. Once the device is set up, the device will measure the data, classify the drop characteristics, and then group the raindrops into different classes of drop sizes.

2.7 PREVIOUS SMALL-SCALE EXPERIMENTAL EROSION RESEARCH

Previous research has been conducted as part of the AU-ESCTF to study and analyze various type cover treatments on a small-scale (2 ft by 4 ft plot size (0.6 m by 1.2 m)) by Wilson (2010). The surface cover treatments studied were: (1) conventional straw, crimped, (2) conventional straw, tackified, (3) wood fiber hydromulch (HM) (Excel® Fibermulch II), (4) straw and cotton hydromulch (Geoskin®), (5) cotton fiber reinforced matrix hydromulch (FRM) (HydraCX^2®), and (6) bonded wheat fiber matrix hydromulch (FM) (Hydrostraw® BFM).

Mulching is defined as an erosion control practice that uses materials such as shredded paper, grass, hay, wood chips, wood fibers, straw, or gravel to stabilize exposed or recently planted soil surfaces (District 2010; Scholl et al. 2012). Surface mulch has been found to be one of the most effective, practical means of controlling runoff and erosion on disturbed land prior to vegetation establishment; however it is most effective when used in conjunction with vegetation (Alabama Soil and Water Conservation Committee 2009; District 2010; Tyner et al. 2011). Researchers (Box and Bruce 1996; Bruce et al. 1995; Sutherland 1998; Sutherland and Ziegler 2006) have reported that mulches used to control erosion have a two-fold advantage: (1) reduce soil loss, and (2) protect grass seeds and soil amendments from being washed away. Additionally, mulches are capable of reducing solar radiation, suppressing fluctuations of soil temperature, reducing water loss through evaporation, increases interception storage capacity, dissipating the kinetic energy from the raindrops impact, and helping to prevent soil crust formation (Bruce et al. 1995; Prats et al. 2016; Rickson 1995; Singer et al. 1981; Sutherland 1998; Turgeon 2002). Research has also

shown that mulching can reduce sediment yields by over 80% when applied at a rate of 2,000 kg/ha (Keizer et al. 2018; Prats et al. 2016).

The purpose of testing conventional straw was to have a traditional, low-cost, widely used erosion control practice to compare to the performance of hydromulch products. Straw is one of the most widely used ground covers used to reduce erosion on construction sites (Babcock and McLauglin 2013), and has been reported to reduce erosion rates by more than 90% if applied at sufficient rates (Mannering and Meyer 1963; McLauglin and Brown 2006; Meyer et al. Foster 1970; Singer et al. 1981). Turgeon (2002) states that straw is also capable of encouraging grass establishment by reducing runoff, increasing infiltration, and improving soil conditions.

Straw crimpers are typically used to crimp or punch straw into the soil when the soil is not too sandy (Babcock and McLauglin 2019). If crimpers are not available or necessary, liquid mulch binders are used to 'tack' mulch by spraying the tack on top of the straw (Alabama Soil and Water Conservation Committee 2009).

There are advantages and disadvantages to using straw mulch for erosion control. The advantages are that it is inexpensive, quick and easy to apply using a straw-blower, capable of achieving efficient grass growth, and water is not needed for application. Straw mulch has also been found to perform as well as or better than hydromulch products when applied in sufficient rates (Lee et al. 2018). Other studies have shown straw mulch to not only reduce soil erosion in the short term, but also by aiding in vegetation establishment through the long-term reduction of soil erosion (Babcock and McLauglin 2011). Conversely, disadvantages of conventional straw include that it does not prevent soil loss as well as more expensive erosion products (e.g., erosion control blankets, compost, etc.), is susceptible to wind if not properly anchored, may introduce weed seeds, and fines from straw blowers can drift long distances (Babcock and McLauglin 2019).

Hydraulically applied mulches, referred to herein as 'hydromulches', have shown continuous evolution and improvement over the past 50 years. Advancements in technology have resulted in the production of equipment and materials that offer enhanced performance and greater productivity over many traditional methods of erosion control. Hydromulch has been shown to meet the required planting depth for small seeded species (McCullough and Endress 2012). In other studies, hydromulch has been shown to reduce the sediment yield by about 75% when compared to bare plots (Eck et al. 2010). There is a knowledge gap between the cost-effectiveness and performance benefits of new products (Morgan and Rickson 1988; National Cooperative Highway Research Program 1980; Sutherland 1998; Weggel and Rustom 1992) such as hydromulches, largely due to newly evolving technologies as well as a lack of research involving hydromulch products.

The introduction of water, refined fiber matrices, tackifiers, super-absorbents, flocculating agents, man-made fibers, plant biostimulants, and other performance enhancing additives to hydromulching practices on slopes has forced federal, state, and local governments to develop hydromulch guidelines. ASTM International (ASTM) has proposed new standards for testing hydraulically-applied erosion control products (HECPs). Also, the Erosion Control Technology Council (ECTC) has divided HECPs into five distinct categories, relevant to their corresponding functional longevity, erosion control effectiveness, and vegetative establishment (Babcock and McLauglin 2019; Erosion Control Technology Council 2008). Specific to this study, the addition of a tackifier to a hydromulch has been shown to increase the effectiveness of the hydromulch as a soil cover due to the tackifier bonding with the soil particles and creating a more hydrophobic environment (Vaughn et al. 2013). Prats et al. (2016) determined that the initial reduction in soil

erosion on a plot treated with hydromulch was attributed to the initial protective cover provided by the mulch to minimize splash erosion.

McLaughlin and Brown (2006) conducted large- and laboratory-scale tests on four ground cover practices: straw mulch, straw erosion control blanket, wood fiber, and a mechanically bonded fiber matrix (MBFM) hydromulch. In their study, it was reported that the ground covers reduced runoff turbidity by a factor of 4 or greater when compared to bare soil. More specifically, on the controlled, laboratory-scale tests, the MBFM reduced average turbidity by approximately 85% and sediment loss by about 86% in comparison to a bare soil control.

Holt et al. (2005) performed laboratory-scale tests on six hydromulch treatments using 2 ft (0.6 m) wide by 10 ft (3.05 m) long by 3 in. (7.62 cm) deep trays at a 15.7% slope. The following six hydromulches were applied by hand at 1,000 lb./ac (lbm/acre) (1,120 kg/ha) and 2,000 lb./ac (2,240 kg/ha): wood hydromulch, paper hydromulch, cottonseed hulls hydromulch, cotton byproduct (COBY) hydromulch produced from stripper waste (COBY Red), COBY produced from picker waste (COBY Yellow), and COBY produced from ground stripper waste (COBY Green). COBY is a term used in Holt's report to represent a patented cotton by product of cottonseed hulls (Holt and Laird 2002). The respective soil treatments with an application rate of 1,000 lb./ac (1,120 kg/ha) achieved soil loss reductions of 35, 58, 84, 90, 80 and 80% for wood, paper, cotton-seed hulls, COBY red, COBY yellow, and COBY green, respectively. When the application rate was increased to 2,000 lb./ac (2,240 kg/ha), the respective soil treatments achieved soil loss reductions of 19, 32, 79, 88, 88, and 68% for wood, paper, cotton-seed hulls, COBY red, COBY yellow, and COBY green, respectively.

Landloch (2002) studied the performance of four hydromulch treatments using fifteen plots that were 16.4 ft long by 4.9 ft wide (5 m long by 1.5 m wide) at a 25% slope. The four

hydromulches tested were paper hydromulch, flax hydromulch, flax plus paper hydromulch, and sugar cane hydromulch, applied at a rate of 893 lb./ac (1,000 kg/ha), 2,232 lb./ac (2,500 kg/ha), 2,900 lb./ac (3,250 kg/ha), and 4,464 lb./ac (5,000 kg/ha), respectively. The respective treatments achieved soil loss reductions of 80, 85, 96 and 96% for paper, flax, flax plus paper and sugar cane.

Benik et al. (2003) developed a study comparing the effectiveness of five treatments, including Soil Guard® which is a bonded fiber matrix (BFM). In their experiments, the BFM was applied at a minimum rate of 3,000 lb./ac (3,360 kg/ha). The BFM reduced average sediment yield by approximately 94%.

Buxton and Caruccio (1979) evaluated 19 soil stabilizing and erosion control treatments, four of them were hydromulches without tackifiers. The plot sizes used were approximately 5 ft. (1.5 m) wide by 10 ft. (3 m) long at a 12 to 15% slope. The four hydromulches tested were Conwed wood fiber mulch, Superior wood fiber mulch, Silva wood fiber mulch, and Pulch; each hydromulch was applied at a rate of 1,200 lb./ac (1,344 kg/ha). In the study of Buxton and Caruccio (1979), effectiveness of the hydromulches were measured using a vegetative maintenance (VM) and erosion control value, which in 1979 was a new parameter in the Universal Soil Loss Equation (USLE), and represented total loss ratio expressed as a decimal. These values ranged from 0.0 to 1.0, where a value of 1.0 means the erosion control practice had no effect in reducing erosion. The VM values for Buxton and Cauccio's (1979) report were translated below in Table 2-3 to measure erosion control performance in soil loss reduction percentage.

Babcock and McLaughlin (2013) evaluated straw mulch, with and without polyacrylamide (PAM), and a wood fiber hydromulch, with and without PAM, on the effectiveness of reducing erosion and improving the water quality of the runoff. The plot sizes used were (3.3 ft by 6.6 ft (1 m by 2 m) on a 33% slope. The plots were subjected to a total rainfall of 1.2 in. (3.05 cm) at an

intensity of 1.5 in./hr (3.7 cm/hr) (50-minute test). The mulch was applied at a rate of 2,000 lb./ac (2,240 kg/ha), while the hydromulch was applied at two separate application rates: 1,750 lb./ac (1,970 kg/ha) and 2,625 lb./ac (2,940 kg/ha). This study found that hydromulch applied at a rate of 2,625 lb./ac (2,940 kg/ha) provided a soil loss reduction of 8% and hydromulch applied at a rate of 1,750 lb./ac (1,970 kg/ha) provided a soil loss reduction of 19% when normalized to a straw mulch application of 2,000 lb./ac (2,240 kg/ha).

Robichaud et al. (2013) developed a study to evaluate the performance of wheat straw mulch and wood hydromulch when used in a post-fire condition to reduce erosion. Their study utilized natural rainfall over several years to evaluate the products. Two separate tests were performed in two different locations. At the first location, the application rate of the wheat straw was 1,963 lb./ac (2,200 kg/ha) and the hydromulch was 981 lb./ac (1,100 kg/ha). The soil loss reduction rates of the wheat straw mulch and the hydromulch were found to be 97% and 65%, respectively, for the first year of the study. At the second location, the application rate of the wheat straw was 4,015 to 5,978 lb./ac (4,500 to 6,700 kg/ha) and the hydromulch was 535 lb./ac (600 kg/ha). The soil loss reduction rates of the wheat straw mulch and the hydromulch were found to be 99% and 19% for the first year, respectively.

Table 2-3 Summary of Reviewed Hydromulch Practices

Study	Type of Hydromulch	Test Scale	Slope	Application Rate, lb./ac (kg/ha)	Soil Loss Reduction (%)
McLaughlin & Brown (2006)	MBFM	large & laboratory	10% and 20%	2,998 (3,360)	86
Holt et al. (2005)	Wood	laboratory	15.7%	1,000 (1,120)	35
	Paper				58
	Cotton-seed hulls				84
	COBY red				90
	COBY yellow			2,000 (2,240)	80
	COBY green				80
	Wood				19
	Paper				32
	Cotton-seed hulls				79
	COBY red				88
	COBY yellow				88
	COBY green				68
Benik et al. (2003)	BFM	large	35%	3,000 (3,360)	94
Landloch (2002)	Paper,	large	25%	892 (1,000)	80
	Flax,			2,230 (2,500)	85
	Flax plus paper,			2,900 (3,250)	96
	Sugar Cane			4,461 (5,000)	96
Buxton and Caruccio (1979)	Conwed*	large	12% to 15%	1,200 (1,344)	77
	Superior*				73
	Silva*				35
	Pulch*				72
Babcock and McLaughlin (2013)	Wood	laboratory	33%	1,758 (1,970)	19
				2,623 (2,940)	8
Robichaud et al. (2013)	Wood	large	various	981 (1,100)	65
				535 (600)	19

Their research evaluated the effectiveness of six different ground cover treatments, normalized to a control treatment, under simulated rainfall on small-scale plots. The process utilized was standardized and repeated across all of the treatments under evaluation.

The validity of this research effort relies heavily on the amount of reproducible data that is collected during experiments that can be used for comparative analyses to evaluate erosion control practice and product performance and effectiveness. The test plots and rainfall simulator

constructed for this research effort were replicas of Shoemaker's (2009) experiments with the exception of the runoff collection device. Each test plot was 2 ft in width by 4 ft in length along the runoff flow direction (0.6 m by 1.2 m) by 3.5 inches (7.62 cm) in depth (Figure 2-1). The size of the test plots were constructed with the purpose of testing erosion control practices with ease, speed, accuracy, and mobility throughout the experiment. The rainfall simulator was constructed using a single FullJet™ ½ HH – 30WSQ nozzle, with a wide-angle uniform square spray area, and medium to large drop size distribution. To regulate flow rate, the inlet hose was attached to a Norgren™ R43-406-NNLA pressure regulator with ½ inch (1.27 cm) port sizes. To maintain a consistent pressure specific to the desired rainfall event, a pressure gauge was attached to the pressure regulator to observe and regulate operating water pressure. The simulator was suspended approximately 5 ft (1.5 m) from the building wall, and 10 ft (3 m) from the floor as shown in Figure 2-1, and rainfall covers approximately a 8 ft by 8 ft (2.4 by 2.4 m) area.

Figure 2-1 Illustration of Rainfall Simulator and Small-Scale Test Plots (Wilson 2010)

Shoemaker's research efforts determined the Christiansen Uniformity Coefficient (CUC) (ASTM International 2019) over the 8 ft by 8 ft (2.4 m by 2.4 m) spray area to range from 83 to 88% (Shoemaker 2009); generally in the center 4 ft by 4 ft (1.2 m by 1.2 m) area.

In Wilson's study, the rainfall in 24 hours for a return period of 2 years for Auburn, Alabama, was selected. The rainfall regime was designed using data available from Shoemaker (2009). The rainfall regime consisted of four separate 15-minute rainfall events, each with a rainfall amount of 1.1 inches (2.8 cm) for a total rainfall amount of 4.4 inches (11.2 cm). The rainfall intensity for this regime is 4.4 in./hr (11.2 cm/hr). There was a 15-minute period of no rainfall between two test events utilized by the researchers for data collection.

2.7.1 Soil Analysis

Soil for the research effort herein was provided by a local grading contractor from a construction site near the Auburn University-Erosion and Sediment Control Testing Facility (AU-ESCTF) located in Opelika, Alabama (32°33'5" N, 85°20'28" W, approximately 14.2 miles (22.9 km) from Auburn, Alabama). A soil analysis was conducted by the Auburn University Soil Testing Laboratory to determine the soil composition. The experimental soil presented a "sandy clay loam" textural class according to the United States Department of Agriculture (USDA) textural classification system with respective composition of 67.5, 2.5, and 30% of sand, silt and clay.

After classifying the soil, a compaction test was conducted. In accordance with local standards for highway construction (ALDOT 2018) on a typical highway embankment, slopes were compacted to 95% compaction. Given the scale of this experiment, hand tamping was selected to be used on the box plots to achieve optimum compaction. To determine the number of drops required to compact the soil, two compaction tests were completed. The first soil

compaction test was to determine the optimum moisture content (OMC) or gravimetric water content of the soil. This was completed using a modified Proctor test, as specified in ASTM D1557-09, Standard Test Methods for Laboratory Compaction Characteristics of Soil Using Modified Effort (ASTM International 2009). The modified Proctor test enabled researchers to develop a Proctor curve representing the moisture content of the soil versus the dry unit weight of the soil, as shown in Figure 2-2.

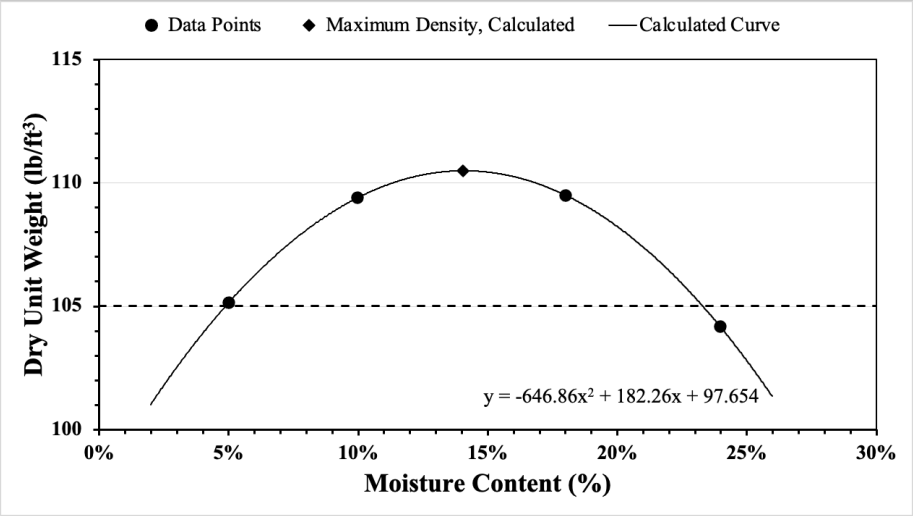

(Note: 1 lb/ft^3 = 16.02 kg/m^3)

Figure 2-2 Proctor Curve for Experimental Soil (Wilson 2010)

The Proctor curve shown in Figure 2-2 illustrates four determined moisture contents (MC) to achieve a specific dry unit weight for the tested soil. An OMC was determined to be 111 lbm/ft^3 (1,762 kg/m^3) at 14% MC by locating the maximum dry unit weight on the Proctor curve. The dotted line shown in Figure 2-2 represents the minimum dry unit weight of 105 lbm/ft^3 (1,682 kg/m^3) required to reach the specified 95% compaction rate over a MC range of 5 to 23%.

The second compaction test, also adopted from Shoemaker (2009), was created to test the number of drops of the hand tamper required to achieve 95% compaction. The purpose of this compaction test was to drop the hand tamper a specified number of times upon a known volume

of compacted soil to determine a corresponding unit weight. Soil with a MC of approximately 14% was loaded into the testing apparatus and a hand tamper was dropped approximately 12 in. (30.5 cm) from the soil surface in a series of 5 sets: 10 drops, 20 drops, 30 drops, 50 drops, and 60 drops. After each set of drops, the known volume of soil was weighed, and a dry unit weight was calculated, and plotted on a graph, shown in Figure 2-3.

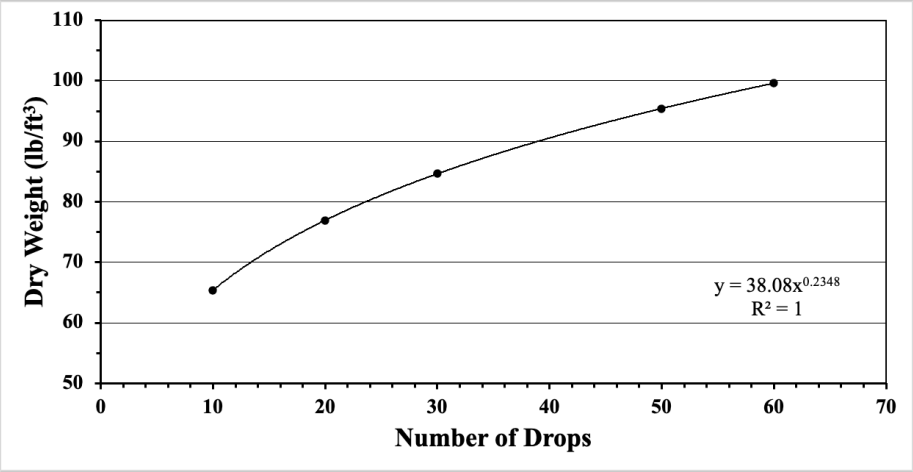

(Note: 1 lb/ft^3 = 16.02 kg/m^3)

Figure 2-3 Number of Drops with a Hand Tamper in Relation to Dry Unit Weight (Wilson 2010)

When compacted, soil will approach a point where it has reached maximum compaction, preventing any further compaction. A regression curve of power function was developed using the five measured points. When soil is no longer further compacted, the soil has reached maximum compaction and the dry unit weight levels off, regardless of energy applied by hand tamping. Using the power function, the specified number of drops of the hand tamper required to reach optimum compaction was calculated (Table 2-4).

Table 2-4 Calculated Dry Unit Weight and Number of Required Drops

Number of Drops	Dry Unit Weight, lbm/ft^3 (kg/m^3)
10	65.4 (1,048)
20	76.9 (1,232)
30	84.6 (1,355)
40	90.5 (1,450)
50	95.4 (1,528)
60	99.6 (1,596)
70	103.3 (1,655)
80	***106.5 (1,706)***
90	109.5 (1,754)
100	112.3 (1,799)

To obtain a minimum of 95% compaction, a minimum dry unit weight of 105 lbm/ft^3 (1,682 kg/m^3) was required, which corresponded to approximately 80 drops of the hand-tamper.

2.7.2 Experimental Design

Seven treatments were tested for this research effort: (1) one bare soil control; (2) conventional straw, crimped; (3) conventional straw, tackified; (4) wood fiber hydromulch; (5) straw and cotton hydromulch; (6) cotton fiber reinforced matrix hydromulch; and (7) bonded wheat fiber matrix hydromulch (Wilson 2010). Two of these treatments are classified as not having tackifiers: conventional straw, crimped and wood fiber hydromulch. The remainder of the products contain a tackifier component to the product. The bare soil treatment serves as the control, and conventional straw treatments were developed as a baseline condition for comparison of traditional mulching practices to newer hydromulch technologies currently being used in the industry. Given the application area of the rainfall simulator, two plots with the same treatment were always tested simultaneously (Figure 2-1) over the full experiment (four 15-minute events). For each of the seven treatments tested, two separate experiments were administered; therefore, there were a total of 4 replicate plots for each treatment. The data for the four replicates of each treatment were averaged first before performing any further analysis.

2.7.3 Test Plot Preparation Prior to Condition Application

To perform this test, the soil was tested to verify the proper moisture content and then loaded into the test plots. The test plots were then compacted in a single layer of 3 in. (7.62 cm) to a density of 95% and scoured with a hand rake to a depth of ¼ in. (6.35 mm). Once the test plots were prepared, the selected products were applied as per the manufacturer's recommended rates.

For each hydromulch product, testing was conducted using a commercially available hydroseeder (TurfMaker 380). Test boards were used to determine the number of passes required over the test plots to provide the manufacturer's specified application rates for each product. The test boards consisted of plywood the same dimensions (2 ft. by 4 ft. [0.6 m by 1.2 m]) as the test plots, without the compacted soil. The applied products were scraped from the test boards and weighed to verify the application rates. The results of determining the number of passes for testing is shown below in Table 2-5.

Table 2-5 Summary Application Rates for Each Hydromulch Product

Hydromulch Product	Manufacturer Required Dry Application Rate, lb./ac (kg/ha)	Equivalent Test Plot Required Dry Application Rate, lb./plot (g/plot)	Averaged Factors[1]	Minimum # of Sprays Required
straw and cotton HM	2,000 (2,241)	~0.37 (~167)	10.1	6
cotton FRM	3,500 (3,923)	~0.64 (~292)	9.7	7
wood fiber HM	2,000 – 2500 (2,241-2,802)	~0.37-0.46 (~167-209)	9.3	9
bonded wheat FM	3,000 (3,362)	~0.55 (~250)	8.9	3

[1] Averaged Factors is the product wet weight divided by the dry weight

Once the minimum number of sprays was determined for each hydromulch product, each product was ready to be applied to test plots and tested accordingly. In order to verify application rates during the testing procedure, test boards were also sprayed in conjunction with the test plots. After the minimum number of sprays were applied to the two test boards and the two test plots,

the test boards were scraped and weighed to check for application consistency to ensure manufacturer recommended rates were achieved on the test plots.

After the test plots were sprayed with the manufacturer specified application rate of the hydromulch, the test plots required time for the products to dehydrate and cure. After applying the product to the test plots, a structure was constructed, shown in Figure 2-4(a), to hold four, 250 Watt ultraviolet-ray bulbs for the purpose of simulating natural sunlight. To ensure consistent drying, the bulbs were oriented on the structure to hang at a 3H:1V slope, which mimics the test plot setup. Lastly, the distance (approximately 18 in. [45.7 cm]) between the bulbs and the hydromulch on the test plots were measured and adjusted to ensure all bulbs were equidistant to the hydromulch surface, as illustrated in Figure 2-4(a). The hydromulch test plots were left to dry for 48 hours (Wilson 2010).

(a) Drying of Test Plots during Hydromulch Testing

(b) Collection from Runoff for Each Test Plot

Figure 2-4 Hydromulch Drying and Runoff Collection for Small-Scale Testing at AU-ESCTF

2.7.4 Data Collection

Collected data for this research included (1) soil loss, (2) runoff volume, and (3) turbidity. The focus was primarily on runoff generated from test plots during rainfall events. Runoff volume

and mass for each 'left' and 'right' test plot (Figure 2-4b) was collected throughout the rain event. Instantaneous turbidity was recorded with a turbidity meter. The runoff volume and turbidity observations were recorded every minute and total 1,680 observations for seven treatments on four plots for four replicates (7×4×4×15). The soil loss observations were recorded every three minutes (560 records = 7×4×4×5). Turbidity measurements were recorded from thoroughly stirred runoff collected at 1-minute intervals using 5-quart (4.7 L) buckets.

To calculate the total soil loss, the runoff volume collected from the plots was filtered through Hayward single-length bags with one-micron size pores. Once all samples were filtered, the bags were place in an oven at 160° F (71.1° C) and dried for 24 hours. After drying, the bags were compared to the weight of the empty bags recorded prior to filtering to determine the amount of eroded soil from each test plot contained within each bag.

2.7.5 Statistical Analyses

The Tukey-Kramer method, a single-step multiple comparison procedure and statistical test, was used to analyze the recorded data and establish statistical significance between treatments (Shoemaker 2009).

2.7.6 Results and Discussion

2.7.6.1 Turbidity Variations

Using the previously outlined procedures, turbidity measurements were recorded for each series of tests from a thoroughly stirred bucket of runoff collected at 1-minute intervals. A summary of the collected results is provided below in Table 2-6. Average turbidity of all four replicate plots for each minute and each treatment was presented in Figure 2-5 for four 15-minutes events for the bare soil (Control) and six erosion control treatments. When compared to the bare

soil treatment, labeled 'Control', turbidity was reduced by at least a factor of 6 for all treatments by the end of the 60-minute test ('Event 4').

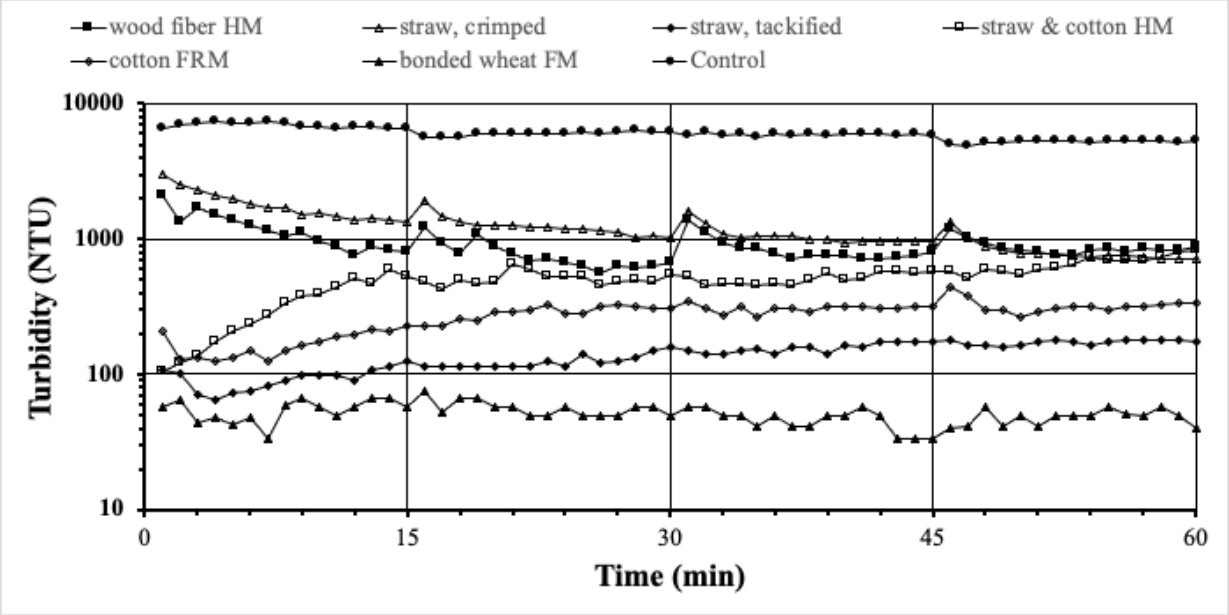

(Note: Average turbidity for each minute was calculated for all four replicate plots for each treatment.)

Figure 2-5 Average Turbidity of Surface Runoff vs. Time

As shown in Figure 2-5, each hydromulch with the exception of the wood fiber HM and the straw and cotton HM were capable of reducing turbidity levels to under 500 NTUs. Two observations can be made from Figure 2-5: (1) the treatments without a polymer-enhanced tackifier (e.g., conventional straw, crimped and wood fiber HM) had higher turbidity values during 'Event 1' and 'Event 2', whereas the turbidity decreased slightly during the last two rainfall events in comparison to treatments with a tackifier; (2) the treatments with tackifiers started with very low turbidity values and steadily increased over the four, 15-minute rainfall events. The bonded wheat FRM was the only product to maintain a steady turbidity of about 60 NTUs throughout the four rainfall events. The improved performance of the treatments containing a tackifier in comparison to the treatments without a tackifier is likely due to the bonding of the tackifier with the soil particles, which in turn creates a more hydrophobic environment (Vaughn et al. 2013).

Table 2-6 shows average turbidity measurements, standard deviation of the average turbidity, and a percent reduction, normalized for the control condition. As shown, the bonded wheat FRM is the most effective treatment in reducing average turbidity of nearly 99%, followed by straw, tackified, cotton FRM; straw and cotton HM, wood fiber HM, and straw, crimped with percent reductions of 98, 95, 92, 85, and 80% respectively. A statistical analysis was conducted and the values for average turbidity were compared to determine if the results were statistically significantly different. The results are denoted by different letters as shown in Table 2-6: 'a' represents significantly different to the control; 'b' represents significantly different to straw and cotton HM; 'c' represents significantly different to straw, crimped; 'd' represents significantly different to cotton FRM; and 'e' represents significantly different to wood fiber HM, and 'f' represents significantly different to bonded wheat FM. Shoemaker (2009) also computed and reported the lower and upper bounds of confidence intervals for all comparison.

Table 2-6 Average Turbidity, Standard Deviation and Percent Reduction of Each Treatment With Respect to the Control of Four 15-minute Events for Surface Runoff

Treatment	Average Turbidity (NTU)[1]	Standard Deviation (NTU)	Percent Reduction
Control	6060	638	-
straw and cotton HM	501[a]	150	92%
straw, crimped	1240[ab]	468	80%
cotton FRM	277[ac]	71	95%
wood fiber HM	930[abd]	285	85%
bonded wheat FM	59[abce]	10	99%
straw, tackified	148[abcef]	35	98%

'1.' Letters following the value show whether it is significantly different ($p < 0.05$) to the referenced treatment: 'a' represents significantly different to the *control*; 'b' represents significantly different to *straw and cotton HM*; 'c' represents significantly different to *straw, crimped*; 'd' represents significantly different to *cotton FRM*; 'e' represents significantly different to *wood fiber HM*, and 'f' represents significantly different to *bonded wheat FM*.

Hydromulches typically include tackifying or bonding agents to bond the mulch particles to the soil surface. Once the hydromulch dries on the soil surface, a crusted, rough surface is formed which is typically a more hydrophobic environment. The crusted surface is designed to

absorb the rainfall and serve as a filtration system to capture soil particles suspended in the stormwater runoff. When the tackifier or bonding agents have been washed away or begin to degrade due to stormwater runoff, the turbidity observed began to increase slightly as shown in Figure 2-5 above for the straw, tackified, cotton FRM; and straw and cotton HM. However, products with stronger tackifying agents such as bonded wheat FM take longer to deteriorate.

The treatments without a tackifier, straw, crimped and wood fiber HM, rely primarily on the mulch material by itself to minimize erosion from the plots. From a soil erosion perspective, these treatments are functioning as a protective layer to minimize the splash erosion created by the rainfall. Splash erosion has been found to be the initial cause of erosion (Angulo-Martínez et al. 2012). An observation was made from Figure 2-5 during the first two rainfall events, which was that the treatments that do not have a tackifying agent applied experienced a higher rate of erosion due to the absence of a tackifying agent to bond the soil particles to the treatment. This initial large concentration of soil in the runoff at the beginning of a rainfall event is due to the splash erosion caused by the raindrops impacting the soil surface. The treatments which contain a tackifying agent lessen this initial erosion by bonding the soil particles with the other material. On the other hand, the products without a tackifying agent lessen the amount of splash erosion by providing a surface cover over the soil particles when compared to the bare soil treatment.

A statistical analysis was completed to confirm observed differences between the control and treatments for turbidity measurements of stormwater surface runoff. ANOVA tables were created using Tukey-Kramer comparison tests to determine statistical significance between individual pairs of groups, as illustrated in Table 2-6. As observed, this table demonstrated that the average turbidities had statistically significant differences between the control and all treatments. All treatments showed significant differences between them in the average turbidity

except for straw and cotton HM and cotton FRM. Also, no significant statistical difference was observed between cotton FRM and bonded wheat FM, cotton FRM and straw, tackified, and bonded wheat FM and straw, tackified. All other treatment comparisons proved to show a statistically significant difference as shown in Table 2-6.

2.7.6.2 Soil Loss

Samples used to calculate soil loss were collected from simulated rainfall runoff every 3 minutes for all experiments conducted. Based on the data collected, it was observed that all treatments had significantly lower levels of soil loss when compared to the bare soil (control). The control condition and the treatments without a tackifying agent (i.e., straw, crimped and wood fiber HM) experienced an initial surge of soil loss due to the breakage of soil aggregates by the impact of raindrops, with the consequent dispersion of fine particles (splash erosion). However, the treatments with tackifiers did not have this surge; a steady increase in soil loss over time for each rainfall event was observed for these treatments. As shown in Figure 2-6, the most effective treatment in reducing soil loss was bonded wheat FM. After the first rainfall event, it was observed that soil loss measurements remained consistent for the remainder of the experiment. The summarized data is provided in Figure 2-6 below.

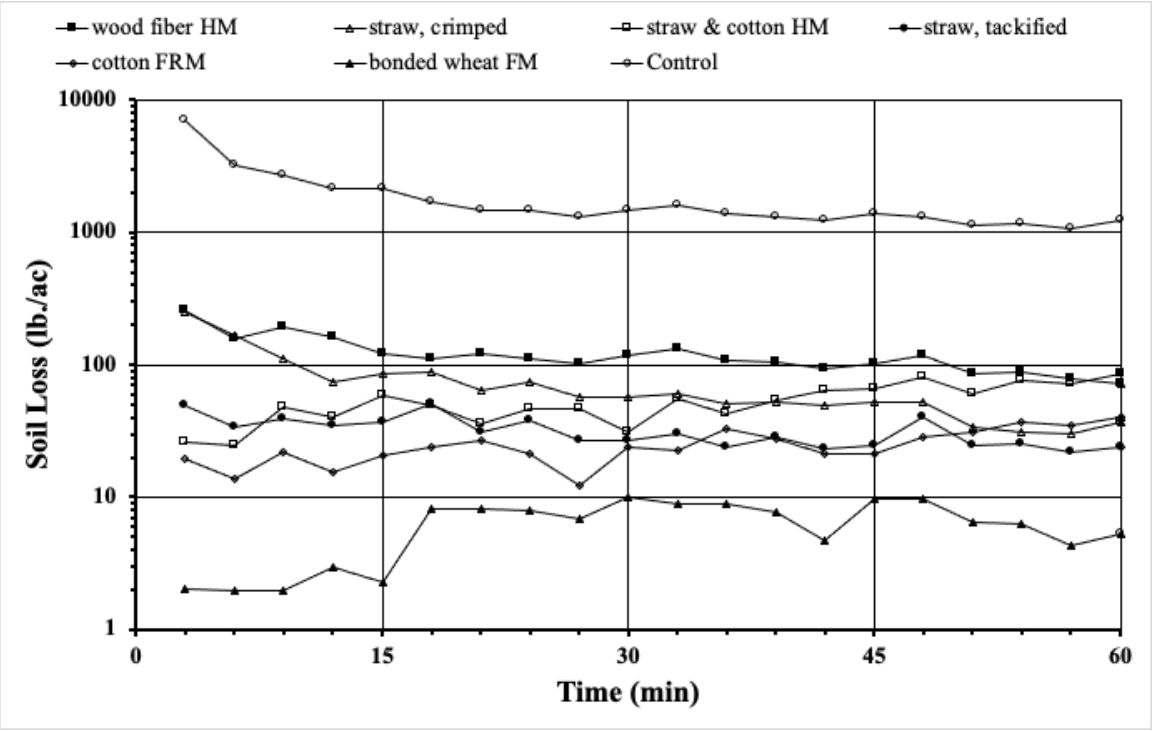

(Note: 1 lb./ac = 1.12 kg/ha)

Figure 2-6 Three-minute Soil Loss vs. Time for All Treatments as Compared to the Control

The control recorded more soil loss than all of the treatments in the first rainfall event by a factor of 17. The most consistent and effective erosion control treatment was bonded wheat FM, maintaining an average soil loss of approximately 10 lb./ac (11.2 kg/ha) over the entire experiment. Wood fiber HM was observed to produce the largest consistent amount of eroded soil, starting at approximately 900 lb./ac (1,008 kg/ha), and decreasing to approximately 450 lb./ac (504 kg/ha) by the last rainfall event. Straw and cotton HM showed initial signs of strength in controlling erosion with 200 lb./ac (224 kg/ha) of cumulative eroded soil, however steadily increased to almost 400 lb./ac (448 kg/ha) by 'Event 4', nearly doubling its initial amount. It was also observed that straw, crimped began with approximately the same amount of cumulative soil loss as wood fiber HM; however after the first two rainfall events, steadily decreased to nearly 200 lb./ac (224 kg/ha),

which are soil loss levels similar to that of straw, tackified and cotton FRM. The cotton FRM averaged 100 lb./ac (112 kg/ha) over the entire experiment. This data is shown in Figure 2-7 below.

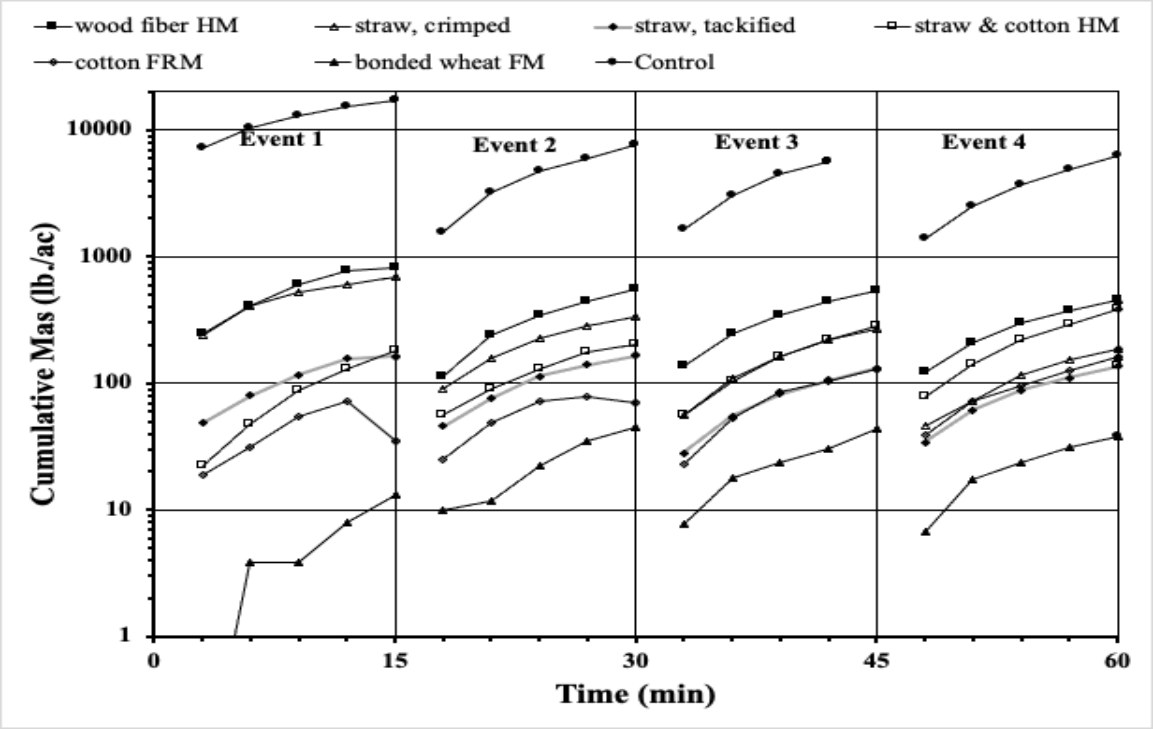

Figure 2-7 Cumulative Soil Loss vs. Time for Six Treatments as Compared to the Control

Table 2-7 presents specific values of average soil loss, standard deviation, and percent reduction for each treatment during each rainfall event. The straw, crimped treatment, when normalized to the control, reduced erosion during the first rainfall event by nearly 96% and increased to approximately 98.9% by the fourth rainfall event. Similarly, straw, tackified and wood fiber HM increased in percent reduction from 'Event 1' to 'Event 4' by 98.9 to 99.2% and 94.9 to 97.4%, respectively. The hydromulches with tackifying agents reacted in a dissimilar way when normalized to the control. Over the rainfall events, percent reductions decreased from 98.9 to 97.8%, 99.5 to 99.1%, and 99.9 to 99.7% for straw and cotton HM, cotton FRM, and bonded wheat FM, respectively. It was observed that this reduction was due to the degradation of the tackifying bonds between the soil and the mulch; contrarily, the increased performance of the non-

tackified treatments was observed to be due to the 'flush effect' of the scoured surface in the first events, exposing the less erodible, compacted, underlying soil.

Table 2-7 Average Soil Loss Over Each 15-minute Rainfall Event Due to Surface Runoff

Condition	Soil Loss [1] lb./ac (kg/ha)	Standard Deviation [2], lb./ac (kg/ha)	Percent Reduction [3], (%)
1st 15-minute rainfall event			
Control	3,470 (3,889)	2,677 (3,000)	-
straw, crimped	138.6 (155.4)	96.4 (108.0)	96.0
straw, tackified	38.2 (42.8)	35.3 (39.6)	98.9
wood fiber HM	177 (198.9)	141.3 (158.4)	94.9
straw and cotton HM	38.2 (42.8)	44.7 (50.1)	98.9
cotton FRM	18.5 (20.7)	11.51 (12.9)	99.5
bonded wheat FM	3.40 (3.81)	2.59 (2.9)	99.9
2nd 15-minute rainfall event			
Control	1,511 (1,694)	189.8 (212.7)	-
straw, crimped	69.2 (77.6)	21.68 (24.3)	98.0
straw, tackified	34.2 (38.3)	34.5 (38.7)	99.0
wood fiber HM	113.4 (127.1)	75.6 (84.7)	96.7
straw and cotton HM	41.8 (46.9)	35.2 (39.5)	98.8
cotton FRM	21.2 (23.8)	15.1 (16.9)	99.4
bonded wheat FM	9.99 (11.2)	3.30 (3.70)	99.7
3rd 15-minute rainfall event			
Control	1,429 (1,602)	236.3 (264.9)	-
straw, crimped	55.3 (62)	121.0 (135.6)	98.4
straw, tackified	26.9 (30.2)	23.8 (26.7)	99.2
wood fiber HM	108.3 (121.4)	75.3 (84.4)	96.9
straw and cotton HM	57.4 (64.3)	47.4 (53.1)	98.3
cotton FRM	26.5 (29.7)	16.3 (18.3)	99.2
bonded wheat FM	9.37 (10.5)	5.17 (5.8)	99.7
4th 15-minute rainfall event			
Control	1,228 (1,377)	194.1 (217.5)	-
straw, crimped	39.4 (44.1)	12.3 (13.8)	98.9
straw, tackified	28.3 (31.7)	25.3 (28.4)	99.2
wood fiber HM	90.8 (101.8)	69.6 (78.0)	97.4
straw and cotton HM	75.2 (84.3)	50.2 (56.3)	97.8
cotton FRM	32.7 (36.7)	21.9 (24.5)	99.1
bonded wheat FM	9.19 (10.3)	3.30 (3.7)	99.7

'1' – Average of 3-minute soil loss (Figure 2-7) for each 15-minute rainfall event
'2' – Standard deviation for average soil loss over an event
'3' – Denotes values normalized by control condition

Continuing the statistical analysis used throughout this research effort, ANOVA procedures with Tukey-Kramer multiple comparison tests were used for the recorded amounts of soil loss. Table 2-8 illustrates statistically significant and insignificant results of average soil loss throughout the experiments. The statistical analysis compared all treatments to the control and

each other. The control proved to be statistically different to all treatments; therefore, each treatment had a significant effect in reducing soil loss when compared the bare soil. No significant differences were found between the comparison to the other treatments. Therefore, it can be concluded from Table 2-8 that statistically, each treatment is capable of significantly reducing and controlling erosion on 3H:1V, compacted fill slopes.

Table 2-8 Cumulative Soil Loss for Four, 15-min Rainfall Events and Calculated Soil Loss Ratio per Treatment

Treatment	Cumulative Soil Loss (A) lb./plot (grams/plot) [2]	Cumulative Soil Loss (A) lb./ft^2 (g/m^2)	*Calculated Soil Loss Ratio[1]
straw, crimped	0.278 (126)[a]	0.347 (1,695)	0.040
straw, tackified	0.117 (53)[a]	0.146 (713)	0.017
wood fiber HM	0.450 (204)[a]	0.562 (2,744)	0.064
straw and cotton HM	0.196 (89)[a]	0.245 (1,197)	0.028
cotton FRM	0.090 (41)[a]	0.113 (552)	0.013
bonded wheat FM	0.029 (13)[a]	0.036 (175)	0.004

'[1]' Soil Loss Ratio normalized to a bare soil value of 0.876 lb./ft^2 (4,281 g/m^2).
'[*]' Soil Loss Ratio calculation: SLR=A/Control, where A is cumulative soil loss in 2nd or 3rd column.
'[2]' The letter "[a]" following the values show that they are significantly different ($p < 0.05$) to the control.

2.7.6.3 Cover-Management Factor

Several studies (Buxton and Caruccio 1979; Clopper et al. 2001; Holt et al. 2005; Landloch 2002; Lipscomb et al. 2006) used a 'cover-factor' or 'cover-management factor' to report erosion control performance. The cover factor is a parameter in the Revised Universal Soil Loss Equation (RUSLE) to represent a comparison of soil loss occurring with the treatment in place to that which occurs in the bare, unprotected condition (Clopper et al. 2001). The RUSLE allows researchers to calculate cover-factors for treatments without testing a bare soil using several different parameters based upon soil type, slope, and rain regimes; Lipscomb et al. (2006) and Clopper et al. (2001) used the RUSLE to calculate cover-factors. However, in Wilson's study (2010), the treatment results are compared to the results of the bare soil control test. This comparison is defined as the "Soil-Loss Ratio". Table 2-8 summarizes the soil loss ratio calculated in the research effort.

According to calculated soil loss ratios of 0.004, 0.013, 0.017, 0.028 0.040, and 0.064 in Table 2-8, the hydromulches can be ranked from most to least effective erosion control practices accordingly: (1) bonded wheat FM, (2) cotton FRM, (3) straw, tackified, (4) straw and cotton HM, (5) straw, crimped, and (6) wood fiber HM.

2.8 SUMMARY

This chapter provides an overview of rainfall simulation including large-scale simulation and intermediate-scale simulation. This review provided the basis for the design of the testing apparatus and the methodology for collection of data and subsequent analysis. A review was also conducted of the previous small-scale research conducted at AU-ESCTF which formed a basis for this study. Many of the methods and procedures reviewed in the previous research were used within this study to ensure consistent and repeatable results.

3 METHODOLOGY

3.1 INTRODUCTION

This chapter describes the rainfall simulator system design, testing methodology, and data collection process developed for the large-scale simulator at AU-ESCTF. The testing methods and procedures for capturing the experimental data are also discussed. The calibration procedures are discussed and identified to ensure the functionality and repeatability of the rainfall simulator. In addition, the modifications to the large-scale methods and procedures to accurately capture the intermediate-scale simulation results are discussed.

3.2 LARGE-SCALE RAINFALL SIMULATOR SYSTEM DESIGN AND CONSTRUCTION

Following ASTM D6459-19, the rainfall simulator includes the use of sprinkler heads, sprinkler risers, pressure gauges, and valves. The ASTM design consists of nine sprinkler risers spaced evenly around the test plot. Raindrop sizes should vary from 0.04 to 0.25 in. (1.0 to 6.0 mm). Furthermore, the risers should be constructed to generate a minimum raindrop fall height of 14 ft (4.3 m). To conduct large-scale testing, a 40 ft (12 m) long by 8.0 ft (2.4 m) wide test plot must be constructed on a 3H:1V slope. The soil veneer used for testing should be placed in two, 6-inch (15 cm) lifts and must consist of either a loam, sand, or clay soil. The drop size distribution for a specific intensity is determined using the flour pan method (Bentley 1904; Laws and Parsons 1943). Specified rainfall intensities are 2.0, 4.0, and 6.0 in./hr (50.8, 101.6, and 152.4 mm/hr). The test consists of three, 20-minute intervals of increasing rainfall intensity for a total of 60 minutes.

The ASTM standard requires apparatus calibration to ensure experimental values for uniformity of rainfall distribution, rainfall intensity, and drop size distribution are similar to natural rainfall. A calibration test consists of running the simulator at a specific intensity for 15 minutes.

A collection of 20 rain gauges should be spaced throughout the test plot to collect rainfall data. The recorded rainfall depth in each rain gauge is analyzed to determine the experimental values for rainfall uniformity and intensity.

3.2.1 Design and Construction of the AU-ESCTF Rainfall Simulator

This section documents the design and construction of a pressurized rainfall simulator with the aim of developing a portable, calibrated simulator capable of producing replicable, simulated rainfall events. The development of this rainfall simulator is in collaboration with the Alabama Department of Transportation to provide the capability to evaluate erosion control practices and products based upon performance under simulated rainfall. This simulator will also provide the industry with much need additional testing options, as there is currently only one simulator within the U.S. that is certified to ASTM D6459 and American Association of State Highway and Transportation Officials (AASHTO) testing requirements. In this study, a rainfall simulator and full-scale test plot were constructed at the Auburn University-Erosion and Sediment Control Test Facility (AU-ESCTF) in Opelika, Alabama. The rainfall simulator design was based on specifications listed in ASTM D6459-19 (ASTM International 2019). The simulator must be capable of producing accurate and repeatable results for three separate rainfall intensities: 2.0 in./hr, 4.0 in./hr, and 6.0 in./hr (50.8 mm/hr, 101.6 mm/hr, and 152.4 mm/hr) . The rainfall simulator design was completed in conjunction with other research projects at AU-ESCTF (Faulkner 2020; Horne 2017). The rainfall simulator consisted of several key components: water supply pond, water delivery system, rainfall simulator risers, rainfall simulator canopies, sprinkler heads, and power supply system.

3.2.2 Water Supply Pond

The water supply pond for this part of the AU-ESCTF consisted of a constructed pond with a typical volume of approximately 25,000 cubic feet of storage, shown in Figure 3-1, below.

Figure 3-1 Aerial view of Large-Scale Rainfall Simulator at AU-ESCTF.

3.2.3 Water Delivery System

The water delivery system consisted of a 3-inch (7.62 cm) NorthStar high pressure pump with a suction head of 26 ft (7.92 m) and total head of 263 ft (80.2 m) installed in the water supply pond and a three inch (7.62 cm) poly vinyl chloride (PVC) distribution system, as shown in Figure 3-2 below.

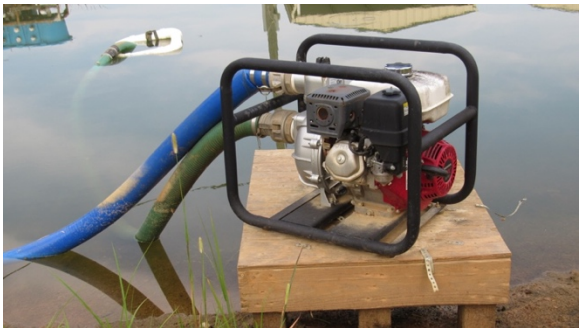

(a) Water supply pump

(b) 3-inch (7.62 cm) distribution system

Figure 3-2 Water Delivery System

3.2.4 Rainfall Simulator Riser and Canopy Design

Each riser was constructed of galvanized steel pipe to support the sprinkler canopy as well as deliver water to the sprinkler heads. A gate valve was installed on the riser to regulate flow. Furthermore, a reducer tee was installed to allow for the attachment of a 0 to 100 psi (0 to 690 kPa) pressure gauge. The riser was supported by a concrete footing as shown in Figure 3-3 (a) below. The risers were also anchored to a 4 inches by 4 inches (10.2 cm by 10.2 cm) nominal pressure treated post to ensure the riser remained plumb and level (Figure 3-3(b)).

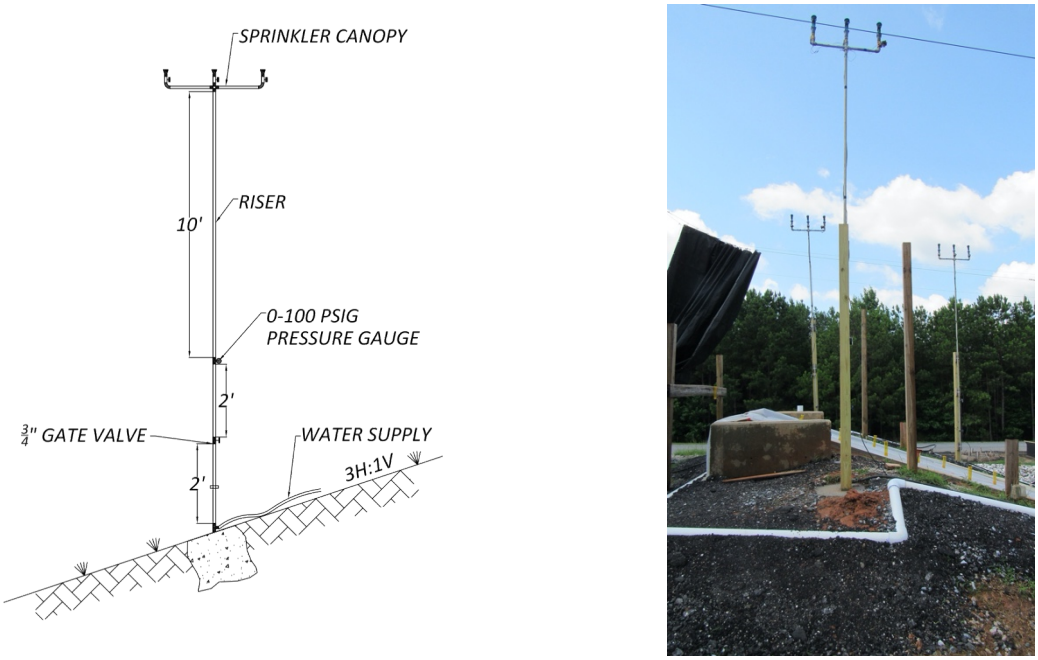

(a) Riser detail (b) Constructed riser

Figure 3-3 Rainfall Simulator Riser Design.

To effectively distribute water over the test plot, a rain canopy, Figure 3-4b, with three sprinkler heads was designed for each of the ten risers. The canopy was designed to allow for each sprinkler head to be individually operated to achieve flow rates displayed in Table 3-1. The Nelson Irrigation sprinkler heads, Figure 3-4a, spray directly out and downward, and the height of the risers was set at 14 ft (4.3 m) to satisfy ASTM D6459 standard for fall height and terminal velocity.

The canopy and all components were constructed of 0.75 in. (19 mm) diameter galvanized steel pipe to provide structural stability as well as to resist corrosion. The canopy connected to the supporting riser through a galvanized steel pipe cross in the center of the canopy.

Solenoid valves were installed upstream of each sprinkler head to allow for individual and automated operation. The use of solenoid valves represents a change from the manually operated ball valves in ASTM D6459-19.

3.2.5 Sprinkler Head Design

As specified in ASTM D6459-19 (ASTM International 2019), the targeted rainfall intensities for the rainfall simulator was designed for 20-minute intervals of 2.0, 4.0, and 6.0 in./hr (50.8, 101.6, and 152.4 mm/hr.), respectively. The rainfall simulator apparatus incorporates solenoid valves to instantaneously alter flow rates by turning on sprinklers to achieve the required intensity over the 60-minute experiment.

After reviewing several commercially available pressurized sprinkler heads, Nelson Irrigation (Walla Walla, Washington, USA) PC-S3000 sprinkler heads (Figure 3-4a) were selected in lieu of nozzles specified in ASTM D6459-19, as the specified nozzles are no longer commercially available. The PC-S3000 sprinkler heads were selected in part due to: their ability to operate at pressures as low as 6.0 psi (41.4 kPa); apply water in a 190° arc; the ability of the equipped spinner plates to shear apart flow in the sprinkler head to generate rain-like droplets; and their capability in interchangeable nozzles that allow for various flow rates. The PC-S3000 use nozzles to control the flow rate through each sprinkler head. At any given pressure, each nozzle allows a specific flow rate through the sprinkler, depending on its size. Furthermore, the sprinkler heads can be equipped with pressure regulators to ensure uniform pressure and thereby a constant

flow rate. Manufacturer specifications for each nozzle size were used to determine the appropriate nozzle sizes for this study.

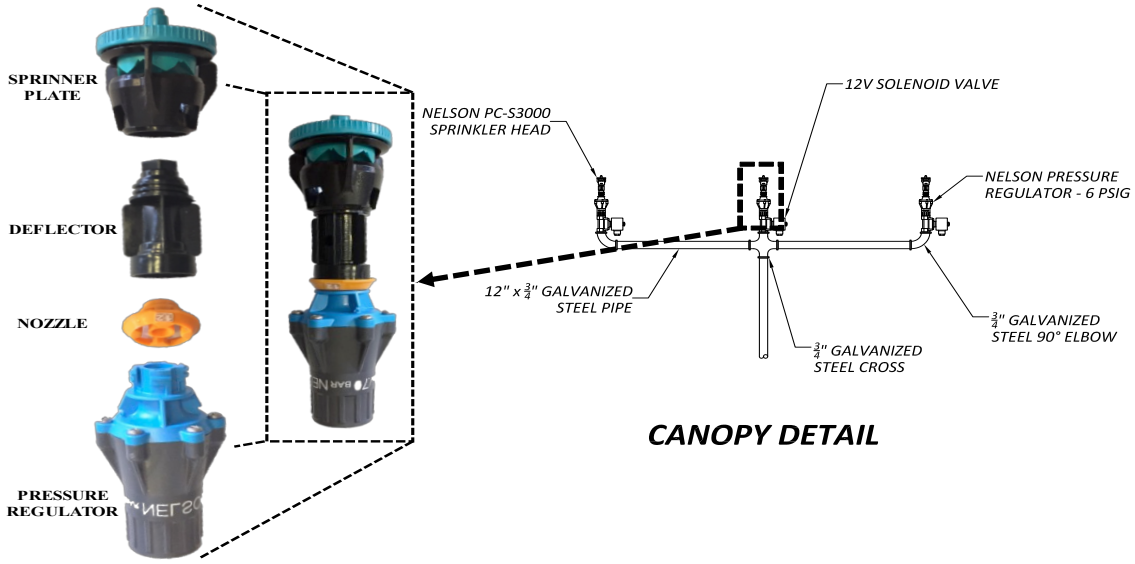

(a) Canopy, Riser, and Anchor Detail

(b) Rain Gauge Layout Constructed

Figure 3-4 Pressurized Rainfall Simulator Layout and Components (Ricks et al. 2019)

Several combinations of selected nozzles (Table 3-1) were used to achieve the variable intensities required to simulate the rainfall event. Initial testing was conducted for the selected nozzle sizes to determine the optimal spacing of sprinkler heads in relation to the rainfall plot gauges. This testing was conducted for each sprinkler considered to determine the optimal distance

from a riser to the predetermined rain gauge layout as shown above. One example of the test data is shown in Figure 3-5, below. The 15-minute duration tests were repeated many times for each sprinkler to generate a data series of rainfall depths at nine rainfall gauges (different distances to the sprinkler) in order to develop the box plots on Figure 3-5. At three rainfall gauges (4, 5.6, and 12 ft [1.22, 1.72, and 3.66 m]) measured rainfall depths did not have much variation so no box plots are shown for them on Figure 3-5.

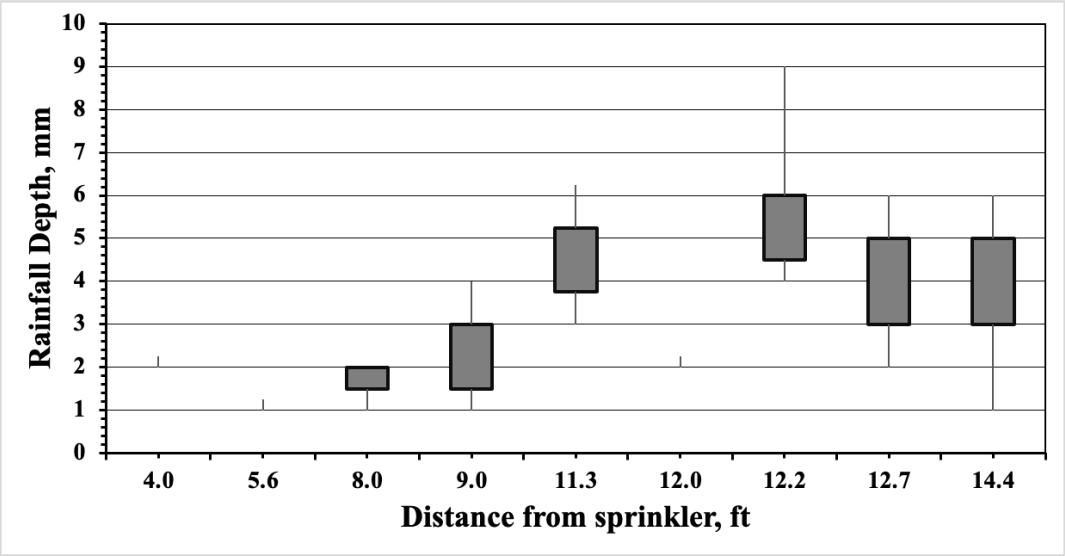

(Note: 1 in. = 25.4 mm)

Figure 3-5 Rainfall Depth Relative to Distance from Nelson PC-S3000 Sprinkler Head with #21 Nozzle at 6 psi (41.4 kPa) for 15-minute Duration Tests

Based on the testing conducted, the following distances were selected for the riser spacing: 5.0 ft (1.52 m) from plot edge and 10.0 ft (3.05 m) center to center as shown in Figure 3-6. As detailed in ASTM 6459-19 (ASTM International 2019), nine risers are specified for the test plot. For this study, an additional riser was installed at the top of the test slope as shown below to provide for a more uniform delivery of simulated rainfall across the plot. As shown in Figure 3-6, the 190° application allows for a large portion of the rainfall to be applied outside the plot area. The ratio of the plot area of application to the overall sprinkler application area is approximately

36%. As shown in Table 3-1, the percentage for the theoretical flow requirement (rainfall depth x plot area) versus the total flow produced (total output for all nozzles) is fairly consistent throughout all three rainfall intensities.

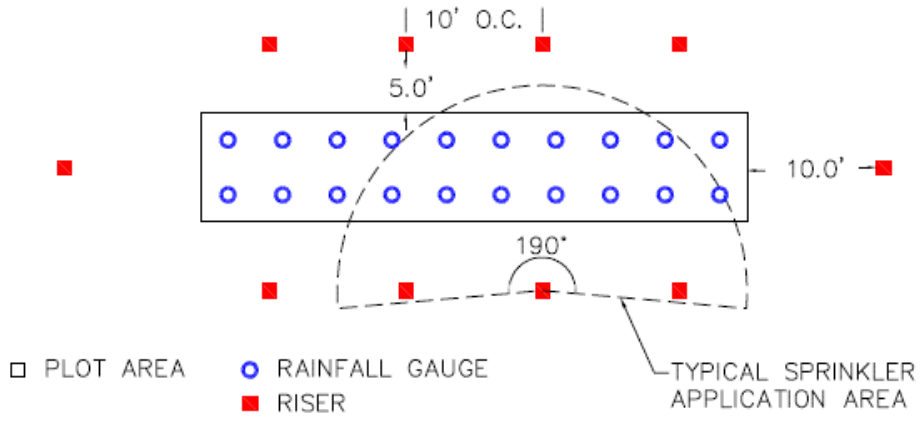

Figure 3-6 Detailed Plan View of Riser and Rainfall Gauge Locations

Table 3-1 Nozzle Combinations

20-minute Test Interval	Number and Type of Nozzles Used	Total Flow, gpm (L/min.)	Theoretical Flow Requirement, gpm (L/min.)	Theoretical vs. Total Flow (%)
1	10–#21[a]	18.4 (69.65)	6.65 (25.17)	36.1
2	15–#21 5–#18[b]	34.4 (130.22)	13.30 (50.35)	38.7
3	21–#21 9–#18	50.9 (192.68)	19.95 (75.52)	39.2

Note: [a] #21–Turquoise yellow nozzle, flow rate at 6 psi (41.4 kPa) = 1.84 gpm (6.96 L/min.); [b] #18–Gray nozzle, flow rate at 6.0 psi (41.4 kPa) = 1.36 gpm (5.14 L/min).

3.2.6 Wind Screen Design

To minimize the impact of cross winds on rainfall simulation experiments, a series of wind screens, suspension cables, and support posts were designed with the goal of reducing wind speeds on the plot to at most 1.0 mi/hr (1.6 km/hr). To support the screens, six, 6.0 in by 6.0 in, 20 ft (12 cm by 12 cm, 6.0 m) nominal lumber posts were installed around the perimeter of the test plot, as shown in Figure 3-4 (b).

3.2.7 Electrical Systems Design

Simulation of variable intensity rainfall was accomplished by installing solenoid valves on the sprinkler canopy. The valves on each canopy were wired with a 7-wire direct burial irrigation control cable to a custom designed electrical control box. The electrical control box consisted of a series of terminal blocks and was designed with three switches to provide control over which valves were active during testing. Two 12-V batteries were wired in parallel to the control box to power the entire valve system. Utilization of electronically controlled valves is an improvement over the current standard (ASTM International 2019) which has been utilized in other rainfall simulators (Sprague and Sprague 2012). The control box was equipped with a toggle switch for each time period of the simulation.

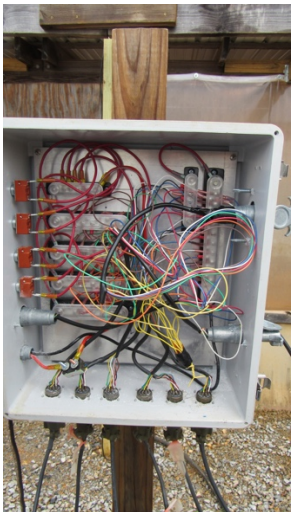

Figure 3-7 Power Supply Control Panel.

3.2.8 Calibration Methods and Procedures

Initially, the rainfall simulator apparatus was calibrated to determine the experimental values for rainfall intensity and uniformity. This process was critical in proving accurate and

repeatable simulated conditions similar to natural rainfall (i.e., uniformity, drop size, and terminal velocity).

According to ASTM D6459-19 (ASTM International 2019), twenty rainfall gauges are required when measuring and calibrating rainfall intensity and distribution. For this study, an additional nine rainfall gauges were installed along the center of the test plot as shown in Figure 3-4b.

For each target rainfall intensity, a calibration test was performed for a duration of 15 minutes. At the end of the test, the rainfall depth in each of the 29 gauges was measured and recorded in centimeters. The recorded values for rainfall depth were then used to calculate CUC using Equation (1), and average rainfall intensity:

$$CUC = 100\left[1.0 - \frac{\sum\left(\left|D_i - D_{avg}\right|\right)}{n \times D_{avg}}\right] \quad (1)$$

where:

CUC = Christiansen's Uniformity Coefficient used to express uniformity of rainfall (%)
D_i = depth of rainfall in the ith gauge (cm)
D_{avg} = average rainfall depth in all gauges (cm),
n = number of gauges

Using Equation (2), experimental rainfall intensities on the test plot were computed and compared to the targeted rainfall intensities for determining the relative errors:

$$i = 60\left[\sum_{j=1}^{J}\frac{D_j}{Jt}\right] \quad (2)$$

where:

i = rainfall intensity (cm/hr)
D_j = depth of rainfall (cm)
J = number of rain gauges

t = test duration (min)

Once the uniformity of rainfall was at least 80% for each target intensity, the raindrop size distribution for each intensity was measured using the flour pan method (Bentley 1904; Laws and Parsons 1943). For each intensity, pans were filled with sifted flour and exposed to rainfall for 2.0 to 4.0 seconds. Raindrops impacting the flour created small pellets that were then sifted, baked, and separated using sieves. The pellets on each sieve were then weighed and counted. This process was repeated three times (at the top, middle, and bottom part of the slope) for each test intensity. Each of the four steps for the flour pan method are depicted in Figure 3-8. Using this information, the average raindrop diameter for each sieve was then calculated using Equation (3) (Laws and Parsons 1943):

$$D_r = \sqrt[3]{\left(\frac{6}{\pi}\right) M\, m_R} \tag{3}$$

where:

D_r = average raindrop diameter (mm)
M = average pellet mass (mg), which is the total mass divided by the number of pellets in each sieve for all three repetitions
m_R is the ratio of the mass of the raindrop to the mass of the pellet and determined using the flour-calibration figure developed by Laws and Parsons (1943)

At the same time, the percent of the mass of the raindrops for each sieve can be determined with respect to total mass of all raindrops measured. The calculated results are shown in Figure 3-9, below.

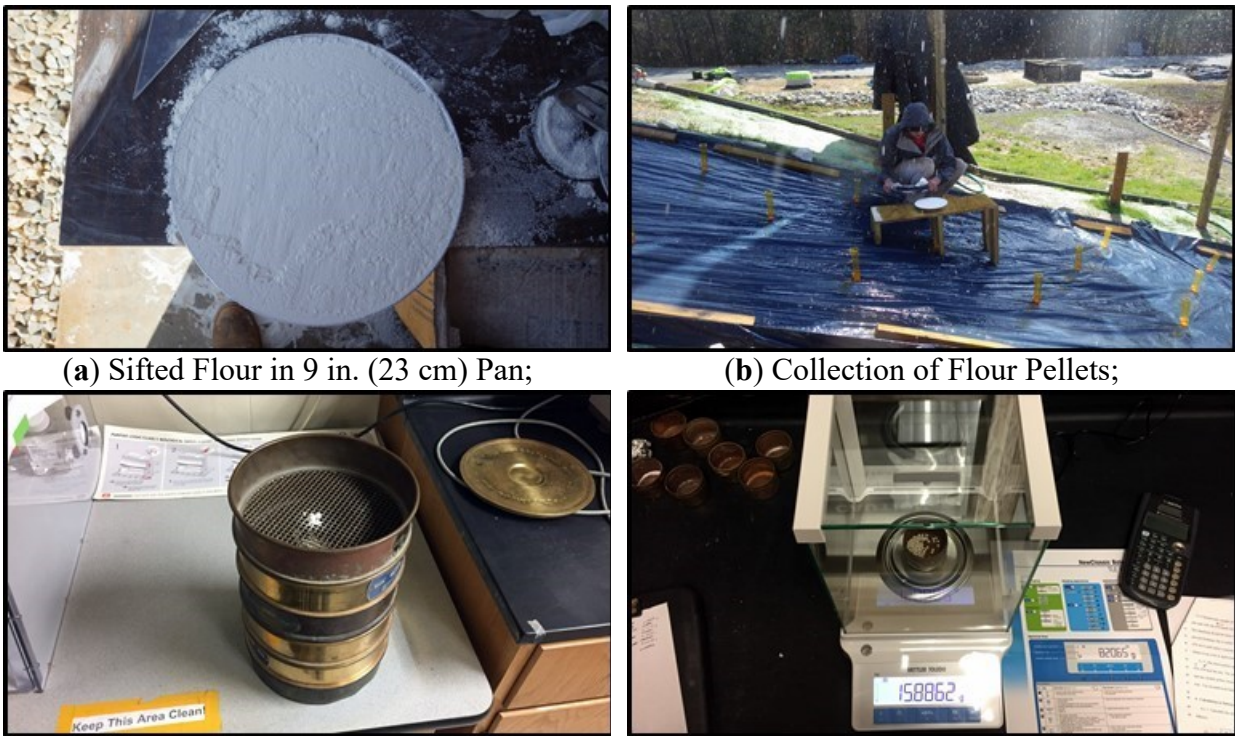

(**a**) Sifted Flour in 9 in. (23 cm) Pan; (**b**) Collection of Flour Pellets;

(**c**) Separating Pellets in a Sieve Stack; (**d**) Weighing Flour Pellets.

Figure 3-8 Drop Size Distribution Testing Procedures

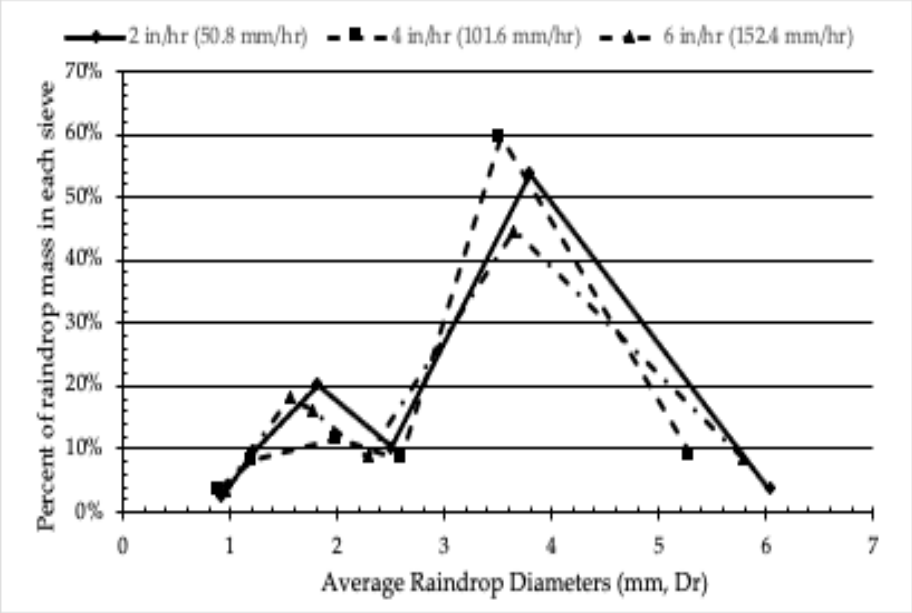

Figure 3-9 Percent of Raindrop Mass vs. Average Raindrop Diameter, D_r, in Each Sieve for Three Rainfall Intensities

Following the calculation of the raindrop size distribution, the kinetic energy generated at each rainfall intensity was calculated to determine rainfall energy, *E*. First, the raindrop fall height was determined by holding a surveyor's rod vertically in front of the center of a single sprinkler riser, extended above the height of the sprinkler nozzles, while the riser was operational. The wetted height was recorded as the average fall height for the raindrops. Next, using the average raindrop diameters computed from the flour pan method, the average volume of the raindrops was calculated using Equation (4):

$$V_{avg} = \frac{4\pi}{3}\left(\frac{D_r}{2}\right)^3 \quad (4)$$

where:

V_{avg} = average volume of raindrops (mm^3)
D_r = average diameter of raindrops (mm)

The diameter of the drops is used with Figure 3-10 to determine the velocity of the drops falling from the height of the rainfall simulator and the terminal velocity. From this, the values for kinetic energy were calculated using Equation (5):

$$KE = 0.5mv^2 \quad (5)$$

where:

KE = kinetic energy (J)
m = average mass of raindrop (kg)
v = velocity of raindrop (m/s)

The final step of the calibration process was to calculate the erosion index using Equation (18).

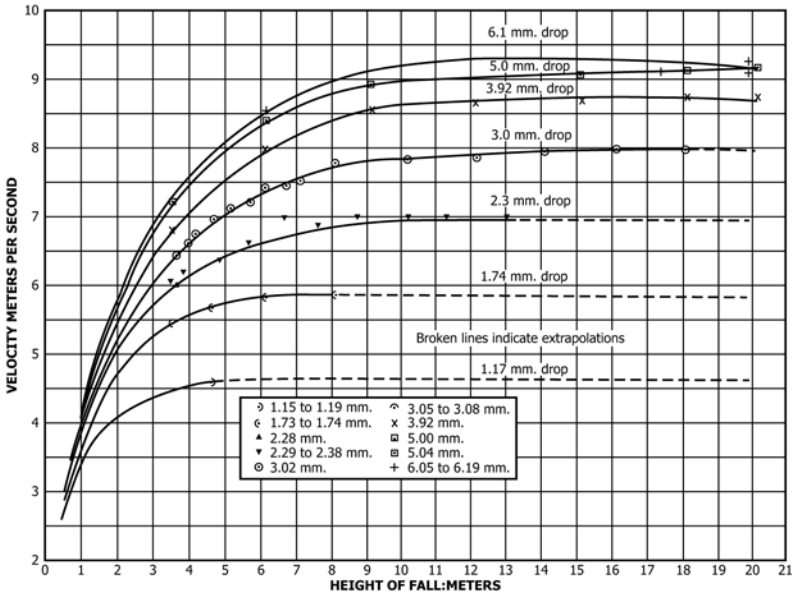

(Note: 1.0 ft = 0.305 m)

Figure 3-10 Fall Velocity of Raindrops as Function of Raindrop Size and Fall Height (ASTM International 2019)

3.2.9 Large-Scale Erosion Plots

Faulkner (2020) completed and detailed the large-scale data used in this study for comparison. The plot size for this data was 8 feet wide by 40 feet long (2.44 m wide by 12.2 m long) on a 3:1 horizontal to vertical slope, consistent with the requirements of ASTM D6459.

3.2.10 Soil Selection

For this research project, the selected soil for testing is a locally sourced loam material in keeping with the recommendations of ASTM 6459-19(ASTM International 2019). Soil was provided by a local grading contractor from a construction site near the AU-ESCTF. A summary of the soil analysis is shown in Table 3-2 below.

Table 3-2 Percent Composition and Classification of Experimental Soil

% Sand	% Silt	% Clay	% Organic Matter	Classification
48	41	11	0	*Loam*

After classifying the soil, a compaction test was conducted to determine the optimum moisture content (OMC) of the soil. This was completed using a modified Proctor test, as specified in ASTM D1557. The modified Proctor test enabled researchers to develop a Proctor curve representing the moisture content of the soil versus the dry unit weight of the soil, as shown in Figure 3-11.

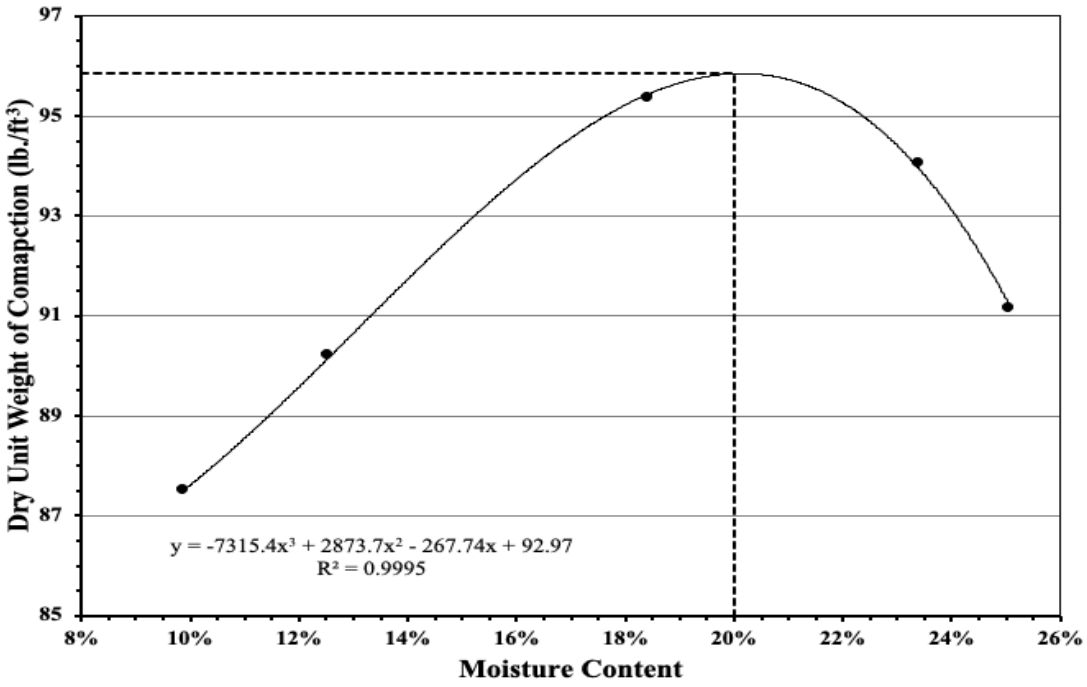

Figure 3-11 Proctor Curve for Experimental Soil

The Proctor curve shown in Figure 3-11 illustrates five determined moisture contents to achieve a specific dry unit weight for the tested soil. An optimum moisture content (OMC) was determined to be 20% moisture content (MC) by locating the maximum dry unit weight on the Proctor curve, i.e., 95.85 lb./ft^3 (1,535 kg/m^3).

3.2.11 Determining Application Rate of Hydromulch Product

In order to determine the application rates for each hydromulch product, testing was conducted utilizing the Turfmaker. Sheets of ½ inch (1.27 cm) plywood were constructed to

represent the size of the small-scale plots (2 ft by 4 ft). The boards were then sprayed with an increasing number of passes with the hydromulcher. The hydromulch was then scraped from the sample boards and dried to determine the application rate. The steps within this process are shown below in Figure 3-12.

(a) Sample boards.

(b) Sample boards at beginning of scraping process.

(c) Hydromulch after being scraped from sample boards.

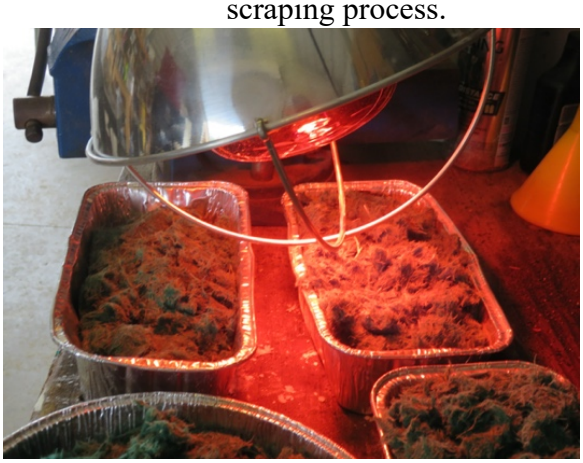

(d) Drying of Hydromulch.

Figure 3-12 Steps of Determining the Hydromulch Application Rate

Table 3-3 Hydromulch Product Application Rates

Hydromulch Product	Recommended Application Rate, lb./ac (kg/ha)	Tested Application Rate, lb./ac (kg/ha)	Number of Passes Determined
EcoFibre	2,500 (2,802)	2,809 (3,148)	5
Terrawood	2,500 (2,802)	2,665 (2,987)	6
Soil Cover	2,500 (2,802)	3,025 (3,391)	8

3.2.12 Data Collection

For the large-scale tests, a total of 12 tests were performed. These tests consisted of three bare soil control tests and three tests for each hydromulch product respectively. Each test was conducted for three separate rainfall intensities of 2 in./hr, 4 in./hr, and 6 in./hr (50.8, 101.6, and 152.4 mm/hr) for 20 minutes in duration for each. During each test, grab samples were taken from the discharge weir every three minutes for the duration of the test. In addition, runoff volumes were captured as well as total sediment that escaped from each plot. Photographs were taken before and after each rainfall interval.

3.2.12.1 Turbidity and Total Suspended Solids (TSS)

Water quality data was obtained from grab samples that were collected from the discharge weir every three minutes throughout the duration of the test. These grab samples were taken from the time when runoff began leaving the plot until all runoff had ceased. The samples were then transferred to the laboratory for analysis in accordance with the "Turbidity and TSS Processing Procedures" at AU-ESCTF provided in the Appendices.

3.2.12.2 Discharge Over Time and Total Soil Loss

For each test, the total discharge of the plot was captured separately for each rainfall intensity. Water depth loggers were utilized to capture depth readings every two minutes during the test by measuring the depth in the capture basin to determine the total discharge. The captured runoff from the test plot was then allowed to settle for a minimum of 24 hours before the excess water was removed. The total dry mass of the sediment was then calculated by weighing the total wet sediment and collecting representative samples to determine the moisture content of the overall sample.

3.3 SMALL-SCALE AND INTERMEDIATE-SCALE TEST DESIGN AND METHODOLOGY

3.3.1 Small-Scale and Intermediate-Scale Test Plots Under Large Rainfall Simulator

While the previous detailed research was used as a basis for the further design and testing of hydromulch products on small-scale rainfall simulation, several key changes were incorporated in the rainfall simulator. In lieu of utilizing a separate rainfall simulator, the rainfall simulator apparatus detailed and constructed for the large-scale testing was utilized. By utilizing the same rainfall simulator for both analyses, the opportunity for error was decreased. The primary difference for the small- and intermediate-scale testing was the modification of the size of the test plots. The primary test plots, referred to as the small-scale plots, were 2 ft in width by 4 ft in length (0.6 m by 1.2 m) as detailed previously (Ricks et al. 2020). The test plots utilized for the loam soil sample were 3.5 inches (8.89 cm) in depth; whereas the topsoil plots were increased to a depth of 5.5 inches (14 cm). In addition, loam bare soil control tests were performed on plot sizes of 4 ft in width by 8 ft in length (1.2 m by 2.4 m). Given the size of the large-scale rainfall simulator, multiple small-scale test plots were placed throughout the rainfall simulator to conduct multiple runs simultaneously. The layout used for the small-scale testing is shown below in Figure 3-13.

(a) Small-Scale Test Plot Layout;

(b) Calibration Gauges, Constructed, for Small-Scale Testing;

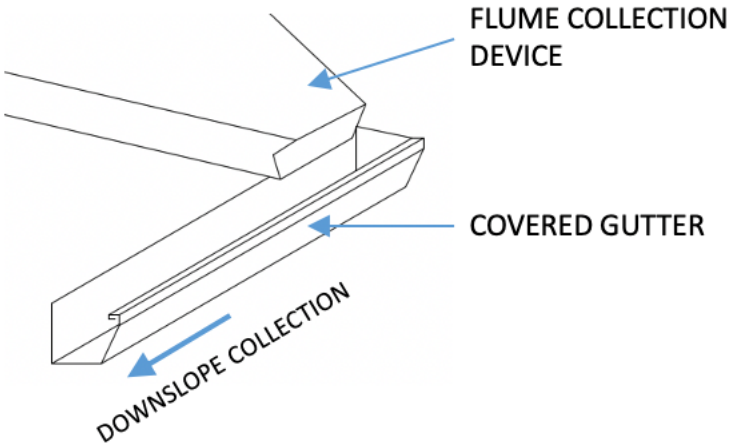

(c) Flume Collection Device for Intermediate- and Small-Scale Testing.

Figure 3-13 Small-Scale Test Plots Under Large-Scale Rainfall Simulator

3.3.2 Calibration Methods and Procedure of Small- Scale and Intermediate-Scale Testing

Calibration tests were performed on each test plot for each individual rainfall intensity. Six rainfall gauges were installed on each test plot as shown in Figure 3-13(b). At the conclusion of each 15-minute calibration test, the rainfall depth in each gauge was measured and recorded in centimeters. From this data, the Christiansen's Uniformity Coefficient (CUC) was calculated as detailed in Section 3.2.10. The targeted uniformity for CUC on the test plot was a minimum of 80%. In order to validate the calibration process, a minimum of ten calibration tests were conducted for each target intensity, if the standard deviation was less than or equal to 0.10 in./hr (2.54 mm/hr). This value was selected as the realistic limit for the simulator to perform in a consistent and repeatable fashion.

Once it was determined that the simulator was performing in a consistent and repeatable process for the specified plot locations, a drop size distribution of each test rainfall interval was conducted in the same method as described previously in Section 3.1. A flour pan test was conducted for each rainfall intensity at each plot location as shown in Figure 3-14. Data obtained from the flour pan method was used to calculate the kinetic energy of the rainfall event. From this data, the plot locations which most closely represented the average kinetic energy of the large-scale tests was used as the bare soil control plot. These plots were utilized to capture water samples which were used to analyze the turbidity and TSS output data. As shown in Table 4-8 below, Plot 4 was the small-scale plot that most closely resembled the kinetic energy of the large-scale plots. This plot was selected for the bare soil control. Plot 5 was selected for the detailed TSS and turbidity analysis of the selected hydromulch products. The remainder of the test plots were used to capture runoff and soil loss data only. In order to properly capture the runoff and soil loss

information from the test plots, improvements were made to the runoff collection device as shown in Figure 3-13(c).

(a) Drop Size Collection Setup Using Flour Pan Method

(b) Drop Size Collection Using Flour Pan Method

Figure 3-14 Flour Pan Testing for Small-Scale Plots

3.3.3 Discussion of Soil Loading and Compaction

Each small- and intermediate-scale test plot was filled with a single lift of soil and then compacted using a hand tamper, similar to the process discussed in Ricks et al. (2020) and shown in Figure 3-16 below. In order to determine the number of drops of the hand tamper required to achieve the desired compaction, testing was conducted utilizing a box of known dimensions and the hand tamper was dropped the desired number of repetitions, see Figure 3-15 below. The volume of soil was then calculated, and the density was determined.

(a) Soil Compaction Testing Box;

(b) Hand Tamper for Soil Compaction Testing.

Figure 3-15 Determining Number of Drops for Soil Compaction

Prior to each test, compaction tests were conducted on each test plot, in accordance with ASTM D2937-10 and ASTM D4643. The desired percent compaction for testing of the loam soil was determined to be 86±6%. The ideal moisture content was 20±5% as shown in Figure 3-11. A similar process was utilized for testing of the topsoil plots as well. The topsoil was loaded in a single lift and compacted using a hand tamper.

(a) Filling of Small-Scale Test Plots;

(b) Scarify Surface of Small-Scale Test Plots.

Figure 3-16 Filling of Test Plots with Soil and Compaction Process.

3.3.4 Data Collection

For the small- and intermediate-scale simulations, the data capture and analysis techniques were similar to the techniques utilized during the large-scale simulations. For each test plot, runoff and total soil loss were captured utilizing the runoff collection devices detailed in Section 3.3.1 and a series of 5-gallon (3,8 L) buckets. Turbidity and TSS were analyzed through the water samples captured for the plots deemed to have the most similar kinetic energy to the large-scale simulation. Both the runoff volumes and water samples were taken on three-minute intervals throughout the duration of the test.

3.3.5 Runoff Depths and Total Soil Loss Calculations

The runoff from each test plot was captured in labeled five-gallon buckets (3.8 L). The depth in each bucket was recorded on the data capture form every three minutes throughout the duration of the test as shown in Figure 3-17 below. Given the consistency of the sizing of the buckets, the runoff depths were applied to Equations (6) and (7) to determine the volume of water (V_d, in^3) at each respective depth (inches) (Rade and Westergren 1990). A summary of the measured depths and corresponding volume of the five-gallon buckets (3.8 L) is provided below in Table 3-4.

Figure 3-17 Runoff Collection Device for Small- and Intermediate-Scale Test Plots

Table 3-4 Small- and Intermediate-Scale Runoff Collection Device Measurements

Depth within Bucket, in. (cm)	Diameter, in. (cm)	Area at Specified Depth, in^2 (cm^2)	Volume at Specified Depth, ft^3 (m^3)
0	10 (25.4)	0.545 (506)	
13.875 (35.2)	11.375 (28.9)	0.706 (656)	0.721 (0.0204)

$$V_d = \frac{\pi h}{12}\left(D_{bot}^2 + D_{bot}D_{top} + D_{top}^2\right) \quad (6)$$

where:

V_d = volume of water (in^3) at respective depth, h
h = measured depth (in)
D_{bot} = diameter at bottom of bucket
D_{top} = diameter at top of bucket

$$z = \frac{1}{2h}\left(D_{top} - D_{bot}\right) \quad (7)$$

where:

z = slope of side wall of cone
h = measured depth (in)
D_{bot} = diameter at bottom of bucket
D_{top} = diameter at top of bucket

Upon completion of the depth measurements, the sediment was allowed to settle in the buckets for a minimum of 24 hours. After 24 hours, the excess water was removed with a vacuum. The buckets were then left to air dry. The bucket and remaining dry soil were then weighed and the soil loss recorded for each bucket.

3.3.6 Turbidity and TSS

The water samples taken from specified test plots were captured using individually labeled 200 mL plastic sampling bottles. Upon completion of the test, the bottles were refrigerated for 24 hours before being transferred to the laboratory for analysis. The samples were tested for turbidity and TSS at the laboratory according to the procedure listed in Appendix A, Section 8.1.

3.4 HYDROMULCH SELECTION

Through discussions with the Alabama Department of Transportation, several types of hydromulch were selected as the erosion control products for testing to be examined in this project. These products were: EcoFibre Plus Tackifier; SoilCover Wood Fiber with Tack; and Terra-Wood with Tacking Agent 3. Each product will be discussed in more detail.

EcoFibre Plus Tackifier is defined as a biodegradable wood fiber hydromulch owned by Profile Products, LLC. It is recommended for installation on moderate slopes of ≤ 2H:1V. The composition of EcoFibre is 97% thermally refined wood fibers and 3% wetting agents including high-viscosity colloidal polysaccharides.

SoilCover Wood Fiber with Tack is defined as a biodegradable wood fiber hydromulch owned by Profile Products, LLC. It is recommended for installation on moderate slopes of ≤ 2H:1V. The composition of SoilCover is 97% thermally refined wood fibers and 3% wetting agents including high-viscosity colloidal polysaccharides.

Terra-wood with Tacking Agent 3 is defined as a biodegradable wood fiber hydromulch owned by Profile Products, LLC. It is recommended for installation on moderate slopes of ≤ 2H:1V. The composition of Terra-wood is 97% thermally refined wood fibers and 3% wetting agents including high-viscosity colloidal polysaccharides. Additional information on each product is provided in the Appendices.

3.5 SOIL LOSS EQUATIONS

3.5.1 Revised Universal Soil Loss Equation (RUSLE)

RUSLE was used to calculate the theoretical soil loss of the various plot sizes, the soil erodibility factor (*K*) of the tested soil on each plot size and the cover management factor (*C*-

factor) of the tested erosion control practices. RUSLE consists of several key variables to calculate soil loss using the following equation (Agriculture 1997):

$$A = R \cdot K \cdot L \cdot S \cdot C \cdot P \quad (8)$$

where:

A = average soil loss per unit of area expressed in the units of *K* and for the period of *R*
R = rainfall-runoff erosivity factor (hundreds ft-ton-in./acre-hour)
K = soil erodibility factor (hundreds acre ft-ton in^{-1})
L = slope length factor (dimensionless)
S = slope steepness factor (dimensionless)
C = cover management factor (dimensionless)
P = support practice factor (dimensionless)

3.5.2 Rainfall-Runoff Erosivity Factor, *R*

The rainfall-runoff erosivity factor, *R*, is determined from the total storm kinetic energy, *E*, and the maximum 30-minute rainfall intensity, I_{30} (Agriculture 1997). The total storm kinetic energy is determined from the unit energy of the storm using the calculated rainfall intensity and the depth of rainfall for the desired storm increment (Clopper et al. 2001). The maximum 30-minute rainfall intensity is calculated using the peak rainfall intensity when the time increment exceeds thirty minutes or by using a weighted average of varying intensities over a 30-minute interval (Early et al., 2003). The formulas for calculating the rainfall-runoff erosivity factor and rainfall energy per unit depth of rainfall per unit area are provided in Equations (**9**) and (**10**), below.

$$R = \frac{\sum_{i=1}^{J}(EI_{30})i}{N} \quad (9)$$

where:

R = rainfall-runoff erosivity factor (hundreds ft-ton-in./acre-hour)
E = total storm kinetic energy (hundred ft-tons/acre)
I_{30} = maximum 30-minute rainfall intensity (in./hr)
N = number of years

$$e = 1099\left(1 - 0.72e^{-1.27i}\right) \quad (10)$$

where:

e = rainfall energy per unit depth of rainfall per unit area (ft-tonf/acre-in)
i = rainfall intensity (in./hr)

3.5.3 Soil Erodibility Factor, *K*

The soil erodibility factor, *K*, is representative of the properties of the soil and the characteristics of the soil profile on overall soil loss. Typically, the *K*-factor is calculated using the other more well-defined terms within RUSLE shown in Equation (8). However, guidance has been provided to estimate the *K*-factor based upon the composition of the soil (Agriculture 1997) as shown below in Figure 3-18.

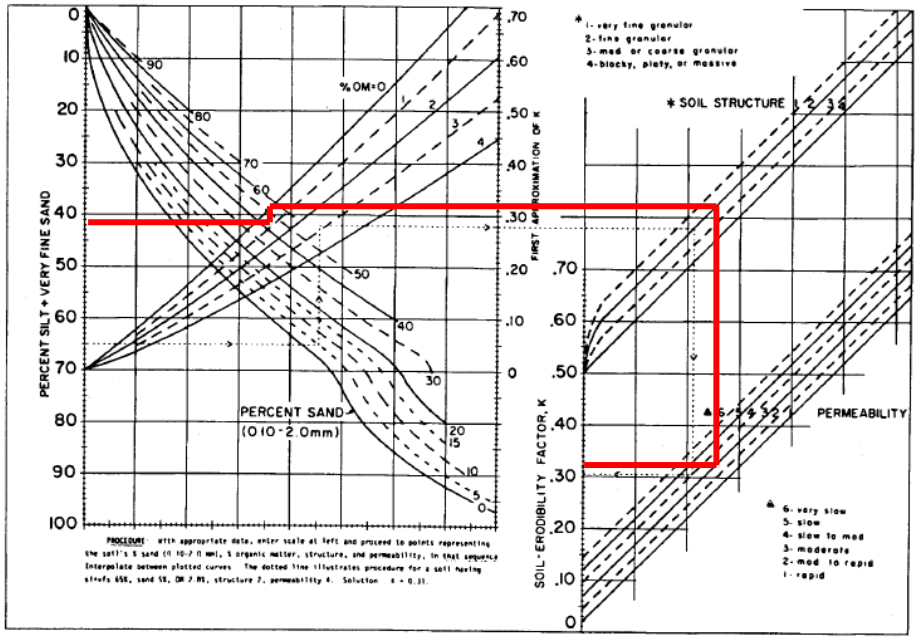

Figure 3-18 Soil-erodibility Nomograph (Agriculture 1997)

The red line shown on Figure 3-18 denotes the estimated *K*-factor for the AU-Loam soil as detailed in Table 3-2. The estimated *K*-factor for the test soil was 0.32.

3.5.4 Length Slope Steepness Factors, *L* and *S*

The slope length factor and slope steepness factor are dimensionless factors related to the topography of a given site and its influence on erosion. The slope length factor, *L*, relates to the

overall length of the slope in question; whereas, the slope steepness factor, *S*, addresses the impact of gradient on erosion. Both factors substantially influence sheet and rill erosion, the factors considered by RUSLE.

The slope length factor is defined by Equations (**11**), (**12**), and (**13**) below.

$$L = \left(\frac{\lambda}{72.6}\right)^{m} \tag{11}$$

$$m = \frac{\beta}{(1+\beta)} \tag{12}$$

$$\beta = \frac{\left(\frac{\sin\theta}{0.0896}\right)}{[3.0(\sin\theta)^{0.8} + 0.56]} \tag{13}$$

where:

L = slope length factor (dimensionless)
λ = horizontal projection of the soil surface slope (ft)
72.6 = the RUSLE unit plot length (ft)
m = a variable slope-length exponent (dimensionless)
β = ratio of rill erosion to interrill erosion (dimensionless)
θ = slope angle

According to RUSLE (Agriculture 1997), in the case of freshly prepared construction slopes, the value calculated for β in Equation (**13**) should be doubled prior to using Equation (**12**) to calculate m.

For the slope steepness factor, *S*, two separate equations are given within RUSLE: the first for slopes less than nine percent and the second where the slope is greater than or equal to nine percent. In the specific case studied herein (slope > 9%), the following equation was used to calculate *S*:

$$S = 16.8\sin\theta - 0.50 \tag{14}$$

where:

S = slope steepness factor (dimensionless)
θ = slope angle

In this study, all test plots have a slope of 3H: 1V, therefore, the slope angle θ is 18.43 degrees, S = 4.813 from Equation 13; β = 1.23 from Equation 12, m = 0.7106 (doubling β for equation 11) , and λ is equal to the plot length times cos θ and then L can be calculated.

3.5.5 Cover Management Factor, *C*

The cover management factor, *C*, within RUSLE is used as a dimensionless ratio to establish the performance of cropping and other management practices on the rate of erosion loss when compared to a standard, in this case a bare soil control plot (Agriculture 1997). Under the premise of testing erosion control products, the *C*-factor is typically calculated, not given, once the *K*-factor for the respective test soil has been established.

3.5.6 Support Practice Factor, P

The support practice factor, *P*, is utilized within RUSLE to account for various soil management practices which may alter the "flow pattern, grade, or direction of surface runoff" (Agriculture 1997). Values have been established within RUSLE through experimental means for various practices commonly found within the agricultural community. For the purpose of the testing conducted within this project, no support practice was installed or evaluated so that P = 1 is used.

3.6 SUMMARY

This chapter provides an overview of the rainfall simulator system design, calibration methodology, and data collection process developed for the large-scale simulator at AU-ESCTF. The testing methods and procedures for capturing the experimental data were also discussed. Modifications of the testing methodology required to complete the s**mall- and** intermediate-scale simulation under the large-scale rainfall simulator were identified.

The rainfall simulator apparatus developed and constructed at the AU-ESCTF can consistently and effectively produce the required rainfall intensities to test various hillslope erosion control materials and practices.

4 RESULTS AND DISCUSSION

4.1 INTRODUCTION

This chapter summarizes and evaluates the experimental results captured through the testing procedures discussed in the previous chapter. The calibration results are presented first for both large- and small-scale test plots. The experimental results of the bare soil control plots for the large-, intermediate-, and small-scale are presented including soil loss, turbidity, discharge, and TSS. The experimental results are also presented for the hydromulch products applied over loam and topsoil, respectively.

4.2 LARGE-SCALE RAINFALL SIMULATION

4.2.1 Calibration Results and Discussion

Calibration experiments were conducted to provide a means to quantify the performance of the rainfall simulator and determine if the apparatus is capable of simulating rainfall with characteristics similar to natural rainfall on a consistent basis. The methods and procedures previously discussed produced a multitude of data in the form of rainfall depth measured from each of the 29 rain gauges after each calibration test.

The data from each test were analyzed to determine the average rainfall intensity and CUC. Finally, the values calculated from the calibration tests for each target rainfall intensity were averaged to provide a generalized report on the performance of the rainfall simulator in terms of experimental rainfall intensity and uniformity of rainfall distribution.

To validate the calibration process, a minimum of ten calibration tests for each intensity were conducted. If the standard deviation was less than or equal to 0.10 in./hr (2.54 mm/hr), testing efforts would proceed to the next interval. A maximum deviation of 0.10 in./hr (2.54 mm/hr) was set as the realistic limit for the simulator performing in a consistent and repeatable fashion. A total

of 30, 15-minute calibration tests were performed. The results from the calibration tests for all test intervals are summarized in Table 4-1.

Table 4-1 Calibration Summary for All Test Intervals

Test Intervals	Average rainfall Intensity, in./hr (mm/hr)	Sample Size	Standard Deviation, in./hr (mm/hr)	Target Intensity, In./hr (mm/hr)	Error (%)
1	2.04 (52.83)	10	0.04 (1.02)	2.0 (50.8)	4.00
2	4.12 (104.65)	10	0.06 (1.52)	4.0 (101.6)	3.00
3	6.07 (154.18)	10	0.07 (1.78)	6.0 (152.4)	1.17

Note: [1]test rainfall intervals are shown on Figure 4-1, 1.0 in. = 25.4 mm.

After analyzing the values in Table 4-1, it was concluded that the rainfall simulator consistently produced rainfall intensities slightly higher than the theoretical target. According to Meyer (1988), the experimental intensities should only vary from the theoretical intensities by a few percent. For the purpose of this study, the benchmark was set at 5.0%. Although the average rainfall intensities were higher than the theoretical target, the standard deviation between the 30 calibration tests was only 0.07 in./hr (1.78 mm/hr). This result ensured that the rainfall simulator was producing repeatable results in terms of rainfall intensity for all test intervals. Figure 4-1 graphically illustrates that the experimental rainfall intensities calculated during calibration were typically slightly higher than the theoretical targets. The intensity produced by the rainfall simulator follows a linear pattern based on the total flow rate in the sprinkler heads. The R^2 value quantifies how accurately the trend line fits the data. With a R^2 value of 0.994, the linear trend line serves as a reliable means for estimating flow rates and corresponding nozzle sizes required to simulate specific rainfall intensities.

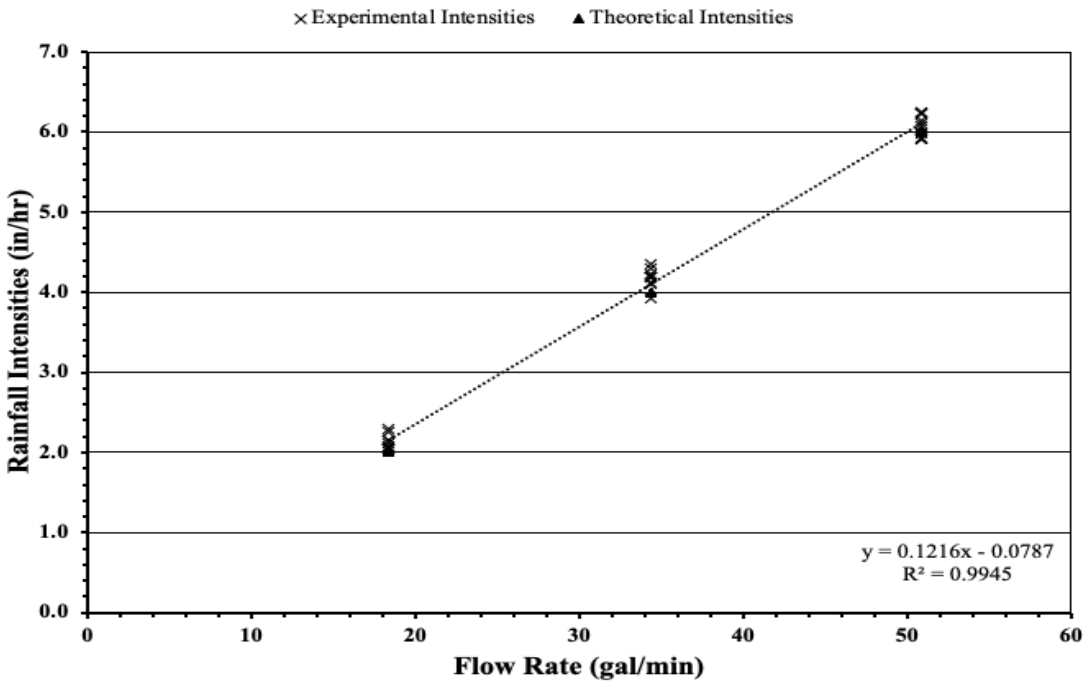

(Note: 1 in./hr = 25.4 mm/hr)

Figure 4-1 Experimental and Theoretical Rainfall Intensities at Different Flow Rates

The average experimental rainfall intensities were used to calculate the *EI* using Equation (**9**) and to compare against theoretical values. *EI* is used in calculating the rainfall-runoff erosivity factor (*R*-factor) used in the RUSLE calculations for expected erosion over a given area. The R-factor is used to quantify the erosive energy of rainfall associated with specific storm events. The results from this analysis are presented in Table 4-2.

Table 4-2 Experimental and Theoretical Erosion Index (EI) Values

Experimental Intensity in./hr (mm/hr)	Target Intensity in./hr (mm/hr)	Experimental Erosion Index (ft-tonf/ac-hr)	Target Erosion Index	Percent Error (%)
2.08 (52.83)	2.0 (50.8)	2,169	2,073	4.60
4.12 (104.65)	4.0 (101.6)	4,510	4,376	3.07
6.07 (154.18)	6.0 (152.4)	6,669	6,592	1.17

The calculated values in Table 4-2 correspond with the results from Figure 4-1. The higher rainfall intensities produced by the rainfall simulator result in greater erosive potential on the test slope. The ensuing result is that higher rates of soil erosion are generated by the simulated rainfall

versus what should be expected from the actual storm event. However, as the rainfall intensities increase, the relative error between the experimental and theoretical values decrease.

To aid in the visualization of the uniformity of rainfall distribution for each test interval, raster surfaces showing rainfall intensity were generated using AutoCAD Civil 3D™ and overlaid on an aerial view of the test plot as shown in Figure 4-2. For each test interval, the rainfall intensities, Figure 4-2 (a), (b), (c), were greatest in the middle of the test plot and lowest at the bottom of the test plot. The average uniformity of rainfall distribution for all tests performed ranged from 87.0 to 87.7%.

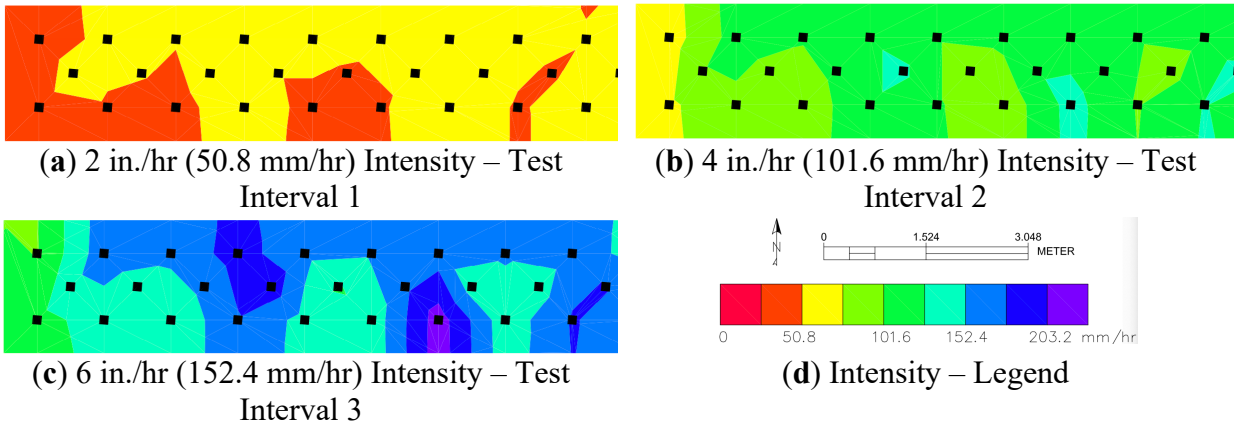

(**a**) 2 in./hr (50.8 mm/hr) Intensity – Test Interval 1

(**b**) 4 in./hr (101.6 mm/hr) Intensity – Test Interval 2

(**c**) 6 in./hr (152.4 mm/hr) Intensity – Test Interval 3

(**d**) Intensity – Legend

Figure 4-2 Rainfall Intensity Raster Surfaces from Calibration Testing

The rain drop diameters produced by the simulator were calculated using the flour pan method. The average drop diameter was then used to calculate the average mass of the rain drops (Table 4-3). At each intensity, the calculated drop diameter was smaller than the theoretical value. Smaller diameter raindrops are produced when pressurized flow is discharged through small nozzle openings.

The values for average drop mass calculated previously were used to determine the experimental kinetic energy generated by the rainfall simulator (Table 4-3). Values for rain drop velocity were estimated based on the diameter of the drop and the height from which the drops fell. In reality, the velocity of the drops is greater than estimated since the drops are projected

from the sprinkler head with an initial outward and downward velocity. However, the actual velocities of raindrops were not quantified in this study.

Table 4-3 Drop Size Distribution Testing and Kinetic Energy of Raindrops

Rainfall Intensity, in./hr (mm/hr)	2.0 (50.8)	4.0 (101.6)	6.0 (152.4)
Average Drop Diameter, in. (mm)	0.094 (2.39)	0.102 (2.58)	0.093 (2.35)
Theoretical Drop Diameter, in. (mm)	0.100 (2.53)	0.113 (2.87)	0.122 (3.09)
Percent Error (%)	5.53	10.10	23.94
Average Drop Mass, lbm (mg)	1.57×10^{-5} (7.13)	1.98×10^{-5} (8.97)	1.49×10^{-5} (6.77)
Velocity of Drop, ft/s (m/s)	20.3 (6.2)	20.7 (6.3)	20.3 (6.2)
Kinetic Energy, lb.-ft^2/s^2 (J)	1.71×10^{-3} (7.24×10^{-5})	1.98×10^{-3} (8.37×10^{-5})	1.66×10^{-4} (7.00×10^{-4})

(Note: 1.0 in. = 25.4 mm)

As shown in Table 4-3 above, the measured average drop diameter (D_{50}, in mm) for each interval was less than the theoretical drop diameters. However, the experimental drop diameters are consistent with other pressurized rainfall simulators as detailed in Bubenzer (1979). As shown in Bubenzer (1979), the median drop diameter for pressured simulators ranged from 0.02 to 0.20 in. (0.6 to 2.6 mm), with the majority of the simulators producing a median drop diameter of 0.08 in. (2.1 mm).

For each rainfall intensity, the kinetic energy of a single raindrop is negligible. However, when combined with the energy of the thousands of other raindrops impacting the slope each second, the summation of this energy would be considerable.

ASTM D6459-19 (ASTM International 2019) is the ASTM International standard test method for determining the performance of rolled erosion control product (RECP) using rainfall simulation. This standard test method is used to quantify rainfall-induced erosion of hillslopes under the protection of RECPs (ASTM International 2019). The test determines the soil erodibility factor, K, of the soil used and the cover management factor, C, of a RECP tested. The data analysis allows for the comparison of C values of different RECPs to understand their relative performance

for controlling erosion. To determine K and C from the Revised Universal Soil Loss Equation (RUSLE), the rainfall-runoff erosivity factor, *R*, must first be determined, which is calculated from the erosion index (*EI*) using Equation (15) (Agriculture 1997):

$$R = \frac{1}{n}\sum_{j=1}^{n}[\sum_{k=1}^{m} EI_k] \tag{15}$$

where:

R = Rainfall Erosivity Factor
EI_k = erosion index for the rainfall event *k*
m = total number of the rainfall events in a year
n = number of years used to obtain average *R* in hundreds of ft·tonf·in./(acre·hr·yr)
E = total storm energy (hundreds ft·tonf/acre)
I_{30} = maximum 30-minute intensity for a given storm event (in./hr)

The total storm energy, *E,* is the total kinetic energy of all raindrops of the storm and directly related to the rainfall intensity. Since *R* is the average erosivity potential from a known set of storm events over a known period of time, each storm within that time period must be individually analyzed using Equation (16) to determine erosivity for each storm event:

$$EI = (E)I_{30} = \left(\sum_{r=1}^{p} e_r \Delta V_r\right) I_{30}(10^{-2}) \tag{16}$$

where:

e_r = rainfall energy per unit depth of rainfall per unit area (ft·tonf/acre·in)
ΔV_r = depth of rainfall for the *r*th increment of the storm hyetograph which is divided into *p* parts

For natural rainfall events, each raindrop reaches its terminal velocity when reaching the ground, and e_r can be calculated as a function of rainfall intensity i_r (in./hr) using Equation (17) in the United States (Agriculture 1997):

$$e_r = 1099[1 - 0.72exp(-1.27i_r)] \; and \; i_r = \Delta V_r / \Delta t_r \qquad (17)$$

For large-scale testing in ASTM D6459-19, evaluations for each RECP are repeated three times, therefore, an annual *R* cannot be developed, only an average *EI* and *C* for three tests are determined for comparing the relative performance of different RECPs. ASTM D6459-19 suggests using Equation (18) to compute *EI* (ASTM International 2019):

$$EI = I \times 1099 \times \left[1 - 0.72e^{(-1.27I)}\right] \qquad (18)$$

ASTM D6459-19 does not provide any specific details to apply Equation (18) but refers to the U.S. Department of Agriculture (USDA) Agriculture Handbook 703 (Agriculture 1997). Equation (18) as described by ASTM D6459-19 misrepresents the original Equations (16) and (17) since there are two *I*s in Equation (18) that represent two different intensities: the first *I* represents I_{30} and the second *I* is intended to represent i_r for the *r*th increment of the storm hyetograph. Also, when using the rainfall simulator (not natural rainfall), each rainfall drop may not reach its terminal velocity and the unit rainfall energy, e_r, cannot be calculated using Equation (17) or (18) directly. In this study, we will discuss the use of the original method in the USDA Agriculture Handbook 703 (Agriculture 1997) to directly compute the erosion index for the large-scale test.

As discussed in Faulkner (2020), the total storm energy from the rainfall simulator was calculated using the drop size information obtained during the calibration testing. A summary of the data is provided in Table 4-4, below.

Table 4-4 Rainfall Simulator Storm Energy (Faulkner 2020)

Rainfall Intensity	2 in./hr (50.8 mm/hr)	4 in./hr (101.6 mm/hr)	6 in./hr (152.4 mm/hr)	Total
Kinetic Energy Rainfall (ft-lbf)	8,729 (1204.6)	17,704 (2,443)	24,266 (3,349)	50,699 (6,996)
Total Storm Energy (ft-tonf/acre)	594 (4.05×10^5)	1,205 (8.22×10^5)	1,652 (1.13×10^6)	3,451 (2.35×10^6)

Note: 1 ft-lbf = 0.138 m-kg
1 ton-ft/acre = 682 kg-m/ha

The maximum thirty-minute rainfall intensity, I_{30}, was calculated using the experimental rainfall intensities of 4.12 and 6.07 in./hr (105 and 154 mm/hr). The I_{30} was determined to be 5.42 inches (138 mm). The experimental rainfall-runoff erosivity factor, R, was then calculated using Equation (**9**) to be 187.

4.2.2 Use of the Erosion Index Equation for Simulated Rainfall

It should be considered that the erosion index described in Equation (16 was developed from analyzing soil erosion resulting from years of naturally occurring rainfall events. This results in an assumption of naturally occurring drop size distribution and the raindrops falling at terminal velocity. For predicting naturally occurring erosion rates based upon this Equation, these assumptions are relatively valid for in-field conditions. However, for synthetic rainfall produced by rainfall simulators, these conditions are difficult to create. For instance, based upon Figure 3-10, a 0.12 in. (3.0 mm) raindrop has to fall approximately 52.5 ft (16.0 m) in a wind-free environment before reaching terminal velocity. ASTM D6459-19 only requires a minimum fall height of 14.0 ft (4.26 m). The nearest drop size plotted for this height in Figure 3-10 is 0.05 in. (1.17 mm) drop diameter, which is smaller than the average drop size produced by most rainfall simulators used for erosion testing. This issue is addressed in ASTM D 6459-19, but only minimally. After calculating the erosion index using Equation (16, the standard specifies that the results of this calculation must then be corrected for the kinetic energy of the drops that are falling at less than terminal velocity. Since no further guidance in the standard is provided for correcting the results of Equation (16, it is left to the user to determine how to adjust.

However, adjusting the output of Equation (16 as the ASTM standard stipulates may not be necessary and potentially improper. It can be seen from this previous discussion that intensity is the correlative variable that helps define the energy of a naturally occurring storm event using

Equations (15, (16, and (17. However, should "correcting Equation (16 for kinetic energy" be performed since the simulators are not producing naturally occurring rainfall energy? The point of using Equations (15, (16, and (17 is to bypass determining the kinetic energy of each storm directly by using intensity as a means of estimating energy. To be able to adjust *EI* from Equation (16, the kinetic energy from the simulated storm must be known. Therefore, since the storm is not naturally occurring and may not be adequately represented by Equation (16, it may be more prudent to simply use the kinetic energy calculations from Equation 9 and directly calculate EI_{30} using the simulator's actual measured kinetic energy, instead of correcting Equation (16 that represents naturally occurring kinetic energy. These concepts require further evaluation and research, which is beyond the scope of this paper.

4.2.3 Bare Soil Control Testing

The purpose of this section is to provide a summary of the relevant collected results from the large-scale test plots that were conducted in the previous research. Additional details and information can be found in Faulkner (2020). Figure 4-3, Figure 4-4, and Figure 4-5 show photos of three repeated bare soil tests taken at the end of each 20-minute testing interval when the rainfall intensity was 2 in./hr, 4 in./hr, and 6 in./hr (50.8, 101.6, and 152.4 mm/hr), respectively.

The first data captured during the tests were the discharge of runoff from the plot. The runoff consisted of both excess water as well as eroded sediment. The discharge per unit time is shown in Figure 4-6 below. As shown below, the discharge from each plot generally followed the same upward projection throughout the test.

As shown in Figure 4-3 at the completion of the first rainfall interval, small rills have begun to form on the lower reaches of the plot. As is consistent with this type of erosion, rills are generally

parallel along a slope and are uniform in spacing and dimension (Service n.d.). This is distinctly shown in Figure 4-3 (c).

Figure 4-4 details the condition of the slope at the end of the second rainfall interval. At that particular time interval, the rills have increased in depth and now classic gully erosion is present. A review of the video available for these tests indicate that gully erosion begins to occur at approximately 38 minutes into the overall test (t = 38 min.). There is however one interval which warrants further discussion. At the beginning of the second rainfall interval (t = 22 min), there is a marked increase in discharge rate over the previously measured value. This is likely the point in time that the surface area of the test plot becomes saturated due to rainfall received during the first interval of the test storm. This time also coincides with the increase in rainfall intensity to 4 in./hr. The increase in total storm energy for the second interval nearly doubles when compared to the first interval (Table 4-4). This increase in energy contributes to additional displacement of soil due to the impact of raindrops. The increase in dislodged soil particles in conjunction with the saturation of the soil surfaces causes the excess runoff to accelerate down the slope thereby increasing the likelihood that soil particles will be transported down the surface of the slope. This would indicate that the length of the slope should be directly related to the volume of sediment removed from the slope.

Significant gully erosion is present at the conclusion of the third rainfall interval as detailed in Figure 4-5. Gully erosion is present for the length of the erosion test plot except for the uppermost section. The excess runoff in this region of the plot has likely not reached an erosive velocity capable of transporting the dislodged soil particles.

(a) Test 1

(b) Test 2

(c) Test 3

Figure 4-3 Bare Soil Plots for Loam Soil at Conclusion of First Rainfall Interval (2 in./hr [50.8 mm/hr])

(a) Test 1

(b) Test 2

(c) Test 3

Figure 4-4 Bare Soil Plots for Loam Soil at Conclusion of Second Rainfall Interval (4 in./hr [101.6 mm/hr])

(a) Test 1

(b) Test 2

(c) Test 3

Figure 4-5 Bare Soil Plots for Loam Soil at Conclusion of Third Rainfall Interval (6 in./hr [152.4 mm/hr])

In addition to capturing the soil loss from each plot, depth loggers were placed within the catch basin to measure the total discharge from the plot including excess runoff and dislodged soil. The volume was recorded every two minutes throughout the duration of the test and is provided below in Figure 4-6.

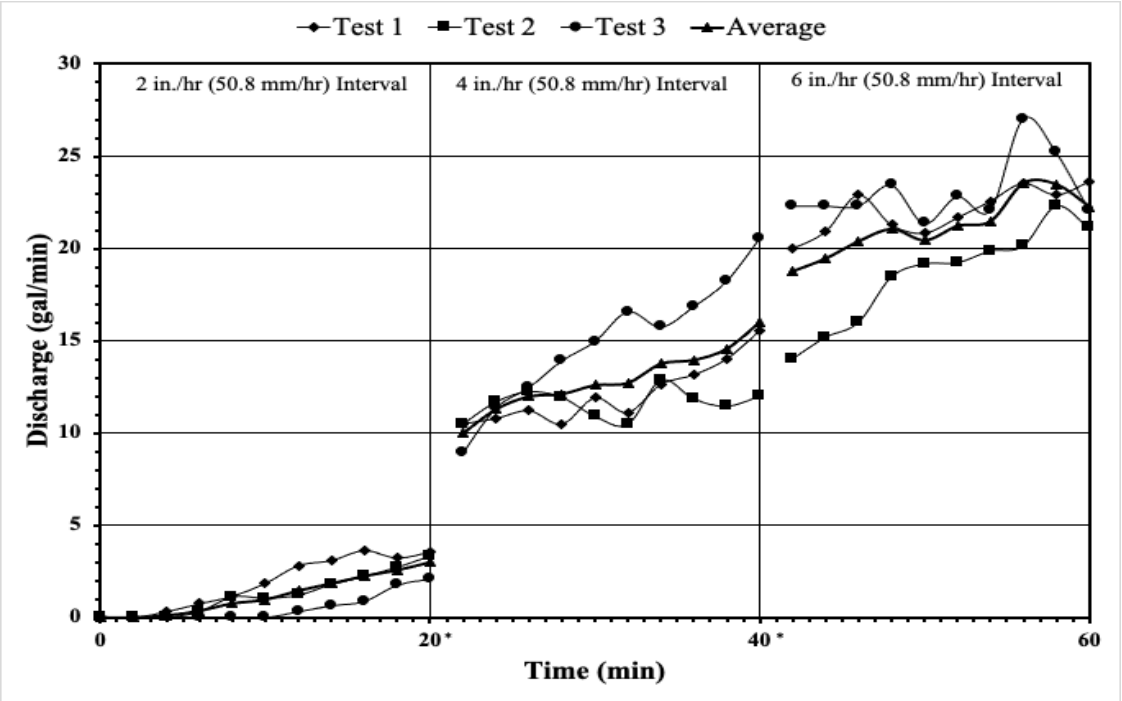

('*'- Denotes 15-minute rest interval for data collection)

Figure 4-6 Discharge Over Time for Large-Scale Bare Soil Plots

The sediment basins were allowed to settle for a minimum of 24 hours before the excess water was removed and measurements taken for the total soil loss as described above. The soil loss for each bare soil control test is shown in Table 4-5 below. The average soil loss for the overall tests was 2,333 pounds (1,058 kg) or 317,580 pounds per acre (355,960 kg/ha). As shown in the table below, there was a significant increase in the amount of soil loss in the plots from the 2 inch per hour interval (50.8 mm/hr) to the 4 inch per hour interval (101.6 mm/hr). The average soil loss for the 2 inch per hour interval (50.8 mm/hr) was only 43 pounds (19.5 kg) (5,853 lb./ac [6,560 kg/ha]); whereas, the average soil loss for the 4 inch per hour interval (101.6 mm/hr) was 775 pounds (352 kg) (105,497 lb./ac [118,246 kg/ha]). The 6 inch per hour interval produced an average soil loss of 1,515 pounds (687 kg) (206,229 lb./ac [231,152 kg/ha]).

Table 4-5 Total Soil Loss in Each Rainfall Interval and Over the Whole Event for Large-Scale Bare Soil Plots

Test Parameters	Test 1	Test 2	Test 3	Average
Rainfall Depth, in (mm)	4.05 (102.9)	4.03 (102.4)	4.07 (103.4)	4.05 (102.9)
Compaction (%)	89.61	86.83	89.27	88.40
Moisture Content (%)	23.86	19.33	20.01	21.07
2 in. per hr Soil Loss, lb. (kg)	54 (24.5)	65 (29.5)	11.1 (5.0)	43.4 (19.7)
4 in. per hr Soil Loss, lb. (kg)	683 (310)	938 (426)	704 (319)	775 (352)
6 in. per hr Soil Loss, lb. (kg)	1,509 (685)	1,347 (611)	1,689 (766)	1,515 (687)
Total Collected Sediment, lb. (kg)	2,246 (1,019)	2,350 (1,066)	2,404 (1,090)	2,333 (1,058)

(Note: 1 inch = 25.4 millimeters, 1 pound = 0.45 kilograms)

After each bare soil test was completed, the water samples collected in 3-minute intervals were allowed to settle for a minimum of 24 hours in the refrigerator and then taken to the laboratory for analysis as described above. The results for the turbidity and total suspended solids are provided in Figure 4-7 and Figure 4-8 below.

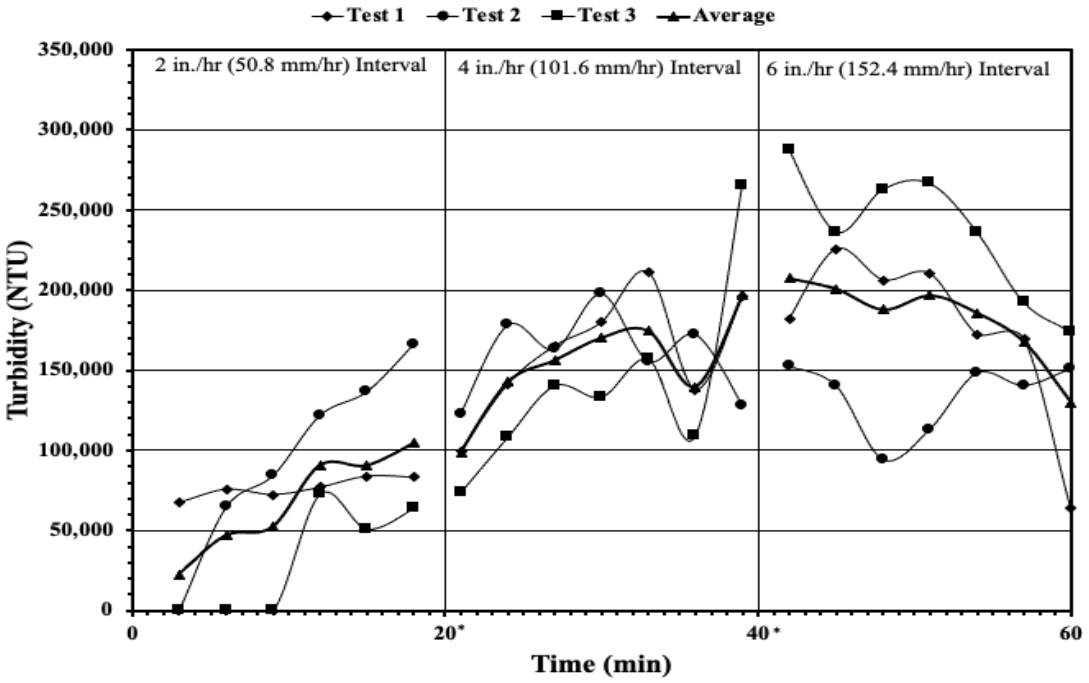

('*' – Denotes 15-minute rest interval for data collection)

Figure 4-7 Turbidity for Large-Scale Bare Soil Plots

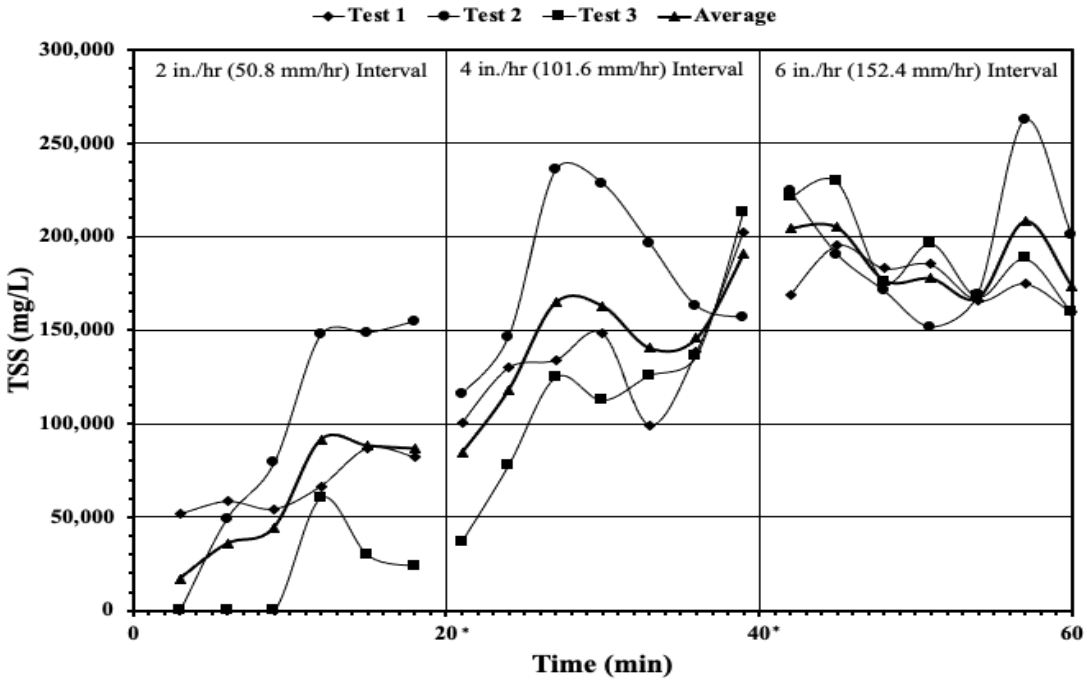

('*' – Denotes 15-minute rest interval for data collection)

Figure 4-8 Total Suspended Solids for Large-Scale Bare Soil Plots

4.2.4 Hydromulch Testing over Loam

Upon completion of each bare soil test, a series of three hydromulch tests were conducted for each product. The average values for the soil loss from the large-scale plots are provided in Table 4-6 below based on three repeated tests. As expected, the hydromulch products provided for significant reductions in total soil loss from the plots when compared to the bare soil control tests. Although all of the hydromulch products exhibited a significant reduction in soil loss when compared to the bare soil control plots, the percent reduction varies significantly by the intensity. Most notably, the hydromulch products exhibited a significant reduction in soil loss for the first rainfall interval (ranging from 80 to 94 percent); however, for the second and third rainfall intervals, the percent reductions dropped significantly to 37 to 61 percent and 47 to 53 percent,

respectively. This is reflected in the turbidity measurements shown in Figure 4-9 and the TSS measurements shown in Figure 4-10.

Table 4-6 Average Soil Loss Results for Hydromulch Products

Rainfall Simulator Data Summary	Bare Soil	EcoFibre	Terrawood	Soil Cover
Rainfall Depth, in (mm)	4.05 (102.9)	4.04 (102.6)	4.06 (103.1)	4.04 (102.6)
Percent Compaction (%)	88.4	87.32	87.47	87.55
Moisture Content (%)	21.07	21.82	19.55	20.39
2 in./hr (50.8 mm/hr) Soil Loss, lb. (kg)	43.4 (19.7)	3.45 (1.56)	8.54 (3.87)	2.67 (1.21)
4 in./hr (101.6 mm/hr) Soil Loss, lb. (kg)	775 (352)	304 (138)	488 (221)	382 (173)
6 in./hr (152.4 mm/hr) Soil Loss, lb. (kg)	1,515 (687)	717 (325)	797 (362)	779 (353)
Total Soil Loss, lb. (kg)	2,333 (1,058)	1,024 (465)	1,293 (587)	1,164 (528)

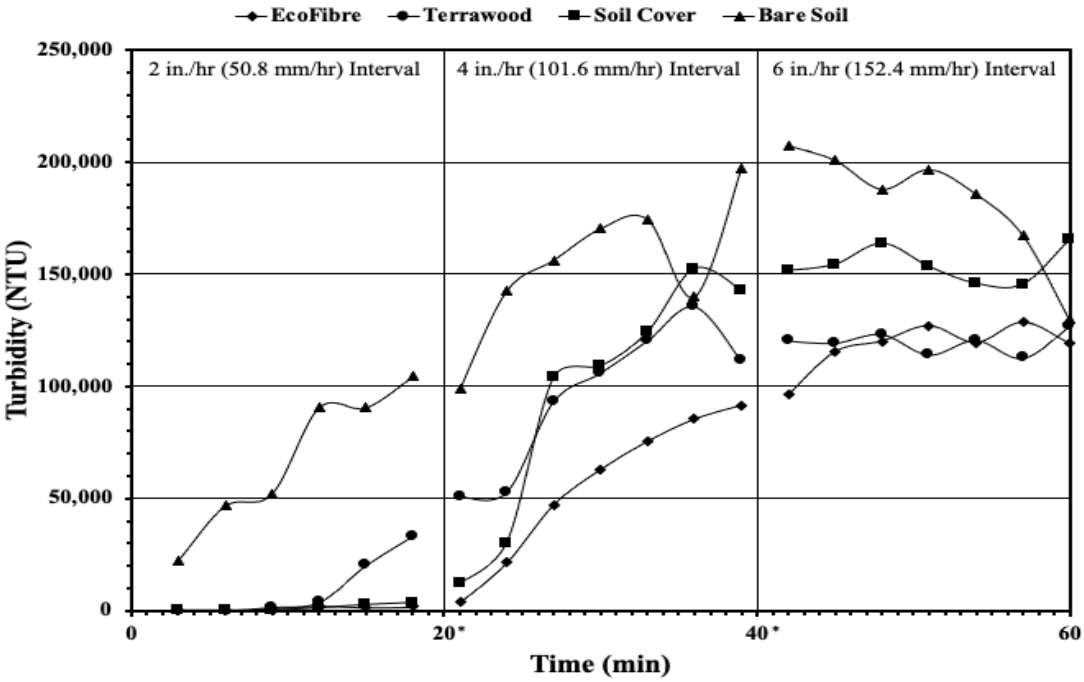

('*' – Denotes 15-minute rest interval for data collection)

Figure 4-9 Average Turbidity for Hydromulch Products

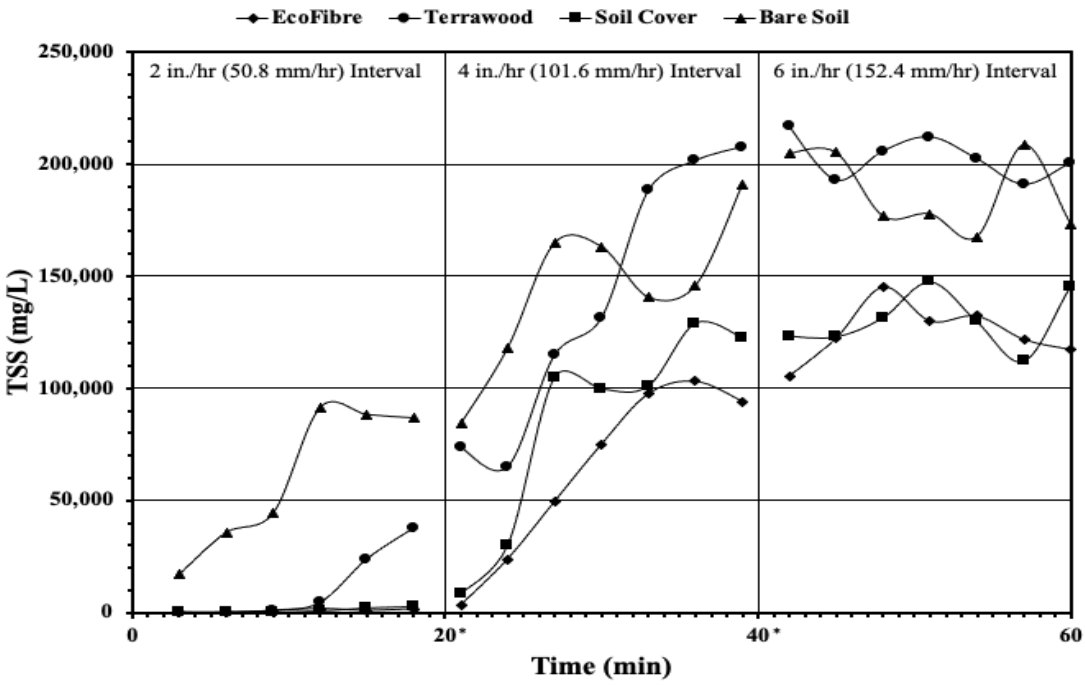

('*' – Denotes 15-minute rest interval for data collection)

Figure 4-10 Average Total Suspended Solids for Hydromulch Products

Figure 4-11 below details the large-scale testing plot at the completion of the first rainfall interval (2 in./hr) for the EcoFibre HM. At this point in time, there is little evidence of soil transportation when compared to the bare soil plots in Figure 4-3. The bare soil plots were beginning to show signs of the development of rill erosion, however, the EcoFibre test plots were not having rill erosion yet, but small percent of EcoFibre covered on the soil (< 5%) started to be washed off from the slope, especially, at the bottom portion.

(a) Test 1

(b) Test 2

(c) Test 3

Figure 4-11 Photographs of EcoFibre HM after First Rainfall Interval (2 in./hr [50.8 mm/hr])

Figure 4-12 details the EcoFibre HM product at the completion of the second rainfall interval (4 in./hr [101.6 mm/hr]). During the second rainfall interval, rill erosion begins to form and by the end of the interval, significant rill erosion is present; at the same time, much more EcoFibre (approximately 70%) was washed off from the slope.

(a) Test 1

(b) Test 2

(c) Test 3

Figure 4-12 Photographs of EcoFibre HM after Second Rainfall Interval (4 in./hr [101.6 mm/hr])

Figure 4-13 details the EcoFibre HM product at the completion of the third rainfall interval (6 in./hr). During the third rainfall interval, rill erosion continues to become more prevalent and by the end of the interval, early signs of gully erosion is present, particularly near the lower portion of the test plot. Some patches of the slope (approximately 20%) were still covered with EcoFibre and did not contribute much to soil loss (splash and sheet-flow erosion).

(a) Test 1

(b) Test 2

(c) Test 3

Figure 4-13 Photographs of EcoFibre HM after Third Rainfall Interval (6 in./hr [152.4 mm/hr])

Figure 4-14 below details the large-scale testing plot at the completion of the first rainfall interval (2 in./hr) for the SoilCover HM. At this point in time, there is little evidence of rill erosion, similar to the EcoFibre HM plots.

(a) Test 1

(b) Test 2

(c) Test 3

Figure 4-14 Photographs of SoilCover HM after First Rainfall Interval (2 in./hr [50.8 mm/hr])

Figure 4-15 details the SoilCover HM product at the completion of the second rainfall interval (4 in./hr). During the second rainfall interval, rill erosion begins to form and by the end of the interval, significant rill erosion is present in two of the tests.

(a) Test 1

(b) Test 2

(c) Test 3

Figure 4-15 Photographs of SoilCover HM after Second Rainfall Interval (4 in./hr [101.6 mm/hr])

Figure 4-16 details the SoilCover HM product at the completion of the third rainfall interval (6 in./hr). During the third rainfall interval, rill erosion continues to become more prevalent and by the end of the interval, signs of gully erosion is present, essentially beginning near the midpoint of the test plot.

(a) Test 1

(b) Test 2

(c) Test 3

Figure 4-16 Photographs of SoilCover HM after Third Rainfall Interval (6 in./hr [152.4 mm/hr])

Figure 4-17 below details the large-scale testing plot at the completion of the first rainfall interval (2 in./hr) for the Terrawood HM. For two of the test plots, there is little evidence of rill erosion at this point in time. However, for Test 3, there is evidence of rill erosion, particularly on the lower portion of the test plot.

(a) Test 1

(b) Test 2

(c) Test 3

Figure 4-17 Photographs of Terra-wood HM after First Rainfall Interval (2 in./hr [50.8 mm/hr])

Figure 4-18 details the Terrawood HM product at the completion of the second rainfall interval (4 in./hr). During the second rainfall interval, rill erosion has now begun to form on three test plots for three repeated tests, similar to the other HM products tested.

(a) Test 1

(b) Test 2

(c) Test 3

Figure 4-18 Photographs of Terra-wood HM after Second Rainfall Interval (4 in./hr [101.6 mm/hr])

Figure 4-19 details the Terrawood HM product at the completion of the third rainfall interval (6 in./hr). During the third rainfall interval, the progression of rill erosion continues and by the end of the interval, signs of gully erosion is present.

(a) Test 1

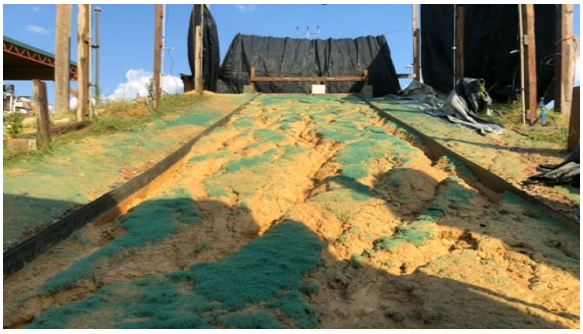

(b) Test 2

(c) Test 3

Figure 4-19 Photographs of Terra-wood HM after Third Rainfall Interval (6 in./hr [152.4 mm/hr])

From a visual assessment, all three hydromulch products performed well during the first rainfall interval (2 in./hr) with little evidence of rill erosion. However, during the second rainfall interval (4 in./hr), the amount of rill erosion increased dramatically. This phenomenon is corroborated by a marked increase in turbidity and TSS during the second rainfall interval as well. This information suggests that the hydromulch products with tackifier function well under rainfall events of less than 2 in./hr intensity. As hydromulch is typically used to provide a temporary ground cover which enables a more permanent grassing alternative to establish root, the evidence herein supports that intention.

4.3 SMALL-SCALE AND INTERMEDIATE-SCALE TEST PLOTS

4.3.1 Calibration Results

For testing the small-scale and intermediate-scale plots under the large-scale rainfall simulator, a calibration process was initiated similar to the process for the large-scale simulation.

Various locations were tested throughout the area of the rainfall simulator until five final locations were chosen. A minimum of ten calibration tests were completed for each rainfall interval. A maximum standard deviation of 0.10 inches was allowed. The results from the calibration tests for all three test intervals are summarized in Table 4-7, below. Average rainfall intensity was determined over ten repeated calibration runs. Average CUC for each test interval was determined from five test-plot locations and over ten repeated calibration runs.

Table 4-7 Calibration Results for Small-Scale Test Plots

Test Interval	Average Rainfall Intensity, in./hr (mm/hr)	Average CUC (%)	Sample Size	Standard Deviation, in (mm)	Target Intensity, in./hr (mm/hr)	Percent Error for Intensity
1	1.9 (48.3)	84.1	10	0.09 (2.29)	2 (50.8)	5.0%
2	4.0 (101.6)	90.9	10	0.10 (2.54)	4 (101.6)	0.0%
3	6.0 (152.4)	95.1	10	0.09 (2.29)	6 (152.4)	0.0%

Once the small-scale locations were determined, raindrop size tests were conducted utilizing the flour pan method described earlier to determine the total energy of the rainfall at each specific location. Due to the number of small-scale plots tested simultaneously, two plot locations were selected using the criteria of similar total energy of the large-scale plots to measure turbidity and TSS. Table 4-8 below provides a summary of the kinetic energy calculations for the small-scale plots. Plot location 4 was selected as the primary bare soil control plot test location due to the similar rainfall energy values when compared to the average large-scale plots. Plot location 5 was selected as the product test location for measurement of turbidity and TSS. All other plot locations were used to measure total runoff volume and volume of soil loss, respectively.

Table 4-8 Kinetic Energy Calculations from Raindrop Data for Small-Scale Plots

Location	$KE_{rainfall}$, ft-lbf (J)	$KE_{totalrainfall}$, ft-tonf (kJ-m)	Total Energy (ft-tonf/acre)	% Different $KE_{totalrainfall}$	%Different – Total Energy
Large-Scale Average		25.45 (69.01)	3,464 (23,213)	-	-
Plot 1	40,303 (54,644)	20.15 (54.64)	2,743 (18,383)	-20.81%	-20.81%
Plot 2	36,677 (49,727)	18.34 (49.73)	2,496 (16,727)	-27.93%	-27.93%
Plot 3	55,955 (75,865)	27.98 (75.87)	3,808 (25,519)	9.95%	9.95%
Plot 4	50,097 (67,923)	25.05 (67.93)	3,410 (22,852)	-1.57%	-1.56%
Plot 5	47,834 (64,854)	23.92 (64.86)	3,256 (21,820)	-6.01%	-6.01%

4.3.2 Bare Soil Results

For the small- and intermediate-scale test plots, similar results were taken as compared to the large-scale rainfall simulations. For each respective test, measurements were taken for total runoff and total soil loss for each plot; in addition to turbidity and TSS measurements taken from the bare soil control plots and a single hydromulch plot for each product tested during the small-scale testing.

As shown in Table 4-9, the average moisture content for the small-scale (2 feet by 4 feet [0.6 m by 1.2 m]) bare soil control plots was 20.3 percent. The average compaction was determined to be 81.6 lbm/ft^3 (1307 kg/m^3). The total soil loss measured for the 2 inch (50.8 mm) rainfall interval was 0.051 lb. (23 grams); for the 4 inch (101.6 mm) rainfall interval was 0.216 lb. (98 grams); and the 6 inch rainfall (152.4) interval was 2.31 lb. (1,049 grams). This equates to an overall total soil loss of 2.58 lb. (1,171 grams). Of the three bare soil control tests, Test 1 resulted with the highest soil loss, which was significantly higher than the other two test plots. The only significant difference between the three small-scale test plots was the moisture content. The test plot from Test 1 also had the highest moisture content for the small-scale test plots. In reviewing the runoff

volumes by time for each test plot (Table 4-10) Test 1 began to experience runoff from the plot at 9 minutes into the first rainfall interval (t = 9) when rainfall was still 2 in./hr (50.8 mm.hr); whereas, Tests 2 and 3 did not register any excess runoff until 24 minutes into the test (t = 24) when rainfall became 4 in./hr (101.6 mm/hr).

Table 4-9 Total Soil Loss for Small-Scale Bare Soil Plots.

	Test 1	Test 2	Test 3	Average
Compaction, lbm/ft^3 (kg/m^3)	85.7 (1,373)	82.1 (1,315)	77.1 (1,235)	81.6 (1307)
Moisture Content, %	23.7	17.4	19.9	20.3
Soil Loss 2 in./hr (50.8 mm.hr) interval, lb. (g)	0.137 (62)	0.00882 (4)	0.00882 (4)	0.051 (23)
Soil Loss 4 in./hr (101.6 mm/hr) interval, lb. (g)	0.425 (193)	0.090 (41)	0.132 (60)	0.216 (98)
Soil Loss 6 in./hr (152.4 mm/hr) interval, lb. (g)	2.79 (1,267)	2.20 (1,000)	1.94 (881)	2.31 (1,049)
Total Soil Loss, lb. (g)	3.36 (1,522)	2.30 (1,045)	2.08 (945)	2.58 (1,171)

Turbidity and TSS summary data are provided in Figure 4-20 and Figure 4-21. Similar to the measured soil loss data, Test 1 resulted in the highest readings for turbidity as well as TSS. As expected, both measures increased with time; however, the measures decreased sharply as the final rainfall interval ended. The flow length (and subsequent time of concentration) of the watershed likely influenced these changes in values.

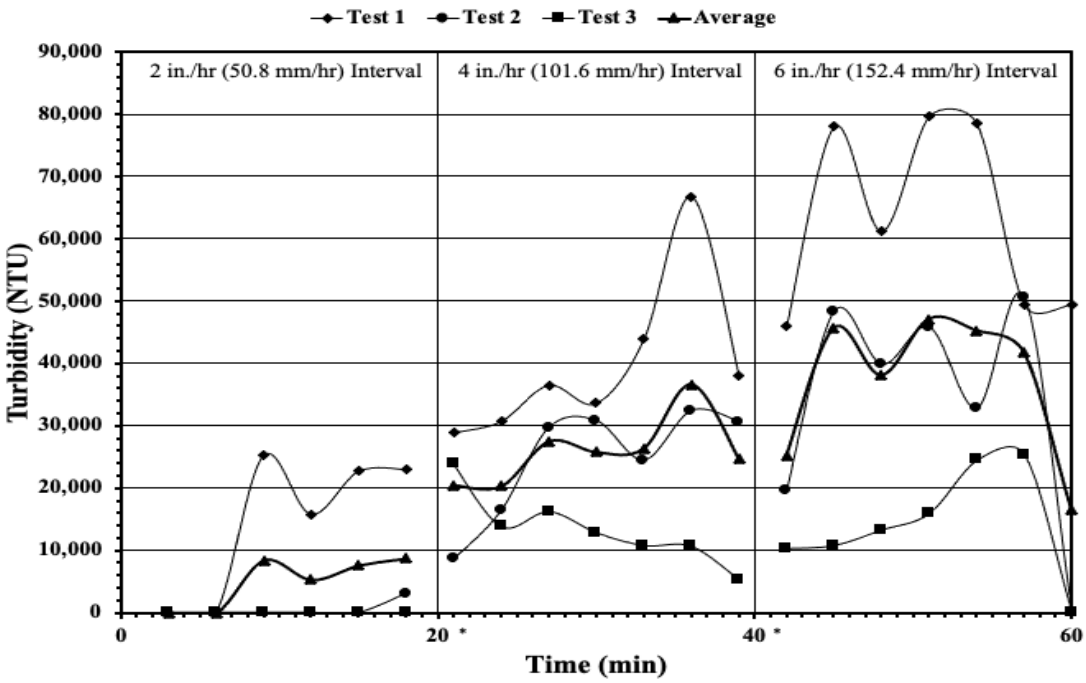

('*' – Denotes 15-minute rest interval for data collection)

Figure 4-20 Turbidity for Small-Scale Bare Soil Control Plots

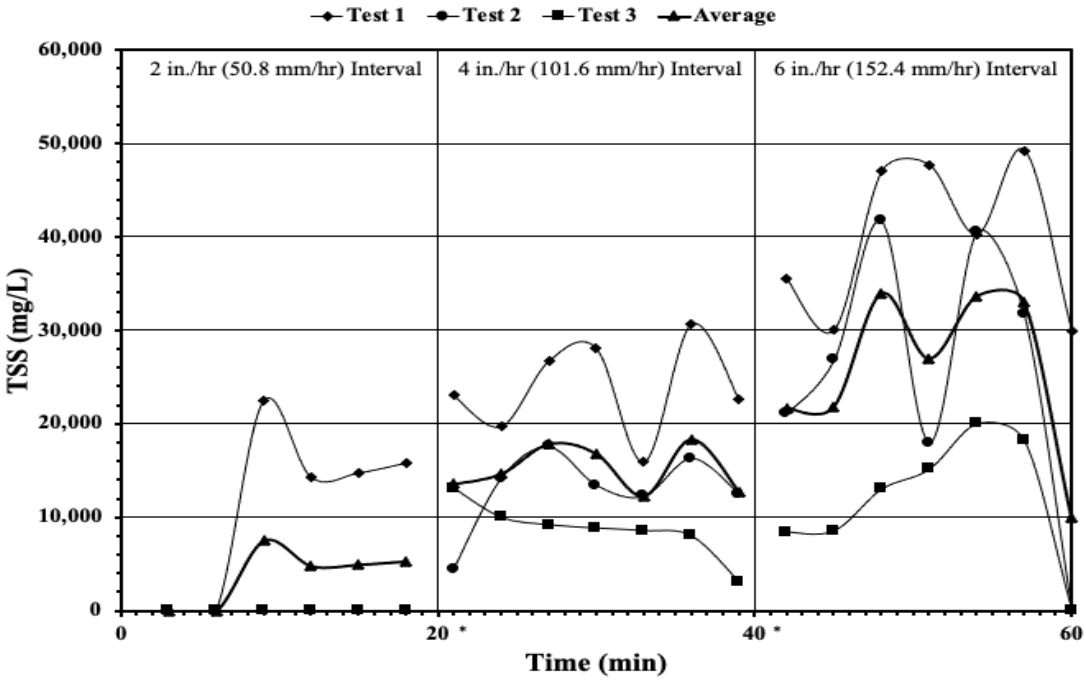

('*' – Denotes 15-minute rest interval for data collection)

Figure 4-21 TSS for Small-Scale Bare Soil Control Plots

Table 4-10 Runoff Volume by Time for Small-Scale Bare Soil Plots

Test Time, min	Bare Soil Plot 1, ft^3 (L)	Bare Soil Plot 2 ft^3 (L)	Bare Soil Plot 3 ft^3 (L)
0	0.00	0.00	0.00
3	0.00	0.00	0.00
6	0.00	0.00	0.00
9	0.02 (0.65)	0.00	0.00
12	0.05 (1.3)	0.00	0.00
15	0.06 (1.79)	0.00	0.00
18	0.09 (2.63)	0.00	0.00
20	0.11 (3.13)	0.00	0.00
21	0.02 (0.65)	0.00	0.00
24	0.09 (2.63)	0.06 (1.79)	0.02 (0.65)
27	0.16 (4.49)	0.13 (3.64)	0.06 (1.79)
30	0.24 (6.76)	0.15 (4.32)	0.13 (3.64)
33	0.29 (8.19)	0.28 (7.83)	0.15 (4.32)
36	0.36 (10.2)	0.35 (10.02)	0.15 (4.32)
39	0.42 (11.89)	0.41 (11.51)	0.18 (5.01)
40	0.42 (11.89)	0.43 (12.08)	0.19 (5.35)
42	0.09 (2.63)	0.09 (2.63)	0.04 (1.14)
45	0.19 (5.35)	0.18 (5.01)	0.07 (1.96)
48	0.29 (8.19)	0.28 (7.83)	0.13 (3.64)
51	0.39 (11.13)	0.39 (11.13)	0.18 (5.01)
54	0.5 (14.1)	0.49 (13.81)	0.2 (5.7)
57	0.59 (16.84)	0.53 (15.11)	0.26 (7.47)
60	0.63 (17.89)	0.63 (17.78)	0.29 (8.19)

As shown in Figure 4-22, no presence of rill erosion is exhibited at the end of the first rainfall interval (2 in./hr [50.8 mm/hr]). This is incongruous with the large-scale plots. The soil visually appears to be becoming saturated, but as stated previously, only Test 1 registered any excess runoff during the first rainfall interval.

(a) Test 1

(b) Test 2

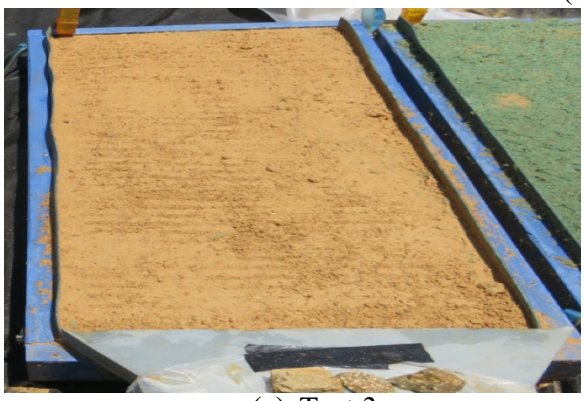

(c) Test 3

Figure 4-22 Photographs of Small-Scale Bare Soil Plots after First Rainfall Interval (2 in./hr [50.8 mm/hr])

Figure 4-23 shows the bare soil control plots at the end of the second rainfall interval (4 in./hr [101.6 mm/hr]). No evidence of rill erosion is present for this interval; however, flow patterns are beginning to visibly form on the lower reaches of the Test 1 plot.

(a) Test 1

(b) Test 2

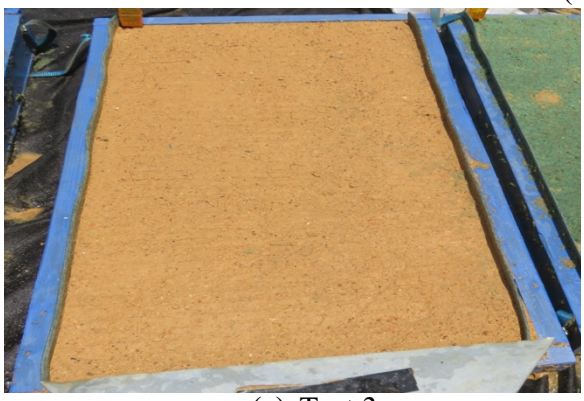

(c) Test 3

Figure 4-23 Photographs of Small-Scale Bare Soil Plots after Second Rainfall Interval (4 in./hr [101.6 mm/hr])

Figure 4-24 details the bare soil control plots after the conclusion of the third rainfall interval. Rill erosion is beginning to occur, most noticeably on the plot from Test 1.

(a) Test 1

(b) Test 2

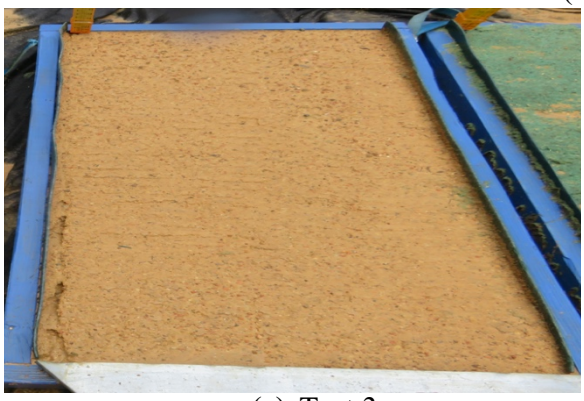

(c) Test 3

Figure 4-24 Photographs of Small-Scale Bare Soil Plots after Third Rainfall Interval (6 in./hr [152.4 mm/hr])

As shown in Table 4-11, the average moisture content for the intermediate-scale (4 feet by 8 feet [1.2 m by 2.4 m]) bare soil control plots was 21.6 percent. The average compaction was determined to be 80.5 lbm/ft^3 (1,289 kg/m^3). The average soil loss measured for the 2 in./hr (50.8 mm/hr) rainfall interval was 0.0838 lb. (38 grams); for the 4 in./hr (101.6 mm/hr) rainfall interval was 4.11 lb. (1,865 grams); and the 6 in./hr (152.4 mm/hr) rainfall interval was 58.6 lb. (26,569 grams). This equates to an overall average total soil loss of 62.8 lb. (28,472 grams). Of the three bare soil control tests, Test 3 resulted with the highest soil loss, which was significantly higher than the other two test plots. The only significant difference between the three intermediate-scale test plots was the moisture content. The moisture content for Test 3 was 23.9 percent, compared to 19.7 and 21.3 percent for Tests 1 and 2, respectively. The increased soil loss in the test plot with

the highest moisture content is consistent with the bare soil results from the small-scale testing. This would suggest that the antecedent moisture condition of a test plot may have a higher impact on plots of smaller scale than corresponding plots of larger scale.

Table 4-11 Total Soil Loss for Intermediate-Scale Bare Soil Plots.

	Test 1	Test 2	Test 3	Average
Compaction, lbm/ft^3 (kg/m^3)	80.2 (1,285)	83.6 (1,339)	77.8 (1,246)	80.5 (1,289)
Moisture Content, %	19.7	21.3	23.9	21.6
Soil Loss 2 in./hr (50.8 mm/hr) interval , lb. (g)	0.157 (71)	0.0441 (20)	0.0485 (22)	0.0838 (38)
Soil Loss 4 in./hr (101.6 mm/hr) interval, lb. (g)	3.73 (1,690)	2.65 (1,201)	5.96 (2,704)	4.11 (1,865)
Soil Loss 6 in./hr (152.4 mm/hr) interval, lb. (g)	35.1 (15,936)	44.1 (19,997)	96.5 (43,775)	58.6 (26,569)
Total Soil Loss, lb. (g)	39.0 (17,697)	46.8 (21,218)	102.5 (46,501)	62.8 (28,472)

Turbidity and TSS summary data are provided in Figure 4-25 and Figure 4-26. The turbidity of all three test plots, except for Test 3 during the third rainfall interval (6 in./hr [152.4 mm/hr]), followed the same general trajectory. Otherwise, both the measurements for turbidity and TSS increased as the test continued.

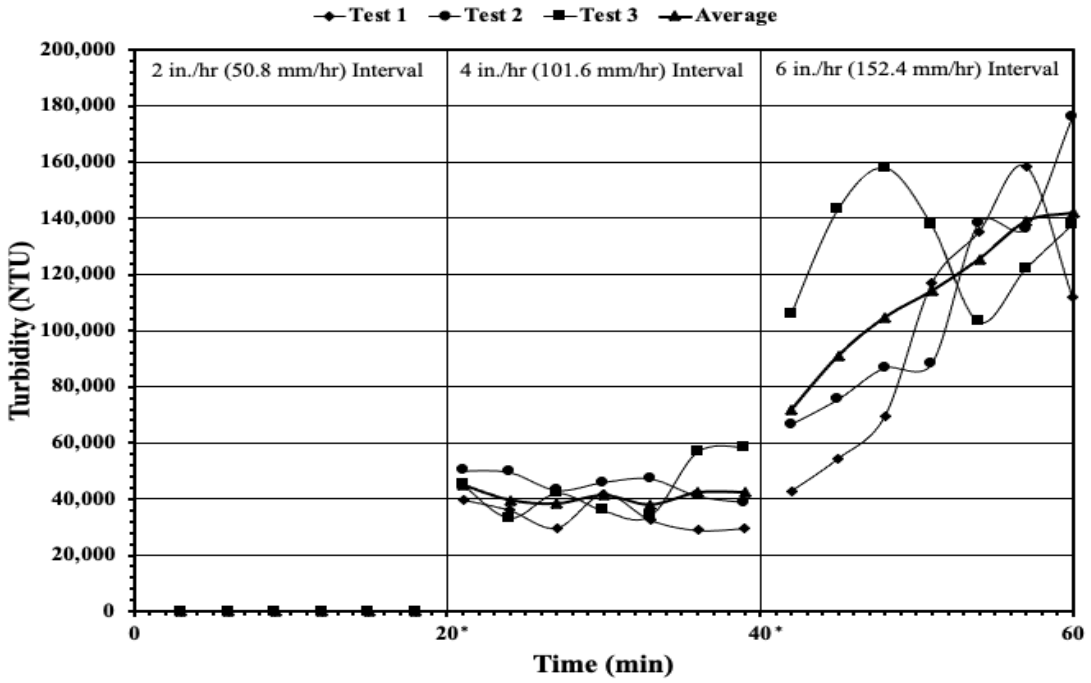

('*' – Denotes 15-minute rest interval for data collection)

Figure 4-25 Turbidity for Intermediate-Scale Bare Soil Plots

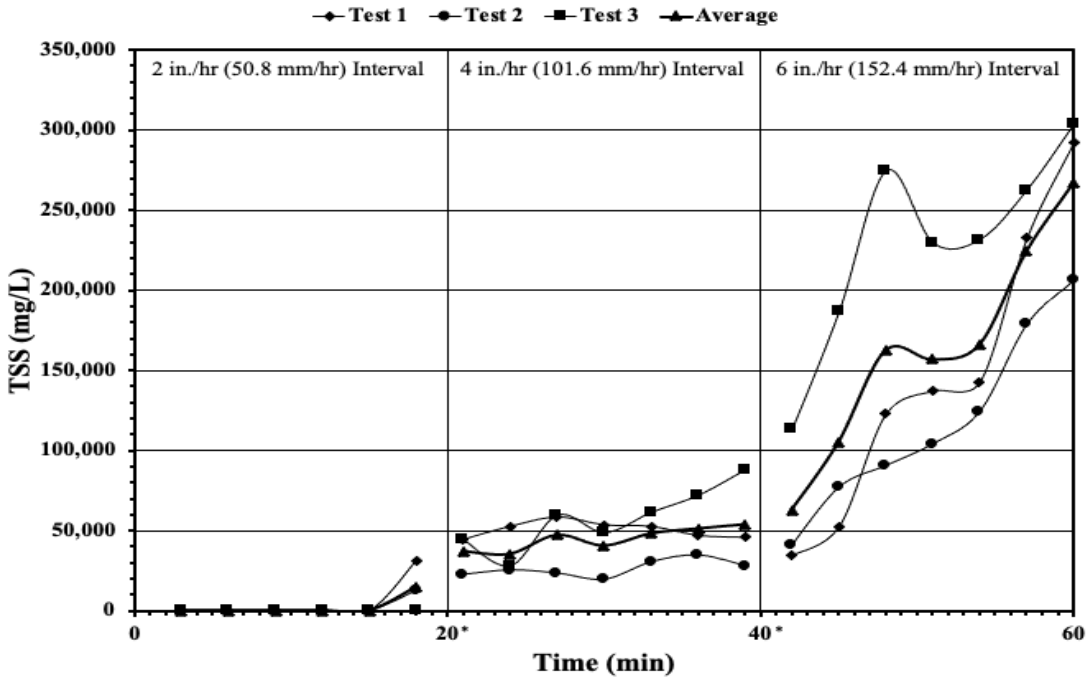

('*' – Denotes 15-minute rest interval for data collection)

Figure 4-26 TSS for Intermediate-Scale Bare Soil Control Plots

The runoff volume by time for each test plot in the intermediate-scale testing was relatively consistent throughout the duration of the test. There was not an interval for any test that exhibited higher excess runoff not in line with the other two control tests. This data is summarized in Table 4-12.

Table 4-12 Runoff Volume by Time for Intermediate-Scale Bare Soil Plots

	Volume of Runoff, ft^3 (L)		
Test Time, min	**Bare Soil Test 1**	**Bare Soil Test 2**	**Bare Soil Test 3**
0	0.00	0.00	0.00
3	0.00	0.00	0.00
6	0.00	0.00	0.00
9	0.00	0.00	0.00
12	0.00	0.00	0.00
15	0.00	0.00	0.00
18	0.01 (0.32)	0.01 (0.32)	0.00
20	0.03 (0.81)	0.02 (0.65)	0.01 (0.16)
21	0.02 (0.48)	0.01 (0.32)	0.02 (0.65)
24	0.25 (7.11)	0.22 (6.23)	0.16 (4.49)
27	0.56 (15.76)	0.52 (14.77)	0.38 (10.76)
30	0.85 (23.95)	0.8 (22.78)	0.67 (18.98)
33	1.18 (33.51)	1.11 (31.32)	0.95 (26.99)
36	1.5 (42.43)	1.42 (40.24)	1.29 (36.54)
39	1.82 (51.68)	1.72 (48.68)	1.61 (45.45)
40	1.97 (55.65)	1.81 (51.13)	1.74 (49.18)
42	0.4 (11.41)	0.37 (10.39)	0.33 (9.46)
45	1 (28.34)	0.92 (26.14)	0.61 (17.35)
48	1.56 (44.16)	1.5 (42.5)	1.28 (36.13)
51	2.24 (63.3)	2.06 (58.25)	2.04 (57.68)
54	2.92 (82.62)	2.6 (73.62)	2.72 (76.99)
57	3.68 (104.07)	3.07 (87.03)	3.47 (98.14)
60	4.62 (130.91)	4.03 (114.13)	4.61 (130.45)

Figure 4-27 details each intermediate-scale test plot at the conclusion of the first rainfall interval (2 in./hr [50.8 mm/hr]). Similar to the small-scale test plots, there is no evidence of rill erosion present at the end of this interval.

(a) Test 1

(b) Test 2

(c) Test 3

Figure 4-27 Photographs of Bare Soil Tests for Intermediate-Scale after the First Rainfall Interval (2 in./hr [50.8 mm/hr])

Figure 4-28 below details each intermediate-scale test plot at the conclusion of the second rainfall interval (4 in./hr [101.6 mm/hr]). Neither Test 1 nor Test 2 exhibit any indication of rill erosion. Test 3, however does show signs of rill erosion forming on the lower portions of the plot area. At this point in the test, the total soil loss for intermediate-scale Test 3 begins to increase dramatically when compared to the other two control tests.

(a) Test 1

(b) Test 2

(c) Test 3

Figure 4-28 Photographs of Bare Soil Tests for Intermediate-Scale after the Second Rainfall Interval (4 in./hr [101.6 mm/hr])

At the conclusion of the third rainfall interval (6 in./hr [152.4 mm/hr]), rill erosion is present on all three test plots of intermediate scale. This is supported by the increase in soil loss for each plot as detailed above. Again, Test 3 exhibits the most advanced stage of rill erosion as evidenced by the number and depth of the rills shown in Figure 4-29 (c).

(a) Test 1

(b) Test 2

(c) Test 3

Figure 4-29 Photographs of Bare Soil Tests for Intermediate-Scale after the Third Rainfall Interval (6 in./hr [152.4 mm/hr])

4.3.3 Hydromulch Products over Loam

As part of the small-scale testing, 2 feet by 4 feet (0.6 m by 1.2 m) plots were tested using the AU-loam soil with various hydromulch products applied. Three such plots were tested for each product. The results are shown in Table 4-13 below. The total soil loss for EcoFibre ranged from 0.289 lb. to 0.425 lb. (131 grams to 193 grams) with an average of 0.355 lb. (161 grams). The total soil loss for Terrawood ranged from 0.815 lb. to 1.92 lb. (370 grams to 872 grams) with an average of 1.40 lb. (635 grams). The total soil loss for SoilCover ranged from 0.385 lb. to 0.868 lb. (175 grams to 394 grams) with an average of 0.590 lb. (268 grams). When compared to the averages obtained during the bare soil control tests, all hydromulch products provided for significant reductions in the overall soil loss as shown. When compared to the bare soil plots, the EcoFibre

product resulted in an 86% reduction in soil loss; the Terrawood product resulted in a 46% reduction in soil loss; and the SoilCover product resulted in a 77% reduction in soil loss.

Table 4-13 Soil Loss (lb. [g]) Comparison of Small-Scale Plots with Hydromulch over Loam

Rainfall Intensity	Plot 1	Plot 2	Plot 3	Average
Bare Soil Control				
2 in./hr (50.8 mm/hr)	0.137 (62)	0.009 (4)	0.009 (4)	0.051 (23)
4 in./hr (101.6 mm/hr)	0.425 (193)	0.09 (41)	0.132 (60)	0.216 (98)
6 in./hr (152.4 mm/hr)	2.791 (1267)	2.203 (1000)	1.941 (881)	2.311 (1049)
Total	3.352 (1522)	2.302 (1045)	2.081 (945)	2.579 (1171)
EcoFibre HM				
2 in./hr (50.8 mm/hr)	0.007 (3)	0.007 (3)	0.046 (21)	0.02 (9)
4 in./hr (101.6 mm/hr)	0.064 (29)	0.086 (39)	0.106 (48)	0.086 (39)
6 in./hr (152.4 mm/hr)	0.218 (99)	0.333 (151)	0.2 (91)	0.251 (114)
Total	0.289 (131)	0.425 (193)	0.352 (160)	0.355 (161)
Terrawood HM				
2 in./hr (50.8 mm/hr)	0.172 (78)	0.139 (63)	0.086 (39)	0.132 (60)
4 in./hr (101.6 mm/hr)	0.46 (209)	0.319 (145)	0.236 (107)	0.339 (154)
6 in./hr (152.4 mm/hr)	1.289 (585)	1 (454)	0.493 (224)	0.927 (421)
Total	1.921 (872)	1.458 (662)	0.815 (370)	1.399 (635)
SoilCover HM				
2 in./hr (50.8 mm/hr)	0.064 (29)	0.022 (10)	0.057 (26)	0.048 (22)
4 in./hr (101.6 mm/hr)	0.379 (172)	0.128 (58)	0.093 (42)	0.2 (91)
6 in./hr (152.4 mm/hr)	0.425 (193)	0.37 (168)	0.236 (107)	0.344 (156)
Total	0.868 (394)	0.52 (236)	0.385 (175)	0.59 (268)

As shown in Figure 4-30 and Figure 4-31, the turbidity and TSS for all tested hydromulch products is reduced significantly when compared to the same-size bare soil control. Contrary to the large-scale plots, the turbidity and TSS do not increase dramatically over time. Given the lack of rill erosion exhibited by the small-scale plots, this result is expected.

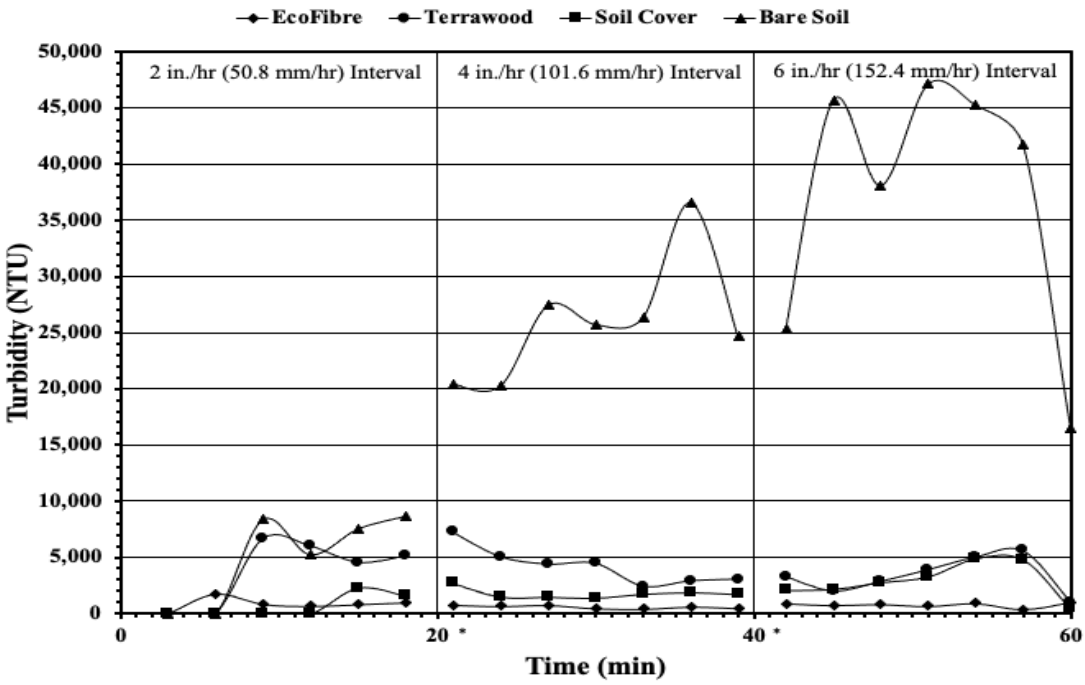

('*' – Denotes 15-minute rest interval for data collection)

Figure 4-30 Turbidity for Hydromulch Products on Loam Using Small-Scale Plots

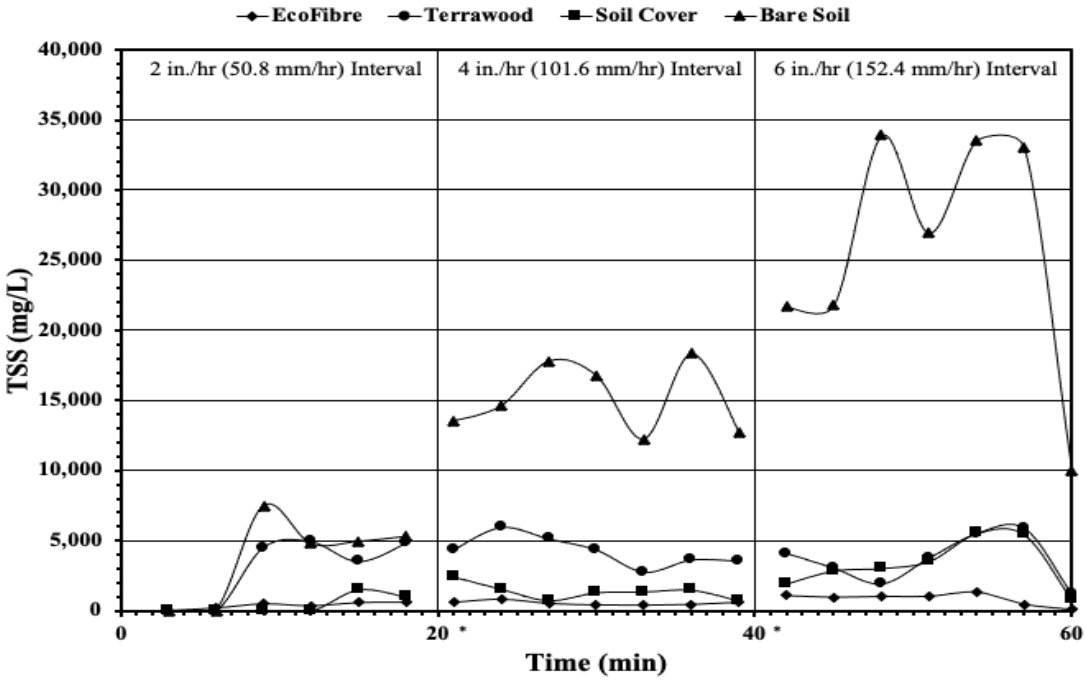

('*' – Denotes 15-minute rest interval for data collection)

Figure 4-31 TSS for Hydromulch Products on Loam Using Small-Scale Plots

Unlike the turbidity and TSS experimental data, the runoff volume for the small-scale hydromulch plots is not suppressed when compared to the same-scale bare soil control plots. This is due to the hydromulch dispersing the raindrops prior to impacting the soil. The dispersed droplets then flow along the top of the hydromulch surface and less moisture is likely absorbed into the test plot. The runoff volume for the hydromulch products on loam is provided in Table 4-14.

Table 4-14 Runoff Volume of Small-Scale Plots by Time for Hydromulch Products on Loam

	Volume of Runoff, ft^3 (L)								
Test Time, min	**EcoFibre on Loam Plot 1**	**EcoFibre on Loam Plot 2**	**EcoFibre on Loam Plot 3**	**Terrawood on Loam Plot 1**	**Terrawood on Loam Plot 2**	**Terrawood on Loam Plot 3**	**SoilCover on Loam Plot 1**	**SoilCover on Loam Plot 2**	**SoilCover on Loam Plot 3**
0	0.00	0.00	0.00	0.00	0.00	0.00	0.00	0.00	0.00
3	0.00	0.00	0.00	0.00	0.00	0.00	0.00	0 (0.103)	0.00
6	0.00	0.00	0.00	0.00	0.00	0.00	0.00	0.01 (0.31)	0.00
9	0.00	0.00	0.01 (0.323)	0.01 (0.31)	0.01 (0.161)	0.00	0.00	0.02 (0.519)	0.00
12	0.03 (0.972)	0.00	0.07 (1.959)	0.03 (0.729)	0.05 (1.3)	0.01 (0.323)	0.02 (0.484)	0.03 (0.729)	0.00
15	0.08 (2.292)	0.01 (0.415)	0.11 (3.129)	0.03 (0.941)	0.09 (2.458)	0.06 (1.794)	0.05 (1.3)	0.05 (1.476)	0.01 (0.161)
18	0.11 (3.129)	0.04 (1.047)	0.16 (4.491)	0.04 (1.261)	0.13 (3.807)	0.09 (2.458)	0.07 (1.959)	0.08 (2.13)	0.01 (0.323)
20	0.14 (3.977)	0.05 (1.476)	0.18 (5.008)	0.06 (1.692)	0.21 (5.878)	0.12 (3.298)	0.09 (2.458)	0.09 (2.625)	0.04 (1.136)
21	0.01 (0.161)	0.01 (0.169)	0.00	0.01 (0.415)	0.01 (0.161)	0.00	0.00	0.01 (0.415)	0.00
24	0.09 (2.458)	0.09 (2.581)	0.09 (2.625)	0.06 (1.692)	0.08 (2.292)	0.05 (1.3)	0.05 (1.3)	0.06 (1.692)	0.02 (0.647)
27	0.15 (4.148)	0.15 (4.355)	0.19 (5.355)	0.13 (3.821)	0.16 (4.663)	0.13 (3.807)	0.13 (3.637)	0.15 (4.286)	0.09 (2.625)
30	0.23 (6.406)	0.24 (6.726)	0.3 (8.552)	0.2 (5.716)	0.29 (8.19)	0.22 (6.23)	0.21 (5.878)	0.24 (6.7)	0.02 (0.484)
33	0.31 (8.916)	0.33 (9.362)	0.38 (10.76)	0.28 (8.067)	0.4 (11.322)	0.31 (8.916)	0.28 (7.83)	0.32 (9.162)	0.2 (5.529)
36	0.4 (11.322)	0.42 (11.888)	0.47 (13.414)	0.37 (10.473)	0.54 (15.362)	0.39 (11.134)	0.35 (10.017)	0.41 (11.576)	0.26 (7.293)
39	0.5 (14.188)	0.53 (14.897)	0.58 (16.352)	0.45 (12.792)	0.64 (17.987)	0.49 (13.8)	0.42 (11.887)	0.48 (13.65)	0.3 (8.552)
40	0.52 (14.773)	0.55 (15.512)	0.62 (17.556)	0.46 (13.044)	0.71 (20.025)	0.52 (14.773)	0.45 (12.647)	0.51 (14.537)	0.33 (9.282)
42	0.06 (1.794)	0.12 (3.476)	0.09 (2.458)	0.02 (0.624)	0.08 (2.125)	0.06 (1.794)	0.05 (1.3)	0.06 (1.692)	0.05 (1.3)
45	0.21 (6.054)	0.21 (6.054)	0.24 (6.759)	0.29 (8.093)	0.21 (6.054)	0.18 (5.181)	0.18 (5.008)	0.2 (5.716)	0.15 (4.148)
48	0.37 (10.574)	0.34 (9.53)	0.43 (12.266)	0.44 (12.496)	0.33 (9.465)	0.26 (7.472)	0.31 (8.734)	0.32 (9.078)	0.29 (8.19)
51	0.5 (14.188)	0.46 (13.03)	0.6 (16.929)	0.5 (14.189)	0.51 (14.578)	0.42 (11.887)	0.45 (12.647)	0.44 (12.541)	0.42 (11.887)
54	0.55 (15.488)	0.58 (16.506)	0.77 (21.915)	0.66 (18.825)	0.61 (17.203)	0.54 (15.362)	0.56 (15.945)	0.46 (12.956)	0.56 (15.955)
57	0.62 (17.486)	0.69 (19.606)	0.93 (26.454)	0.82 (23.228)	0.77 (21.87)	0.68 (19.339)	0.74 (20.838)	0.66 (18.624)	0.7 (19.932)

60	0.7 (19.717)	1.14 (32.42)	1 (28.414)	1.04 (29.556)	0.99 (27.992)	0.82 (23.192)	0.89 (25.294)	0.78 (22.1)	0.81 (23.069)

4.3.4 Hydromulch Products over Topsoil

As part of the small-scale testing, 2 feet by 4 feet (0.6 m by 1.2 m) plots were tested using the topsoil with various hydromulch products applied. Three such plots were tested for each product. Table 4-15 details the experimental soil loss captured from each small-scale plot with the respective hydromulch products over topsoil. The total soil loss for EcoFibre ranged from 151 grams to 365 grams with an average of 230 grams. The total soil loss for Terrawood ranged from 192 grams to 294 grams with an average of 258 grams. The total soil loss for SoilCover ranged from 126 grams to 255 grams with an average of 204 grams. The average results for the hydromulch products over topsoil are generally consistent with the average experimental results obtained when the products were tested over loam soil. Table 4-16 details the runoff volume for each small-scale plot with hydromulch over topsoil. The average peak runoff values for each hydromulch ranged from 1.09 to 1.14 ft^3 (0.031 to 0.032 m^3), compared to the hydromulch over loam average peak runoff range of 1.02 to 1.14 ft^3 (0.029 to 0.032 m^3). Effectively, the peak runoff volumes are equivalent for the hydromulch products on the small-scale test plots regardless of soil.

Table 4-15 Soil Loss (lb. [g]) of Small-Scale Plots with Hydromulch over Topsoil

Rainfall Intensity	Plot 1	Plot 2	Plot 3	Average
EcoFibre HM				
2 in./hr (50.8 mm/hr)	0.018 (8)	0.011 (5)	0.009 (4)	0.013 (6)
4 in./hr (101.6 mm/hr)	0.123 (56)	0.079 (36)	0.117 (53)	0.106 (48)
6 in./hr (152.4 mm/hr)	0.664 (301)	0.243 (110)	0.26 (118)	0.388 (176)
Total	0.805 (365)	0.333 (151)	0.386 (175)	0.507 (230)
Terrawood HM				
2 in./hr (50.8 mm/hr)	0.075 (34)	0.15 (68)	0.024 (11)	0.084 (38)
4 in./hr (101.6 mm/hr)	0.185 (84)	0.117 (53)	0.225 (102)	0.176 (80)
6 in./hr (152.4 mm/hr)	0.388 (176)	0.157 (71)	0.388 (176)	0.311 (141)
Total	0.648 (294)	0.423 (192)	0.637 (289)	0.569 (258)
SoilCover HM				
2 in./hr (50.8 mm/hr)	0.044 (20)	0.013 (6)	0.013 (6)	0.024 (11)
4 in./hr (101.6 mm/hr)	0.11 (50)	0.035 (16)	0.121 (55)	0.088 (40)
6 in./hr (152.4 mm/hr)	0.353 (160)	0.229 (104)	0.428 (194)	0.337 (153)
Total	0.507 (230)	0.278 (126)	0.562 (255)	0.45 (204)

Table 4-16 Runoff Volume of Small-Scale Test Plots by Time for Hydromulch Products over Topsoil

Test Time, min	Volume of Runoff, ft^3 (L)								
	EcoFibre on Topsoil Plot 1	EcoFibre on Topsoil Plot 2	EcoFibre on Topsoil Plot 3	Terrawood on Topsoil Plot 1	Terrawood on Topsoil Plot 2	Terrawood on Topsoil Plot 3	SoilCover on Topsoil Plot 1	SoilCover on Topsoil Plot 2	SoilCover on Topsoil Plot 3
0	0.00	0.00	0.00	0.00	0.00	0.00	0.00	0.00	0.00
3	0.00	0.00	0.00	0.00	0.00	0.00	0.00	0.00	0.00
6	0.00	0.00	0.00	0.00	0.00	0.00	0.00	0.00	0.00
9	0.00	0.00	0.00	0.02 (0.647)	0.00	0.00	0.02 (0.647)	0.00	0.00
12	0.02 (0.647)	0.01 (0.323)	0.01 (0.161)	0.03 (0.972)	0.01 (0.323)	0.00)	0.05 (1.3)	0.01 (0.161)	0.01 (0.161)
15	0.08 (2.292)	0.04 (1.136)	0.02 (0.647)	0.06 (1.629)	0.04 (1.136)	0.03 (0.809)	0.08 (2.125)	0.02 (0.484)	0.02 (0.647)
18	0.11 (3.129)	0.07 (1.959)	0.04 (1.136)	0.08 (2.125)	0.08 (2.125)	0.03 (0.972)	0.1 (2.793)	0.04 (1.136)	0.05 (1.3)
20	0.14 (3.977)	0.09 (2.625)	0.05 (1.464)	0.1 (2.793)	0.12 (3.298)	0.09 (2.458)	0.14 (3.977)	0.04 (1.136)	0.06 (1.629)
21	0.00	0.00	0.00	0.00	0.00	0.00	0.00	0.00	0.00
24	0.03 (0.972)	0.04 (1.136)	0.02 (0.484)	0.09 (2.458)	0.06 (1.794)	0.04 (1.136)	0.06 (1.794)	0.02 (0.484)	0.04 (1.136)
27	0.05 (1.464)	0.1 (2.961)	0.07 (1.959)	0.14 (3.977)	0.14 (3.977)	0.11 (3.129)	0.15 (4.148)	0.05 (1.3)	0.12 (3.298)
30	0.08 (2.292)	0.13 (3.807)	0.13 (3.637)	0.21 (6.054)	0.2 (5.704)	0.15 (4.319)	0.23 (6.582)	0.09 (2.625)	0.17 (4.835)
33	0.14 (3.977)	0.2 (5.704)	0.19 (5.355)	0.3 (8.371)	0.26 (7.472)	0.21 (6.054)	0.33 (9.282)	0.12 (3.298)	0.24 (6.759)
36	0.24 (6.937)	0.25 (7.115)	0.26 (7.472)	0.39 (11.134)	0.35 (9.833)	0.28 (8.01)	0.42 (11.887)	0.13 (3.807)	0.29 (8.19)
39	0.35 (10.017)	0.33 (9.282)	0.3 (8.552)	0.49 (13.8)	0.42 (11.887)	0.34 (9.649)	0.5 (14.188)	0.18 (5.008)	0.36 (10.203)
40	0.42 (11.887)	0.33 (9.282)	0.31 (8.916)	0.54 (15.362)	0.49 (13.994)	0.37 (10.388)	0.54 (15.165)	0.19 (5.355)	0.39 (11.134)
42	0.07 (1.959)	0.01 (0.161)	0.01 (0.161)	0.04 (1.136)	0.02 (0.647)	0.03 (0.972)	0.06 (1.794)	0.02 (0.647)	0.06 (1.629)
45	0.24 (6.759)	0.09 (2.625)	0.09 (2.625)	0.18 (5.181)	0.15 (4.148)	0.15 (4.319)	0.2 (5.529)	0.11 (3.129)	0.19 (5.355)
48	0.42 (11.887)	0.19 (5.355)	0.21 (6.054)	0.32 (9.099)	0.28 (7.83)	0.27 (7.651)	0.37 (10.574)	0.2 (5.704)	0.31 (8.916)
51	0.61 (17.242)	0.3 (8.371)	0.37 (10.388)	0.53 (14.969)	0.43 (12.266)	0.42 (11.887)	0.53 (14.969)	0.29 (8.19)	0.45 (12.647)
54	0.81 (22.834)	0.45 (12.647)	0.49 (13.8)	0.66 (18.776)	0.99 (28.023)	0.53 (14.969)	0.66 (18.606)	0.31 (8.837)	0.59 (16.624)
57	0.99 (28.041)	0.55 (15.608)	0.59 (16.761)	0.86 (24.25)	0.55 (15.564)	0.63 (17.93)	0.82 (23.159)	0.41 (11.488)	0.7 (19.94)
60	1.13 (32.018)	0.66 (18.701)	0.68 (19.155)	1.07 (30.331)	0.72 (20.457)	0.81 (22.979)	1 (28.383)	0.52 (14.596)	0.85 (24.157)

Figure 4-32 details the testing performed with EcoFibre HM on both topsoil (plots 3, 6, and 7, Figure 4-32a,b) and loam (plots, 1, 2, and 5, Figure 4-32a) after the conclusion of each rainfall interval. The topsoil plots have been labeled accordingly in Figure 4-32; all other plots shown are tested over AU-loam soil. As shown in Figure 4-32, minimal displacement of the hydromulch product occurred during the test. No evidence of rill erosion is present on the hydromulch plots.

Figure 4-33 details the testing performed with Terrawood HM on both topsoil (plots, 1, 6, and 7, Figure 4-33a, b) and loam (plots 2, 3, and 5, Figure 4-33a) after the conclusion of each rainfall interval. Similar to the results of the EcoFibre HM, minimal displacement of the hydromulch product has occurred. No evidence of rill erosion is present.

Figure 4-34 details the testing performed with SoilCover HM on both topsoil (plots 3, 6, and 7, Figure 4-34a, b) and loam (plots 1, 2, and 5, Figure 4-34a) after the conclusion of each rainfall interval. As evidenced by all hydromulch products tested on the small-scale plots, minimal displacement of the hydromulch product has occurred during the test. Contrary to the large-scale testing, no evidence of rill erosion is present on the small-scale test plots.

(a) 2 in./hr (50.8 mm/hr) Interval – Plots 1, 2, 3, and 5

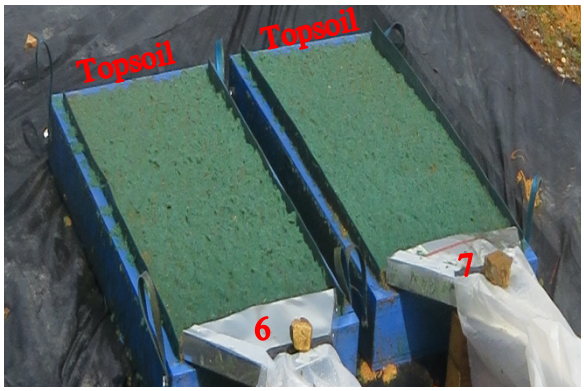

(b) 2 in./hr (50.8 mm/hr) Interval – Plots 6 and 7

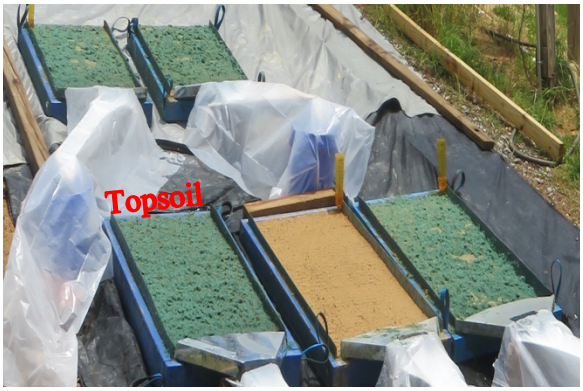

(c) 4 in./hr (101.6 mm/hr) Interval – Plots 1, 2, 3, and 5

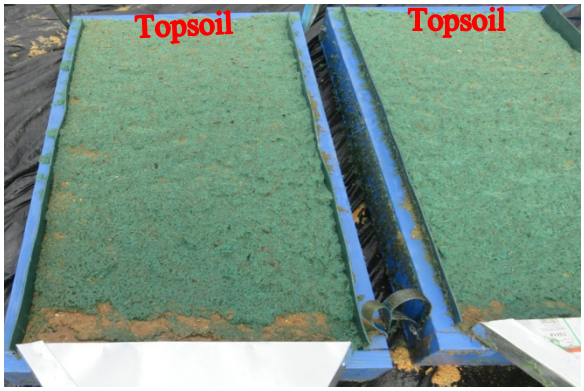

(d) 4 in./hr (101.6 mm/hr) Interval – Plots 6 and 7

(e) 6 in./hr (152.4 mm/hr) Interval – Plots 1, 2, 3, and 5

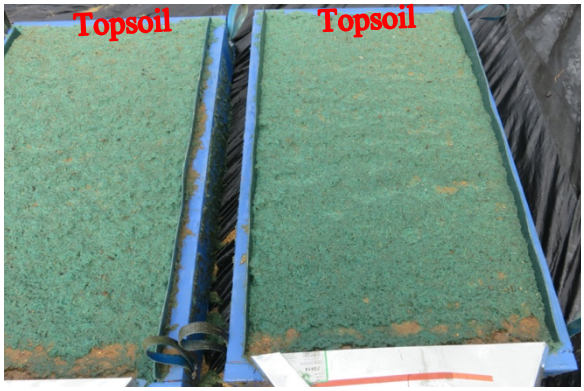

(f) 6 in./hr (152.4 mm/hr) Interval – Plots 6 and 7

Figure 4-32 Photographs of EcoFibre HM on Loam or Topsoil using Small-Scale Plots after Each Rainfall Interval

(a) 2 in./hr Interval – Plots 1, 2, 3, and 5

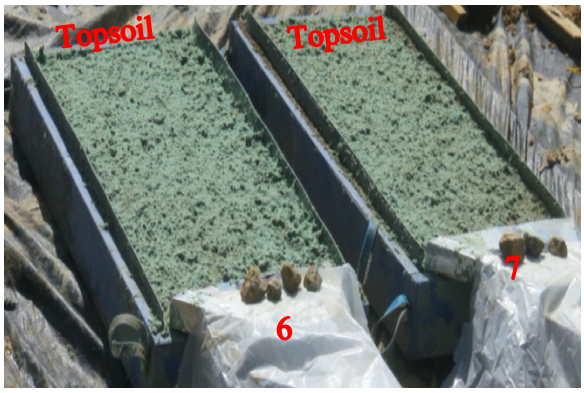

(b) 2 in./hr Interval – Plots 6 and 7

(c) 4 in./hr Interval – Plots 1, 2, 3, and 5

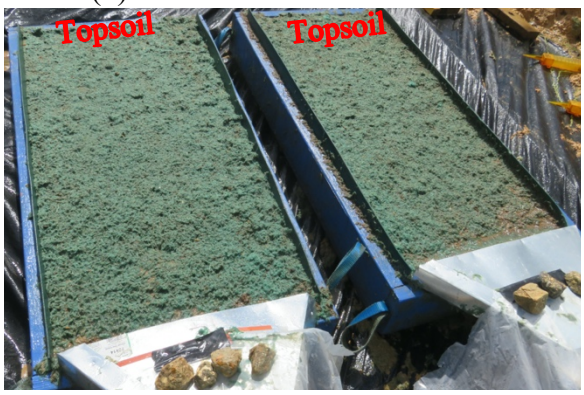

(d) 4 in./hr Interval – Plots 6 and 7

(e) 6 in./hr Interval – Plots 1, 2, 3, and 5

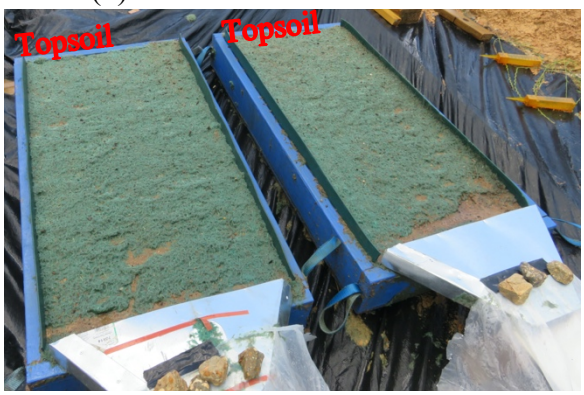

(f) 6 in./hr Interval – Plots 6 and 7

Figure 4-33 Photographs of Terrawood HM on Topsoil and Loam Using Small-Scale Plots after Each Rainfall Interval

(a) 2 in./hr (50.8 mm/hr) Interval – Plots 1, 2, 3, and 5

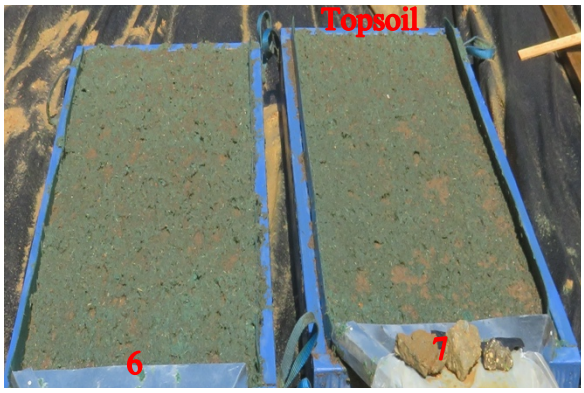

(b) 2 in./hr (50.8 mm/hr) Interval – Plots 6 and 7

(c) 4 in./hr (101.6 mm/hr) Interval – Plots 1, 2, 3, and 5

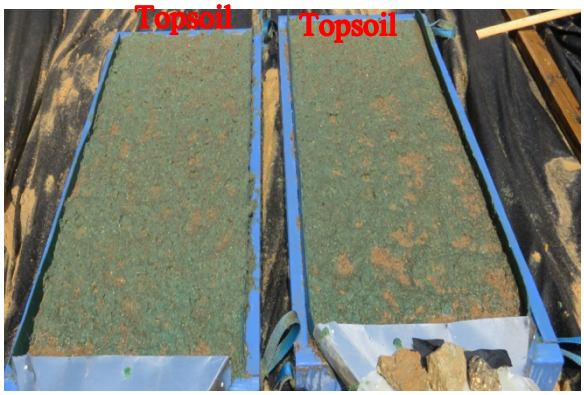

(d) 4 in./hr (101.6 mm/hr) Interval – Plots 6 and 7

(e) 6 in./hr (152.4 mm/hr) Interval – Plots 1, 2, 3, and 5

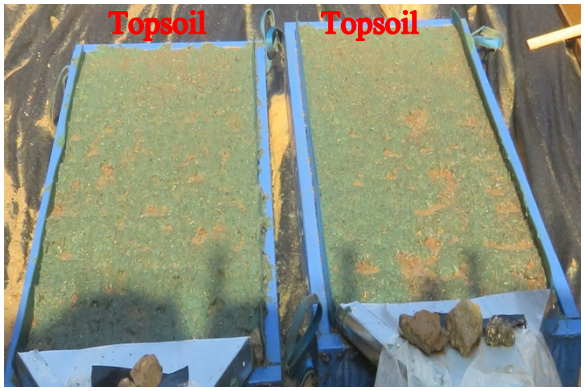

(f) 6 in./hr (152.4 mm/hr) Interval – Plots 6 and 7

Figure 4-34 Photographs of SoilCover HM on Topsoil and Loam Using Small-Scale Plots after Each Rainfall Interval

4.4 SUMMARY

In this study, the results of three sizes of bare soil control test plots were evaluated by the AU-ESCTF large-scale rainfall simulator to ensure the same rainfall conditions. In addition,

hydromulch products over loam soil were evaluated for two different scales: large- and small-scale test plots. The selected hydromulch products were also tested over topsoil. A summary of the average soil loss from each scenario is provided below in Table 4-17.

Table 4-17 Summary of Average Soil Loss under Rainfall Simulation

Soil Type	Erosion Control Practice	Scale of Rainfall Simulation	Soil Loss, lb. (kg)			
			2 in./hr (50.8 mm/hr)	4 in./hr (101.6 mm/hr)	6 in./hr (152.4 mm/hr)	Total
Loam	Bare Soil	Large	43.4 (19.7)	775 (352)	1515 (687)	2,333 (1,058)
	Bare Soil	Intermediate	0.0838 (0.038)	4.11 (1.865)	58.6 (26.569)	62.8 (28.472)
	Bare Soil	Small	0.051 (0.023)	0.216 (0.098)	2.31 (1.049)	2.58 (1.171)
	EcoFibre	Large	3.45 (1.56)	304 (138)	717 (325)	1024 (465)
	EcoFibre	Small	0.02 (0.009)	0.086 (0.039)	0.251 (0.114)	0.355 (0.161)
	Terrawood	Large	8.54 (3.87)	488 (221)	797 (362)	1293 (587)
	Terrawood	Small	0.132 (0.060)	0.339 (0.154)	0.927 (0.421)	1.399 (0.635)
	SoilCover	Large	2.67 (1.21)	382 (173)	779 (353)	1164 (528)
	SoilCover	Small	0.048 (0.022)	0.2 (0.091)	0.344 (0.156)	0.59 (0.268)
Topsoil	EcoFibre	Small	0.013 (0.006)	0.106 (0.048)	0.388 (0.176)	0.507 (0.23)
	Terrawood	Small	0.084 (0.038)	0.176 (0.08)	0.311 (0.141)	0.569 (0.258)
	SoilCover	Small	0.024 (0.011)	0.088 (0.04)	0.337 (0.153)	0.45 (0.204)

EcoFibre consistently outperformed the other two hydromulch products as evidenced by the smallest average soil loss, regardless of soil or scale of simulation. EcoFibre was followed by SoilCover and finally by Terrawood. A further analysis of the relationship between the scale of testing and product performance will be covered in the following chapter.

5 COMPARISON OF DATA

5.1 INTRODUCTION

This chapter compares the experimental bare soil control results of each test-plot scale and the relationship between the soil loss and several variables of each scale plot. Several factors will be evaluated including test plot area, test plot length, and the horizontal projection of the plot length (λ). Furthermore, the *K*-factor for the experimental loam soil and the *C*-factor for the tested hydromulch products are calculated based on the experimental data. The percent reduction for each hydromulch product will be determined for both the large- and small-scale test plots.

5.2 BARE SOIL CONTROL PLOTS

For this project, three different plot sizes were tested as bare soil control plots using loam soil: three hundred and twenty square feet (8 ft width by 40 ft length); thirty-two square feet (4 ft by 8 ft); and eight square feet (2 ft by 4 ft). Each plot size was tested in triplicate. The testing was completed under the same large-scale rainfall simulator (Figure 3-2) to minimize error in rainfall energy. For each plot, the total soil loss, total runoff, turbidity, and TSS were captured as previously discussed.

5.2.1 Soil Loss

The first step taken was to analyze the total soil loss results of the various scales of testing methods using a multiple regression analysis. The dependent variable in this analysis was soil loss. The independent variables selected for testing were (1) area of test plot and (2) flow length of test plot. The results of the analysis show a strong correlation between soil loss and area of the test plot. The results also show a strong correlation between soil loss and the total flow length of the test plot. The results are shown below in Figure 5-1, Figure 5-2, and Table 5-1.

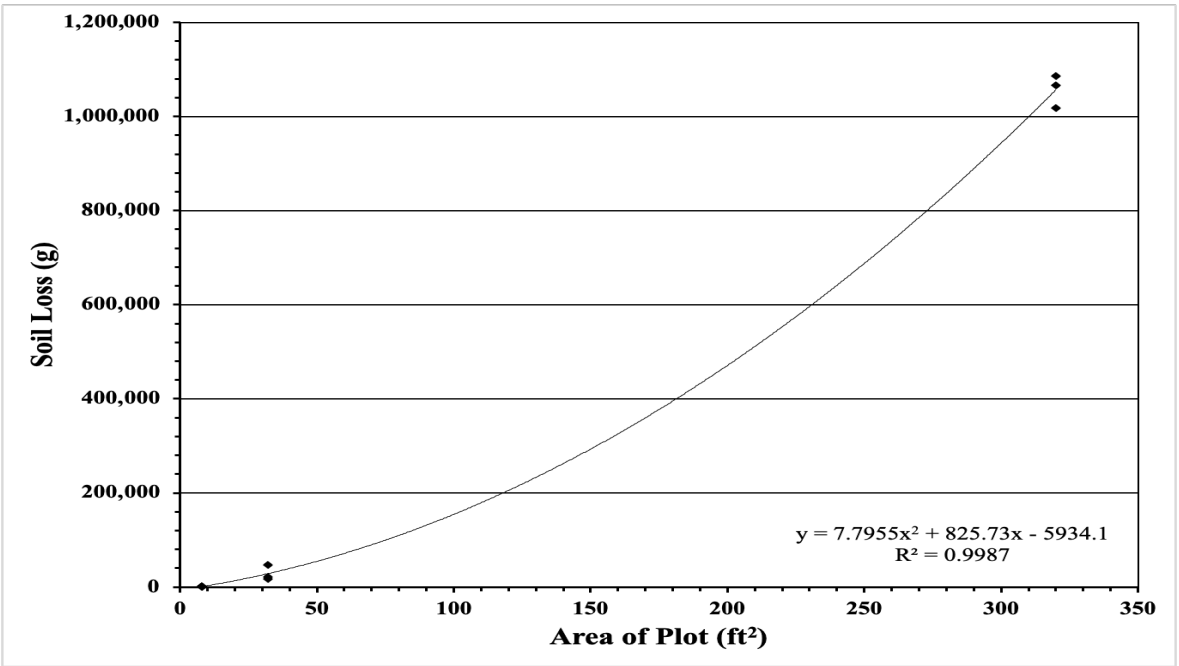

Figure 5-1 Total Soil Loss v. Area of Plot

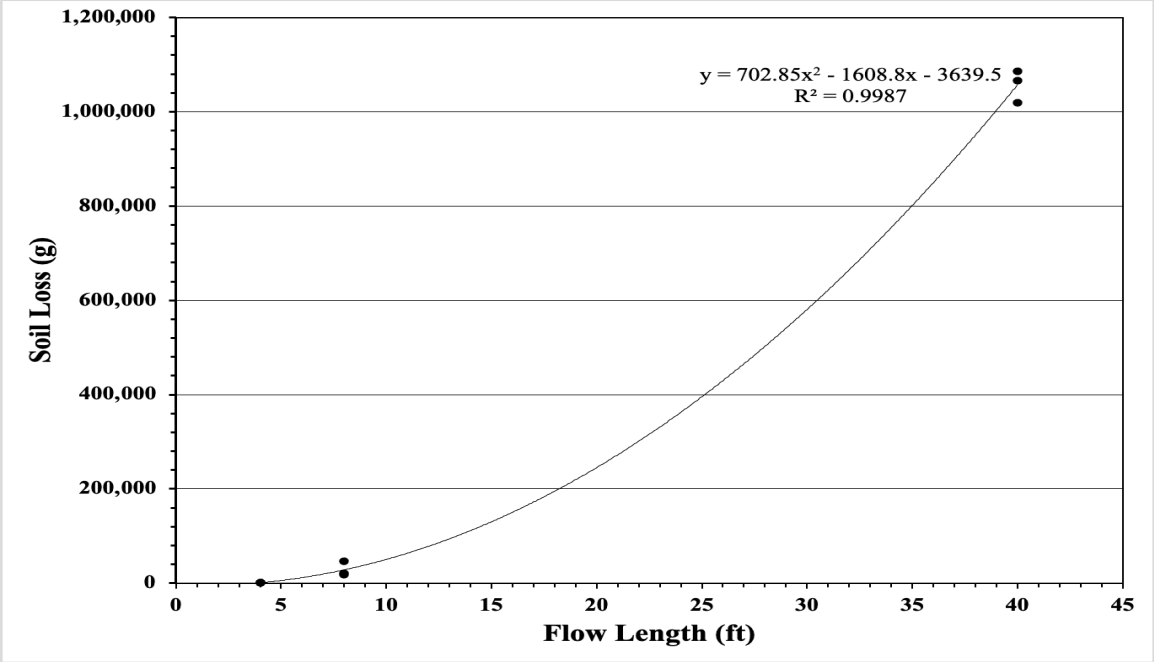

Figure 5-2 Soil Loss vs. Flow Length for Bare Soil Plots

As indicated in the data shown above, both the area of the plot and the total plot length were deemed to be significantly related to the soil loss generated as evidenced by having a P-value less than 0.05. However, both independent variables shared similar fit to the measured data as

well as similar P-values. In order to further analyze the relationship of the independent variables, the soil loss for each scenario was then divided by the width of the respective plot to create the soil loss per unit width. This variable was then treated as the dependent variable and compared to the independent variables of (1) area of test plot and (2) flow length of test plot. The results are provided in Figure 5-3, Figure 5-4, and Table 5-1 below.

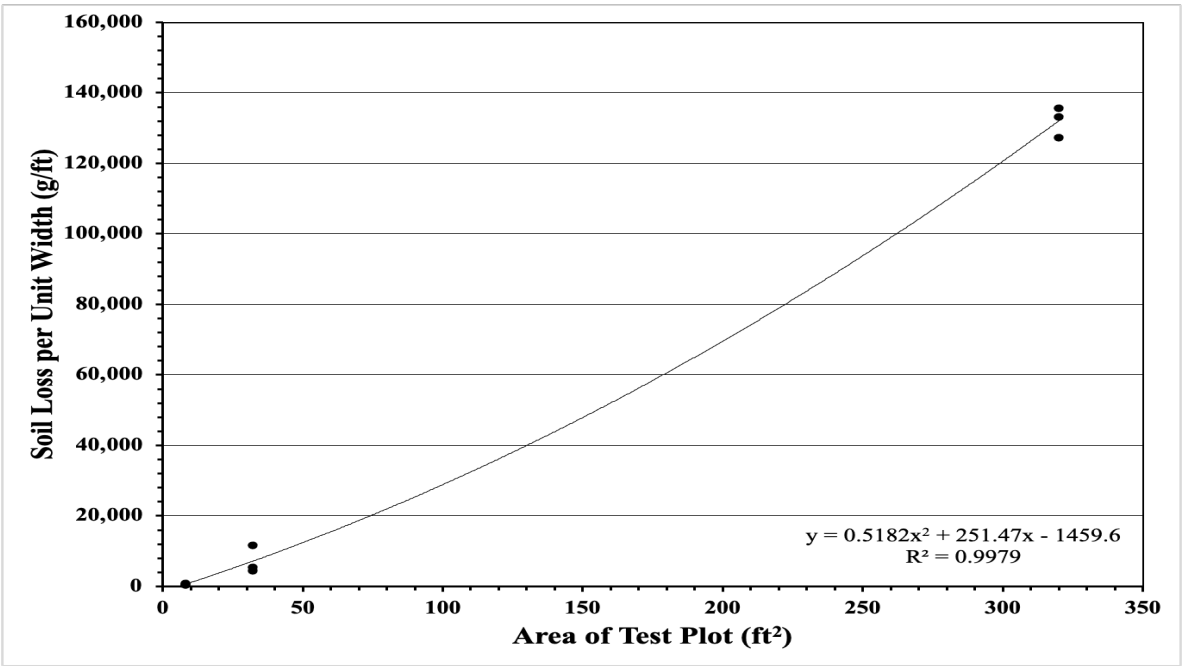

Figure 5-3 Soil Loss per Unit Width vs. Area of Test Plot

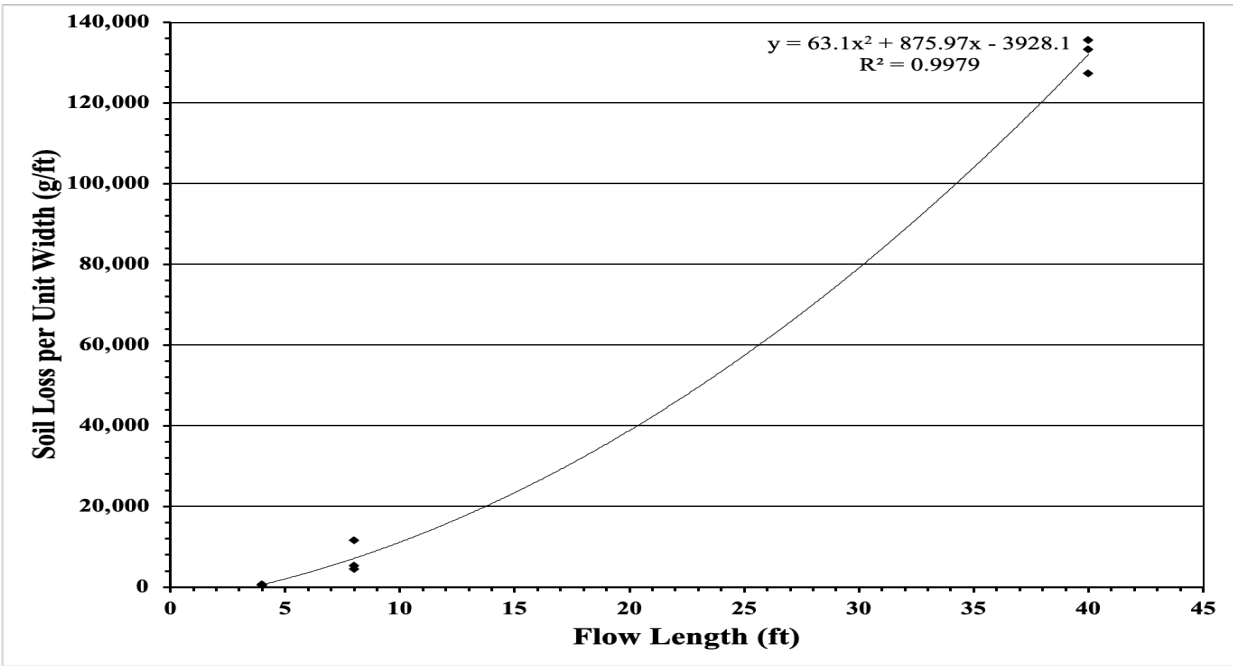

Figure 5-4 Soil Loss per Unit Width vs. Flow Length

Table 5-1 Results from Multiple Regression Analysis of Bare Soil Plots

Dependent Variable	Independent Variable	R^2 Value	P Value
Soil Loss	Area of Test Plot	0.9987	<0.0001
	Flow Length	0.9987	<0.0001
Soil Loss per Unit Width	Area of Test Plot	0.9979	<0.0001
	Flow Length	0.9979	<0.0001

Again, both independent variables have a strong correlation to the soil loss per unit width as evidenced by a P-value less than 0.05. In looking at the regression data, both of the independent variables exhibit a strong correlation to both soil loss and soil loss per unit width as evidenced by a P-value of less than 0.0001.

Based on the regression data, both the plot area and flow length are useful indicators of the total soil loss generated for the given storm. The data gathered over the tested plot sizes indicate the opportunity to utilize flow length and plot area as useful factors to scale up soil loss results. This could provide additional justification for testing on a smaller scale at a reduced cost and scaling the data up to estimate soil losses on a larger area.

5.2.2 Soil Loss Calculations using RUSLE

As discussed previously, RUSLE was used to evaluate the measured soil loss from each size of erosion control plots when compared to theoretical soil loss. The first step in this process was to evaluate the theoretical soil loss for each plot scale. Using the equations defined in Section 3.5, the variables required for the soil loss calculations were determined. The results are summarized in Table 5-2 and Table 5-3. The angle β is multiplied by two to get β', which is required for determining *LS* for "soil highly susceptible to rill erosion…most likely to occur on steep, freshly prepared construction slopes." (Agriculture 1997). This is the case of this testing study when the slope is a 3 horizontal versus 1 vertical (much larger than 9%). The exponent *m* is determined using Equation (**12**) with β' instead of β.

Table 5-2 Common RUSLE Factors

Factor	Value
θ	18.4°
β	1.23
β` = 2β	2.45
m	0.711
S-factor	4.81
R-factor	187
K (theoretical)	0.32
C-factor	1
P-factor	1

Table 5-3 Calculated RUSLE Factors for all Plot Sizes

	Small-Scale	Intermediate-Scale	Large-Scale
Test Plot Area, ft^2 (m^2)	8 (0.74)	32 (2.97)	320 (29.73)
Slope Length, ft^2 (m^2)	4 (1.22)	8 (2.44)	40 (12.19)
λ, ft (m)	3.8 (1.16)	7.59 (2.31)	37.95 (11.57)
L-factor (dimensionless)	0.123	0.201	0.631

Using these variables, the theoretical soil loss for the respective plot sizes were calculated using Equation (8). The results are provided in Table 5-4 below. The percent error for the large-

scale plots ranges from 9.9 percent to 15.8 percent. However, as the plot size decreases the percent error dramatically increases. This suggests as the plot size increases, the use of RUSLE to calculate soil loss becomes more applicable. For the large-scale plots of this study, the overall flow length is 40 feet (12.19 m), which corresponds to a λ value of 37.95 feet (11.57 m). The unit plot length defined in RUSLE is 72.6 feet (22.13 m). Based on our tested data, the results suggest that increasing the plot length to the standard unit plot length would continue to lower the percent error. The theoretical soil loss results were then compared to the experimental soil loss values measured during each test. The results have been plotted in Figure 5-5.

Table 5-4 Theoretical Soil Loss Determined using RUSLE Compared with Experimental Soil Loss

Plot	Theoretical Soil Loss, ton/acre (kg/ha)	Experimental Soil Loss, ton/acre (kg/ha)	Percent Error
Large-Scale	181.5 (406869)	152.9 (342756)	-15.8%
		163.6 (366742)	-9.9%
		159.9 (358448)	-11.9%
Intermediate-Scale	57.8 (129570)	26.6 (59629)	-54.0%
		31.8 (71286)	-45.0%
		69.8 (156471)	20.8%
Small-Scale	35.3 (79132)	9.14 (20489)	-74.1%
		6.27 (14055)	-82.2%
		5.67 (12710)	-83.9%

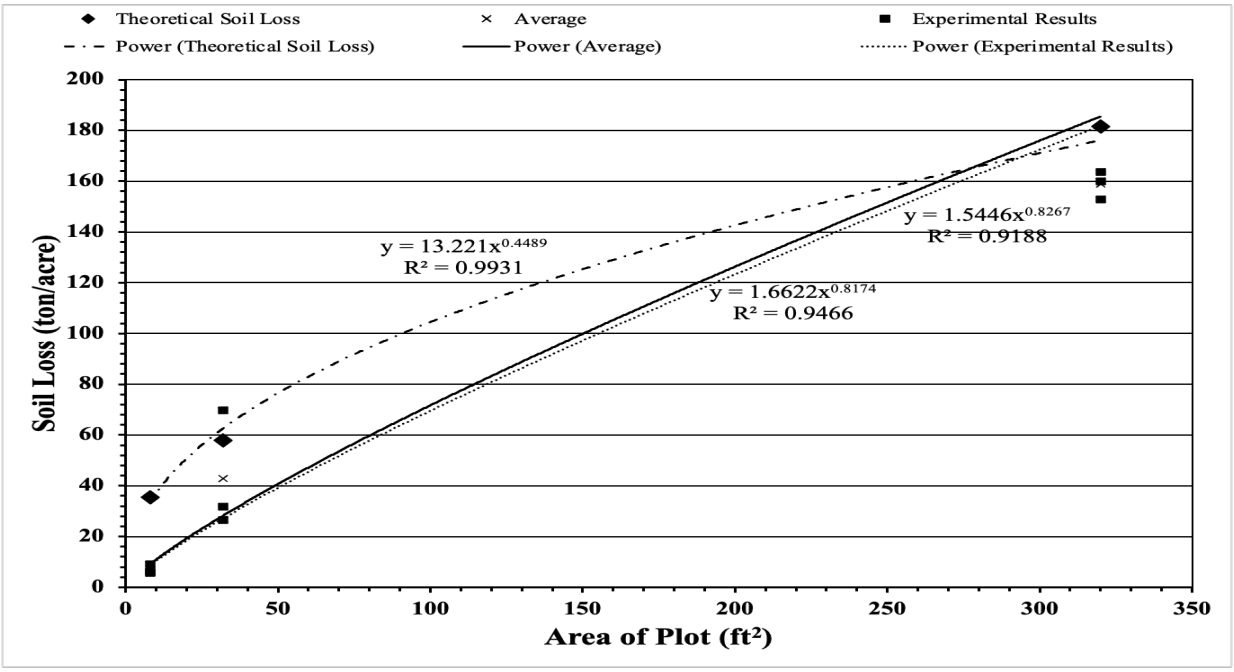

Figure 5-5 Soil Loss Per Area (ton/acre) vs. Area of Plot – Theoretical and Experimental

To further investigate the relationship between soil loss and the length of the plot, the soil loss was plotted against the horizontal projection of the slope length, λ (Table 5-3). The results are shown in Figure 5-6 below. The theoretical soil loss trendline follows a definite power function with a coefficient of 13.702 and an exponent of 0.7105. By simply plotting the trendline of the experimental soil losses, the data are skewed due to the wide variation in λ, and the overall limited number of data points. However, by using the theoretical soil losses as a guide, the experimental soil losses were fit to a power function in two different methods. The first method was to maintain the exponent of the theoretical equation (0.7105) and use the Solver function of Excel to determine the optimum value of the coefficient. This is accomplished through minimizing the root of the mean squares between experimental and fitted/calculated soil loss. The second method was to use

the Solver function of Excel to determine the optimum values of both the exponent and coefficient. The results are tabulated in Table 5-5 below.

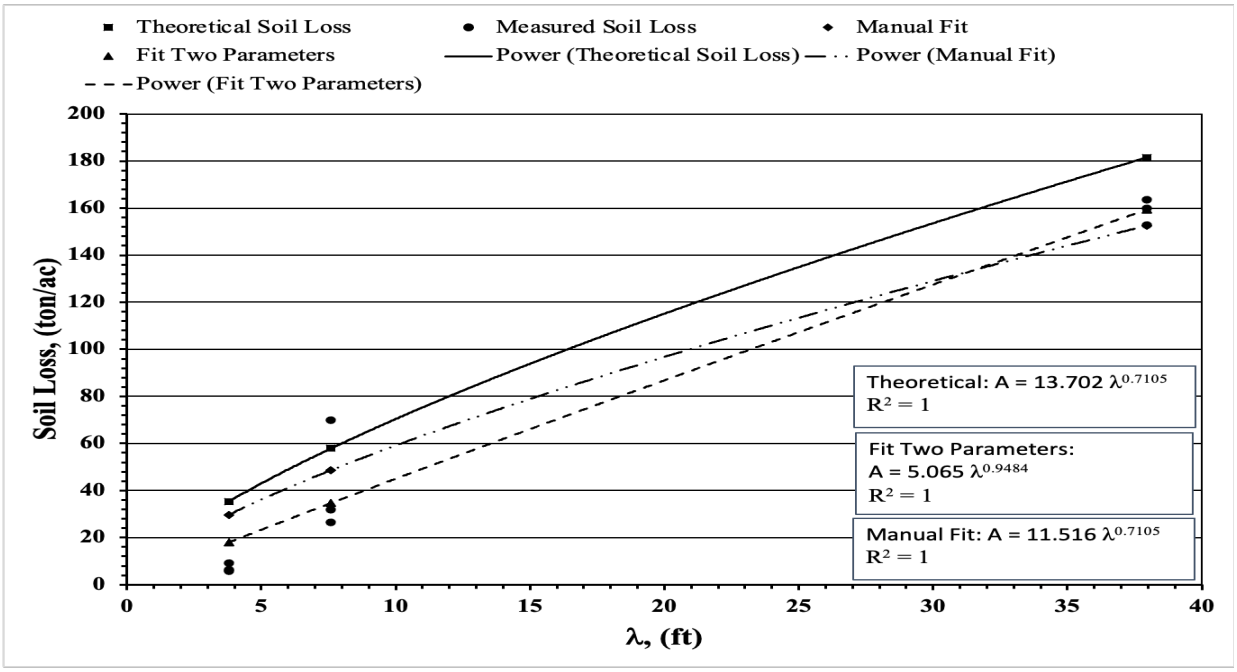

Figure 5-6 Theoretical and Experimental Soil Loss vs. Horizontal Projection of Slope Length, λ for All Plot Sizes Including Fitted Equations

Table 5-5 Numerical Solution for Power Function Fitting of Measured Soil Loss Data

		Manual Fit				Fit Two Parameters	
λ, ft (m)	Measured Soil Loss, ton/ac. (tonnes/ha)	Calculated Soil Loss from Equation, ton/ac. (tonnes/ha)	Square of Difference $[ton/ac.]^2$ $(tonnes/ha)^2$		λ, ft (m)	Calculated Soil Loss from Equation, ton/ac. (tonnes/ha)	Square of Difference $[ton/ac.]^2$ $(tonnes/ha)^2$
3.8 (1.16)	9.1 (20.4)	29.7 (66.59)	423.1 (2133.07)		3.8 (1.16)	17.9 (40.1)	77.6 (389.3)
3.8 (1.16)	6.3 (14.12)	29.7 (66.59)	549.1 (2752.35)		3.8 (1.16)	17.9 (40.1)	136.3 (676.4)
3.8 (1.16)	5.7 (12.78)	29.7 (66.59)	577.6 (2895.3)		3.8 (1.16)	17.9 (40.1)	150.6 (748.2)
7.6 (2.32)	26.6 (59.64)	48.6 (108.96)	486.3 (2432.86)		7.6 (2.32)	34.6 (77.6)	65.2 (321.7)
7.6 (2.32)	31.8 (71.3)	48.6 (108.96)	281.2 (1418.7)		7.6 (2.32)	34.6 (77.6)	7.8 (39.4)
7.6 (2.32)	69.8 (156.49)	48.6 (108.96)	448.1 (2259.14)		7.6 (2.32)	34.6 (77.6)	1235.3 (6228.1)
38 (11.58)	152.9 (342.8)	152.5 (341.91)	0.1 (0.8)		38 (11.58)	159.3 (357.2)	41.9 (205.9)
38 (11.58)	163.6 (366.79)	152.5 (341.91)	123.3 (619.32)		38 (11.58)	159.3 (357.2)	18.3 (92.9)
38 (11.58)	159.9 (358.5)	152.5 (341.91)	55.2 (275.25)		38 (11.58)	159.3 (357.2)	0.4 (1.8)
Exponent	**Calculated Coefficient**	**Root of Mean Squares**			**Exponent**	**Calculated Coefficient**	**Root of Mean Squares**
0.7105	11.516	18.09			0.948	5.065	13.9

The fitting of the experimental data (soil loss versus λ) to the power functions of the Manual Fit analysis results in a uniform 16 percent error when compared to the theoretical soil loss; whereas, when compared to the Fit of the Two Parameters equation, the percent error is nearly 50 percent at the small-scale plots. As the λ value increases, the percent error of the Fit of the Two Parameters equation begins to converge as indicated by the reduction in the percent error to 40.2 percent for the intermediate scale plots and 12.2 for the large-scale plots.

5.2.2.1 Determination of Experimental K-factor

In order to validate the assumption of the *K*-factor, 0.32, used to develop the theoretical soil loss, calculations were performed to determine the experimental *K*-factor using the following equation:

$$K = \frac{A}{R \cdot L \cdot S \cdot C \cdot P} \tag{19}$$

For the large-scale and intermediate-scale plot sizes, the experimental *K*-factor was determined to be 0.28 and 0.24, respectively. For the small-scale plot size, however, the experimental K-factor was determined to be 0.06. This is due to the lack of rill erosion exhibited on the small-scale plots. The flow length is inadequate to allow for the transportation of the dislodged sediment caused by splash erosion.

5.2.3 Total Discharge from Test Plots

The total runoff of each plot size was collected every three minutes throughout the duration of each test. The test data for each plot size was then recorded and averaged for each respective plot size. The discharge was then normalized over the area of the plot size. The average runoff per unit area was then plotted against the time for each respective plot size and is shown below in Figure 5-7. The total discharge of all plot sizes follows the same general trajectory. However, over time, the discharge from the large-scale plots begins to increase at a more rapid rate when compared to the other two plot sizes. During the second rainfall interval, the slope of the curve of the large-scale plots increases dramatically at a rate of nearly 0.125 gal/ft^2/min. (5.10 L/m^2/min) compared to approximately only 0.075 gal/ft^2/min. (3.06 L/m^2/min) for the intermediate scale plots. Since the test plots were evaluated under the same rainfall simulator; thereby ensuring the volume of the rainfall per unit area is consistent for all plot sizes, the variance in discharge per unit

area shows that the large-scale plots in fact have a larger response factor to the rainfall event than the intermediate- and small-scale plots.

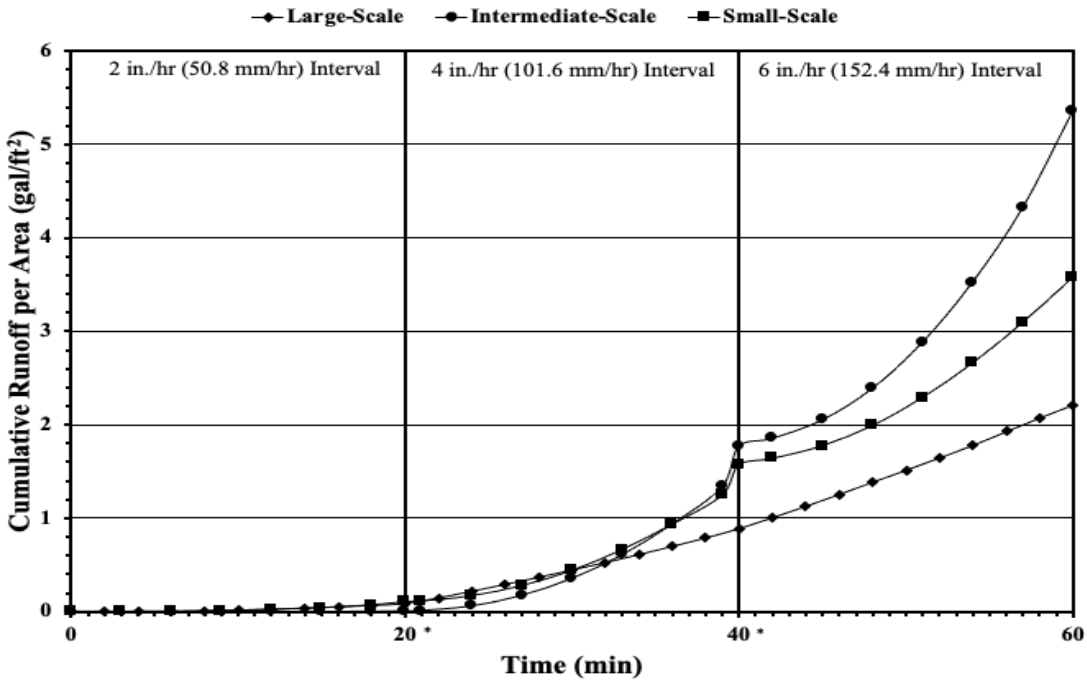

('*' – Denotes 15-minute rest interval for data collection)

Figure 5-7 Cumulative Runoff per Unit Area versus Time for Bare Soil Plots

The cumulative runoff rate by unit area is shown below in Table 5-6. The small-scale plots of produced approximately 71% of the runoff of the large-scale plots when compared by the unit area; whereas, the intermediate-scale plots produced approximately 86%. These results indicate that the small-scale plots are providing a much lower representation of the total discharge generated per unit area as compared to the intermediate-scale plots and the large-scale plots.

Table 5-6 Cumulative Runoff per Unit Area for Each Plot Size

Plot Size	Peak Runoff per unit area, gal/ft² (L/m²)	Percent Difference, %
Large	6.65 (271.2)	-
Intermediate	5.75 (234.3)	14%
Small	4.70 (191.5)	29%

5.2.4 Turbidity and TSS

Turbidity and TSS were also captured through grab samples from each bare soil control test plot every three minutes throughout the duration of the test. The results obtained from each test was then averaged with the results of the other tests on that specific plot size. This data is shown in Figure 5-8 and Figure 5-9, below. While the turbidity of the sampled runoff generally increased for all plot sizes over the duration of the test, the turbidity of both the small-scale and intermediate-scale plots was significantly less than that of the large-scale plot. The reduced turbidity of the water for both the intermediate-scale and small-scale plots is likely due to the reduced flow length of the excess runoff as it travels down the slope. For the large-scale plots, the travel time of the excess runoff is significantly greater than that of the smaller scale plots; thereby increasing the opportunity for the runoff to transport dislodged sediment.

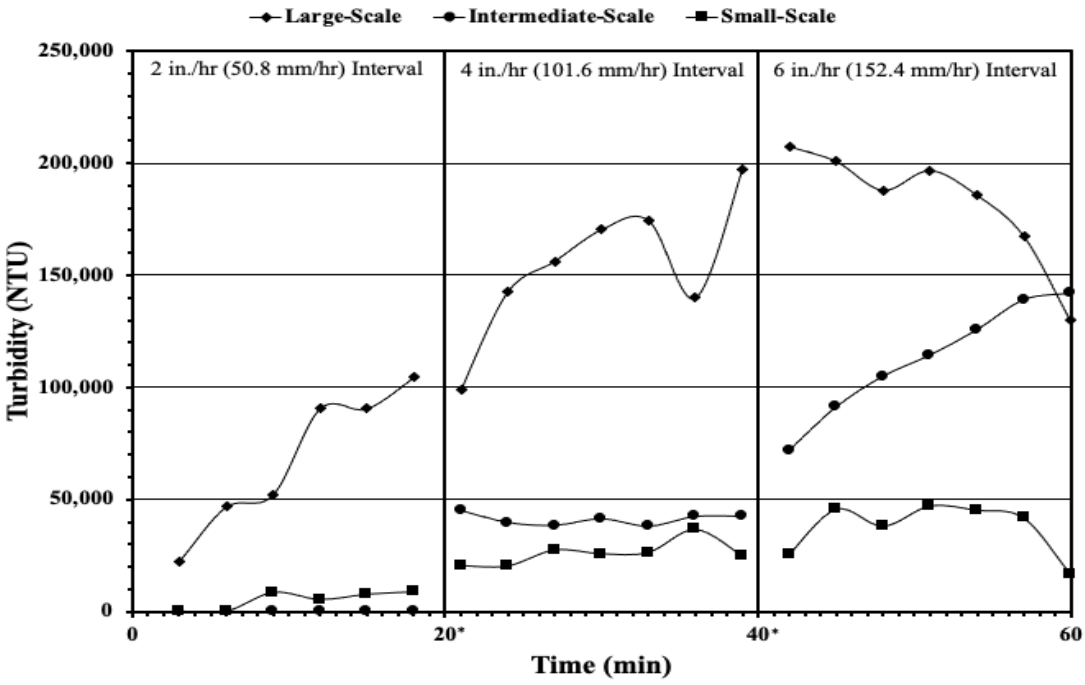

('*' – Denotes 15-minute rest interval for data collection)

Figure 5-8 Average Turbidity for All Plot Sizes

Similarly, the average TSS for each plot size increased over the duration of the test, as the rainfall intensity increased. However, both the small-scale and intermediate-scale plots produced TSS values that were significantly less than the large-scale plots. This data is consistent with the other results described previously which indicate that the small-scale and intermediate-scale plots are not providing similar results when the data is normalized to the area of the respective test plots.

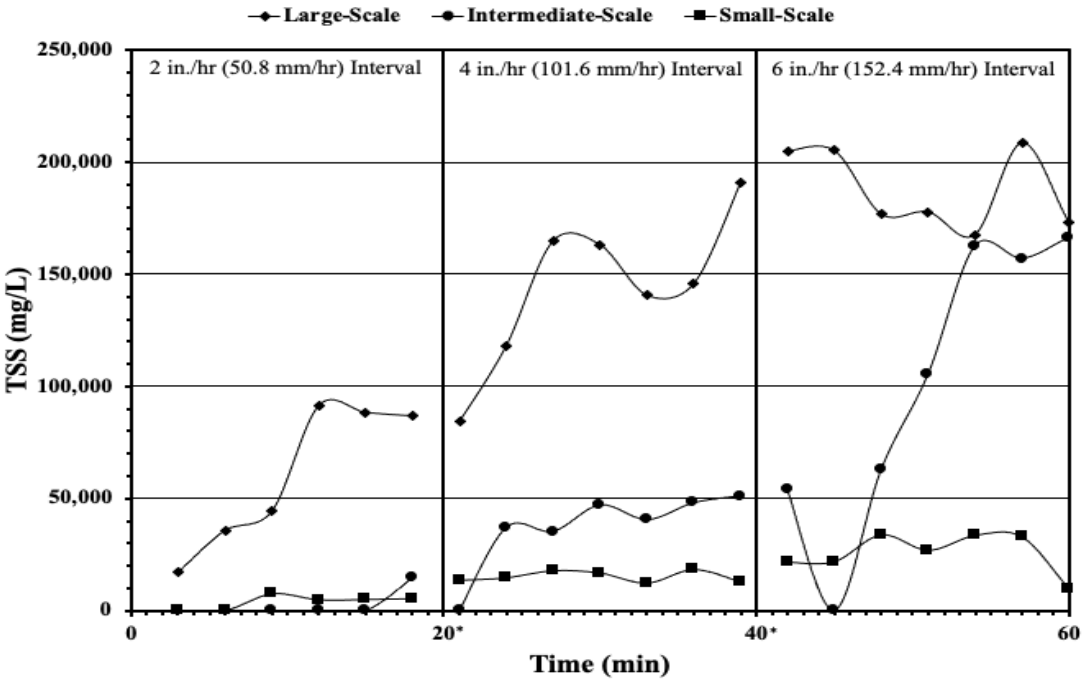

('*' – Denotes 15-minute rest interval for data collection)

Figure 5-9 Average Total Suspended Solids versus Time for Bare Soil Plots

5.3 PLOT SIZE VARIATION OF HYDROMULCH PRODUCTS

For this project, three hydromulch products were applied and tested over loam soil using two different plot sizes of three hundred and twenty square feet (29.7 m^2) and eight square feet (0.74 m^2). Each product was tested on three separate plots of each size. The testing was completed under the same rainfall simulator to minimize error in rainfall energy. For each plot, total soil loss and the total runoff volume were captured. The total soil for each size plot is shown in Table 5-7 below.

Table 5-7 Total Soil Loss by Plot Size for Hydromulch Products over Loam

Average Total Soil Loss per Unit Area lb./ft^2 (kg/m^2)			
	EcoFibre	**Terrawood**	**SoilCover**
Large-Scale	2.24 (10.94)	2.49 (12.16)	2.43 (11.88)
Small-Scale	0.04 (0.22)	0.17 (0.85)	0.07 (0.37)
Percent Difference	98%	93%	97%

One of the key comparisons commonly made during erosion control research has been the percent reduction of soil loss of a cover treatment when compared to a bare soil control plot. This value is typically considered as a cover-factor. According to the manufacturer (LLC 2010), the established maximum cover factor for the tested hydromulch products is 50. The experimental large-scale results in this study closely resemble this recommendation. However, the small-scale results for both EcoFibre and SoilCover far exceed the manufacturer's recommendation as summarized in Table 5-8.

Table 5-8 Plot Size Percent Reduction when Compared to Bare Soil Control

	Percent Reduction		
	EcoFibre	**Terrawood**	**SoilCover**
Large-Scale	56%	45%	50%
Small-Scale	86%	46%	77%
Percent Difference	35%	2.2%	35%

When compared to the large-scale plots, the total soil loss from the small-scale plots is considerably smaller per unit area. The total soil loss per unit area on the small-scale plots was only two to seven percent of the large-scale plots. This is likely due to the hydromulch bonding directly with the top layer of soil particles and holding them in place. Even though the intensity of the rainfall, and subsequently the kinetic energy, is increasing over time in all cases, the shorter

flow length of the small-scale plots prevents the runoff from entering into significant rill erosion as evidenced by Figure 5-10 below.

(a) Large-Scale

(b) Small-Scale

Figure 5-10 Large-Scale and Small-Scale Erosion at Test Conclusion

5.4 HYDROMULCH PRODUCTS OVER LOAM AND TOPSOIL ON SMALL-SCALE PLOTS

For this project, three hydromulch products were applied to small-scale plots in triplicate over topsoil. The testing for the small-scale topsoil plots was completed under the same rainfall simulator as the small-scale loam plots. Total soil loss and total runoff were captured for the small-scale topsoil plots. The total soil loss results for both the small-scale topsoil plots and loam plots are provided in Table 5-9 below.

Table 5-9 Soil Loss Comparison for Hydromulch Products

	2 in./hr (50.8 mm/hr) interval soil loss, lb. (g)	4 in./hr (101.6 mm/hr) interval soil loss, lb. (g)	6 in./hr (152.4 mm/hr) interval soil loss, lb. (g)	Total Soil Loss, lb. (g)
EcoFibre over Topsoil	0.013 (6)	0.106 (48)	0.388 (176)	0.507 (230)
EcoFibre over Loam	0.02 (9)	0.086 (39)	0.251 (114)	0.355 (161)
Percent Difference	-50%	19%	35%	30%
Terrawood over Topsoil	0.084 (38)	0.176 (80)	0.311 (141)	0.569 (258)
Terrawood over Loam	0.132 (60)	0.34 (154)	0.928 (421)	1.4 (635)
Percent Difference	-58%	-93%	-199%	-146%
SoilCover over Topsoil	0.024 (11)	0.088 (40)	0.337 (153)	0.45 (204)
SoilCover over Loam	0.049 (22)	0.201 (91)	0.344 (156)	0.591 (268)
Percent Difference	-100%	-128%	-2%	-31%

As shown on the previous table, the soil loss from topsoil varied significantly when compared to the loam soil. Although a loam soil is specified in ASTM D6459-19 as the preferred test medium, in field practice, final stabilization practices, such as hydromulch, are often applied over topsoil instead of loam or another type of soil. Given the wide variance between the soil loss results of topsoil versus loam and the significant variance between the small-scale and large-scale loam bare soil control test plots, it is likely that if the hydromulch was tested over topsoil on the large-scale test plots, there would be an exponential increase in the volume of soil displaced and transported on the large-scale test plot. Since installation of hydromulch over topsoil is such a common practice, additional studies are required to evaluate the true effectiveness of hydromulch as a stabilization technique on construction sites.

5.5 *C*-FACTORS OF HYDROMULCH PRODUCTS BY PLOT SIZE

In order to evaluate the effectiveness of the tested hydromulch products, each product was evaluated for both large-scale and small-against the bare soil control plots to determine the cover management factor, *C*, utilized in RUSLE. Utilizing the experimental *K*-factor for each scale plot, the *C*-factor was then calculated from RUSLE using Equation (**20)**. The results are tabulated in Table 5-10 below. The *C*-factor for the small-scale plots were significantly smaller for both the EcoFibre and SoilCover products when compared to the large-scale equivalent. This is due to the lack of rill erosion exhibited on the small-scale plots. However, the experimental *C*-factors for the Terrawood product was nearly identical for both large- and small-scale plots. This is due to one small-scale test plot which experienced significantly more soil loss than the other similar plots. If the results from that single test are removed, the *C*-factor for Terrawood would be 0.44.

$$C = \frac{A}{R \cdot K \cdot L \cdot S \cdot P} \qquad \textbf{(20)}$$

Table 5-10 Experimental *C*-factors for Hydromulch Products at Large- and Small-Scale

	Large-Scale	Large-Scale *C*-factor	Small-Scale	Small-Scale *C*-factor
Experimental K-factor	0.28		0.06	
Experimental Bare Soil Control Plots Average Soil Loss, ton/ac (kg/ha)	158 (354,121)		7.03 (15,756)	
EcoFibre Experimental Average Soil Loss, ton/ac (kg/ha)	70.6 (158,234)	0.44	0.966 (2,165)	0.15
SoilCover Experimental Average Soil Loss, ton/ac (kg/ha)	79.2 (177,509)	0.5	1.609 (3,606)	0.24
Terrawood Experimental Average Soil Loss, ton/ac (kg/ha)	88.1 (197,456)	0.55	3.811 (8,541)	0.58

5.6 SUMMARY

Several variables were considered when comparing the experimental bare soil control results from each plot scale. The most significant relationship between the soil loss and the variables considered was the relationship to the horizontal projection of the slope length, λ. Utilizing the theoretical discharge from RUSLE, an equation was developed to identify relationship between soil loss and λ. The experimental data suggests that the soil loss is a function of the horizontal projection of the slope length as detailed in Table 5-5, above, and Equation (22, below.

The *K*-factor for the experimental soil was calculated to be 0.28 on the large-scale plots and 0.24 on the intermediate-scale plots. This is consistent with the suggested nomograph provided in RUSLE ($K = 0.32$). For the small-scale plots, however, the calculated *K*-factor was significantly less (0.06). Based on the literature provided in RUSLE, RUSLE is intended to calculate both sheet erosion and rill erosion. However, based on the visual inspection of the small-scale plots, minimal

rill erosion was present throughout the duration of the test. This supports the finding of the soil loss being a function of the horizontal projection of the flow length.

The *C*-factor was determined from the experimental data for the hydromulch products tested over loam. For the large-scale test plots, the *C*-factor was determined to be near the manufacturer's recommendation of 0.5. However, for the small-scale plots, the *C*-factor was calculated to be significantly lower for two of the products (EcoFibre 0.15, SoilCover 0.24). Terrawood returned a *C*-factor of 0.58 which closely resembled the factors calculated on the large-scale test plots.

6 CONCLUSIONS AND RECOMMENDATIONS

The overall goal of this research was to compare the test results of different size erosion control plots under rainfall simulation to determine if there is a direct relationship to the size of a tested erosion control plot and the experimental results. This goal was accomplished through the development of a large-scale rainfall simulator (8 ft width by 40 ft length [2.4 m by 12.2 m) to test both bare soil control plots as well as three separate hydromulch products in triplicate. The large-scale rainfall simulator was also utilized to deliver the required rainfall on small-scale plots (2 ft in width and 4 ft in length [0.6 m by 1.2 m]) for both bare soil control plots and the same hydromulch products as were tested on the larger scale. In addition, three bare soil control plots were also tested under the same rainfall simulator for an intermediate-scale test plot (4 ft in width by 8 ft in length [1.2 m by 2.4 m]).

It was determined through experimentation that the large-scale bare soil plots had an average soil loss of 2,333 lb. (7.29 lb./ft^2 [1,058 kg or 35.6 kg/m^2]). The small-scale bare soil plots had an average soil loss of 2.58 lb. (0.323 lb./ft^2 [1.17 kg or 1.58 kg/m^2]). The intermediate scale bare soil plots had an average soil loss of 62.8 lb. (1.96 lb./ft^2 [28.5 kg or 9.56 kg/m^2]). The significant difference in soil loss per unit area can be attributed to the various stages of erosion found in the test plots. The large-scale plots experienced significant rill erosion and the early signs of gully erosion; whereas the small-scale plots experienced very limited rill erosion. An analysis was conducted to determine the relationship between the soil loss for each size test plot and the distance λ as defined in RUSLE. The theoretical soil loss for each plot resulted in the following relationship:

$$A_{Theoretical} = 13.702\lambda^{0.7105} \qquad (21)$$

Through data analysis, the optimum equation for the experimental data given the nine sample points was determined to be:

$$A_{Experimental} = 5.065\lambda^{0.9484} \quad (22)$$

Overall, the experimental soil loss data was found to compare well with the theoretical soil loss estimated through RUSLE. The theoretical *K*-factor as determined in RUSLE was calculated to be 0.32. The experimental *K*-factor was determined to be 0.28 and 0.24 for the large-scale and intermediate-scale simulations, respectively. However, the *K*-factor for the small-scale plots was estimated at only 0.06. This determination supports the theory that in order to accurately evaluate different erosion control products, testing should be conducted on larger scale test plots.

The next objective was to evaluate the percent reduction of three separate hydromulch products over two different scale test plots when compared to a bare soil control. The large-scale tests resulted in *C*-factors of 0.44, 0.50 and 0.55 for EcoFibre HM, SoilCover HM, and Terrawood HM, respectively. These values are in line with the manufacturer's recommendation of a maximum *C*-factor of 0.50. The small-scale tests however, resulted in *C*-factors of 0.15, 0.24 and 0.58 for EcoFibre HM, SoilCover HM, and Terrawood HM, respectively. The results for both EcoFibre HM and SoilCover HM are likely caused by the lack of minimal rill erosion experienced on the small-scale plots.

The hydromulch products were tested on small-scale plots for both loam and topsoil. The soil loss from the topsoil plots varied significantly when compared to the loam soil. The average soil loss for the topsoil plots when compared to the loam plots ranged from 30% to 146%. Although a loam soil is specified in ASTM D6459-19 as the preferred testing medium, field practice dictates that hydromulch and other soil stabilization practices are applied to topsoil. Given the variance of the soil loss, it is safe to say that additional testing is required to evaluate the effectiveness of hydromulch on topsoil and reliance on loam as a testing medium may provide inaccurate results in field practice.

In summary, the large-scale rainfall plots performed as expected in regard to standards across the industry. The hydromulch products tested resulted in *C*-factors consistent with manufacturer recommendations. The bare soil control plots also similarly resulted in soil loss results similar to the theoretical soil loss calculated using RUSLE. However, the small-scale plots and intermediate-scale plots did not produce similar results. The expected soil loss for the small-scale plots was significantly less than the theoretical soil loss. In addition, the calculated *C*-factors for two of the hydromulch products tested were significantly less than the manufacturer's recommendations. All of the results point to the fact that the limited slope length of the small- and intermediate-scale plots significantly impacts the erosion processes on the slope and subsequently the soil loss.

6.1 LIMITATIONS OF STUDY AND FUTURE RESEARCH

This study has presented the findings of measuring the soil loss for large-, intermediate-, and small-scale test plots under a single rainfall simulator. During the testing and analytical processes, several conditions were noted where improvements could be made to further the development of the research:

1) Given the difference in scale of the tested control plots, additional research is needed on plot sizes between the experimental intermediate-scale (4 ft in width by 8 ft in length [1.2 m by 2.4 m]) and the experimental large-scale (8 ft in width by 40 ft in length [2.4 m by 12.2 m]). Additional data points in this area would provide further confirmation of the analysis herein on the relationship of λ to total soil loss.
2) Further investigation should be completed on the testing of hydromulch products over topsoil. In most instances, hydromulch is field applied to slopes which are dressed in topsoil, to encourage permanent vegetation growth. The experimental results conducted in this study resulted in a percent difference ranging from 2 to nearly 200 percent when

comparing hydromulch application over topsoil to loam. Additional testing should be conducted on the large-scale plots to verify the findings and make recommendations.

3) Further discussion and investigation should be completed to evaluate the intensity of the rainfall events used for testing. As evidenced by the continued degradation of the hydromulch product on the large-scale test plots as the intensity of rainfall increased, further discussion is warranted to determine if the design intent of hydromulch (which is a temporary soil stabilization measure) is exceeded by the tested rainfall.
4) Given the temporary purpose of hydromulch to function as a soil stabilization measure to aid in the establishment of permanent vegetation, future research should be conducted to evaluate the use of hydromulch in conjunction with other biological (seed) means of permanent soil stabilization. The use of hydromulch could then be compared with other chemical and mechanical means of temporary soil stabilization to evaluate the effectiveness of erosion control in conjunction with permanent vegetation.
5) The wind screens on the existing rainfall simulator should be improved to lessen the amount of prep time required to test products. The wind screens are a critical component of the rainfall simulator in order to minimize the impact of wind on the falling raindrops. Currently, the system is extremely manual, although improvements were made during this study to modify the method of attachment of the curtains to the steel cables. Ideally, the curtains would be equipped with a mechanized pulley system which would dramatically reduce the deployment and retraction times of the simulator.
6) The control box should be relocated outside of the wind screens of the rainfall simulator. During the final two intervals of testing, the area around the control box becomes

saturated and slippery. If the control box was simply relocated outside of the wind screens, the intervals could be operated manually without entering the testing area.

7) The side slopes of the large-scale test plot should be improved to allow access to mechanized equipment to repair/modify the testing slope. Currently, a significant amount of manual labor is required to prepare the slopes for testing as well as any modification to the test soil. If the test plot was accessible to mechanized equipment, the required delay between tests could be reduced.

6.2 ACKNOWLEDGEMENTS

This research is based on a study sponsored by Alabama Department of Transportation. The author greatly acknowledges the financial support. The findings, opinions, and conclusions expressed in this report are those of the author and do not necessarily reflect the view of the sponsor.

7 REFERENCES

Agriculture, United States Department of. 1997. *Predicting Soil Erosion by Water: A Guide to Conservation Planning With the Revised Universal Soil Loss Equation (RUSLE)*.

Alabama Soil and Water Conservation Committee, (ASWCC). 2009. *Alabama Handbook for Erosion Control, Sediment Control, and Stormwater Management on Construction Site and Urban Areas: Volume 2*. Montgomery, Alabama.

ALDOT. 2018. *Standard Specifications for Highway Construction*.

Angulo-Martinez, M., S. Begueria, A. Navas, and J. Machin. 2012. "Splash Erosion under Natural Rainfall on Three Soil Types in NE Spain." *Geomorphology* 175–176:38–44.

Angulo-Martínez, M., S. Beguería, A. Navas, and J. Machín. 2012. "Splash Erosion under Natural Rainfall on Three Soil Types in NE Spain." *Geomorphology* 175–176:38–44.

ASTM International. 2009. *ASTM D1557-09, Standard Test Methods for Laboratory Compaction Characteristics of Soil Using Modified Effort (56,000 Ft-Lbf/Ft3 (2,700 KN-m/M3))*. West Conshohocken, Pennsylvania.

ASTM International. 2019. *ASTM D-6459-19: Standard Test Method for Determination of Erosion Control Blanket (ECB) Performance in Protecting Hillslopes from Rainfall-Induced Erosion*. West Conshohocken, Pennsylvania.

Babcock, D. L. and R. A. McLauglin. 2011. "Runoff Water Quality and Vegetative Establishment for Groundcovers on Steep Slopes." *Journal of Soil and Water Conservation* 66(2):132–41.

Babcock, D. and R. A. McLauglin. 2013. "Erosion Control Effectiveness of Straw, Hydromulch, and Polyacrylamide in a Rainfall Simulator." *Journal of Soil and Water Conservation* 68(3):221–27.

Babcock, D. and R. A. McLauglin. 2019. "Mulch Options for Erosion Control on Construction

Sites." Retrieved November 24, 2019 (https://content.ces.ncsu.edu/mulch-options-for-erosion-control-on-construction-sites).

Benik, S. R., B. N. Wilson, D. D. Biesboer, B. Hansen, and D. Stenlund. 2003. "Performance of Erosion Control Products on a Highway Embankment." *Transactions of the ASAE* 46(4):1113–19.

Bentley, W. A. 1904. "Studies of Raindrops and Raindrop Phenomena." *Monthly Weather Review* 32:450–56.

Birt, L. N., R. A. Persyn, and P. K. Smith. 2007. "Evaluation of an Indoor Nozzle - Type Rainfall Simulator." *Applied Engineering in Agriculture* 23(3):283–87.

Box, J. E. Jr. and R. R. Bruce. 1996. "The Effect of Surface Cover on Infiltration and Soil Erosion." Pp. 107–23 in *Soil Erosion, Conservation and Rehabilitation*, edited by M. Aggasi. New York: Dekker.

Brady, N. C. and R. R. Weil. 2014. *The Nature and Properties of Soils*. 14th ed. Upper Saddle River, New Jersey: Prentice Hall.

Bruce, R. R., G. W. Langdale, L. T. West, and W. P. Miller. 1995. "Surface Soil Degradation and Soil Productivity Restoration and Maintenance." *Soil Science Society of America Journal* 59:654–60.

Bubenzer, G. D. 1979. "Rainfall Characteristics Important for Simulation." Pp. 22–34 in *Proceedings of the Rainfall Simulator Workshop*. Tuscon, AZ.

Bubenzer, G. D. and L. D. Meyer. 1965. "Simulation of Rainfall and Soils for Laboratory Research." *Transactions of the ASABE* 8(1):73.

Bubuenzer, G. D. n.d. "Inventory of Rainfall Simulators." *Proceedings of the Rainfall Simulator Workshop* 120–30.

Buxton, H. and F. T. Caruccio. 1979. *Evaluation of Selective Erosion Control Techniques*. Cincinnati, Ohio.

Clopper, P. E., M. Vielleux, and T. Johnson. 2001. "Quantifying the Performance of Hillslope Erosion Control Best Management Practices." *American Society of Civil Engineering*.

Company, American Excelsior. n.d. "Erosionlab."

Covert, A. and P. Jordan. 2009. "A Portable Rainfall Simulator: Techniques for Understanding the Effects of Rainfall on Soil Erodibility." *Watershed Management Bulletin* 13(1):5–9.

District, Mile High Flood. 2010. "Chapter 7 Construction BMPs." Retrieved November 24, 2019 (https://udfcd.org/wp-content/uploads/uploads/vol3 criteria manual/Chapter 7 Construction BMPs.pdf).

Early, Justin J., Paul E. Clopper, and Anthony Johnson. 2003. "Quantitative Erosion Contorl Product Testing Under Simulated Rainfall." Conference paper in the International Erosion Control Association (IECA) 2003 conference.

Eck, B., M. Barrett, A. McFarland, and L. Hauck. 2010. "Hydologic and Water Quality Aspects of Using a Compost/Mulch Blend for Erosion Control." *Journal of Irrigation and Drainage Engineering* 136(9):646–55.

Elbasit, M. A., C. S. Ojha, Z. Ahmed, H. Yasuda, A. Salmi, and F. Ahmed. 2015. "Rain Microstructure and Erosivity Relationships under Pressurized Rainfall Simulator." *Journal of Hydrologic Engineering* 20(6):6015001–6.

Erosion Control Technology Council, (ECTC). 2008. "Erosion Control Product Categories." Retrieved November 24, 2019 (https://www.ectc.org/product-selection-by-category).

Faulkner, Brian. 2020. "Evaluation of Erosion Control Practices under Large-Scale Rainfall Simulation Following ASTM D6459 Standard Test Methods." Auburn University.

Fernández-Raga, M., J. Ocampo, J. Rodrigo-Comino, and Saskia D. Keesstra. 2019. “Rainfall Simulation Experiments : A Laboratory Study.” *Water* 11(1228):1–21.

Foltz, R. B. and J. H. Dooley. 2003. “Comparison of Erosion Reduction Between Wood Strands and Agricultural Straw.” *Transactions of the ASABE* 46(5):1389–96.

Gascho, G. J., R. D. Wauchope, J. G. Davis, C. C. Truman, C. C. Dowler, J. E. Hook, H. R. Sumner, and A. W. Johnson. 1998. “Nitrate - Nitrogen, Soluble, and Bioavailable Phosphorus Runoff from Simulated Rainfall After Fertilizer Application.” *Soil Science Society of America Journal* 62:1711–18.

Grismer, M. 2012. “Standards Vary in Studies Using Rainfall Simulators to Evaluate Erosion.” *California Agriculture* 66(3):102–7.

Holt, G. A., M. Buser, D. Harmel, K. Potter, and M. Pelletier. 2005. “Comparison of Cotton-Based Hydro-Mulches and Conventional Wood and Paper Hydro-Mulches-Study 1.” *The Journal of Cotton Science* 9:121–27.

Holt, G. A. and J. W. Laird. 2002. “COBY Products and a Process for Their Manufacture.”

Horne, M. 2017. “Design and Construction of a Rainfall Simulator for Large - Scale Testing of Erosion Control Practices and Products.” Auburn University.

Keeper, Mobile Bay. 2017. “Construction Site Stormwater.” Retrieved November 13, 2020 (https://www.mobilebaykeeper.org/construction-stormwater).

Keizer, J. J., F. C. Silva, D. C. S. Vieira, O. González-Pelayo, I. Campos, A. M. D. Vieira, S. Valente, and S. A. Prats. 2018. “The Effectiveness of Two Contrasting Mulch Application Rates to Reduce Post-Fire Erosion in a Portuguese Eucalypt Plantation.” *Catena* 169(January):21–30.

Kim, K. S., J. D. Choi, and K. S. Kweon. 2001. “Effect of PAM Application on Soil Erosion of a

Sloping Field with a Chinese Cabbage Crop." in *ASAE Annual International Meeting*. Sacramento, CA.

Landloch. 2002. "Studies of Hydromulch Effectiveness." *National Centre for Engineering in Agriculture Publication* 1000455(1).

Lascano, R. J., J. T. Vorheis, R. L. Baumhardt, and D. R. Salisbury. 1997. "Computer - Controlled Variable Intensity Rain Simulator." *Soil Science Society of America Journal* 61(4):1182–89.

Laws, J. O. and D. A. Parsons. 1943. "The Relation of Raindrop Size to Intensity." *Transactions of the American Geophysical Union* 24:452–60.

Lee, G., R. A. McLaughlin, K. D. Whitely, and V. K. Brown. 2018. "Evaluation of Seven Mulch Treatments for Erosion Control and Vegetation Establishment on Steep Slopes." *Journal of Soil and Water Conservation* 73(4):434–42.

Lipscomb, C. M., T. Johnson, R. Nelson, and T. Lancaster. 2006. "Comparison of Erosion Control Technologies: Blown Straw vs. Erosion Control Blankets." *Land and Water*.

LLC, PROFILE Products. 2010. "Section 32 92 16.16 - Hydraulic Seeding: Hydraulic Mulch - Wood with Tackifier Specification." 3.

Mannering, J. V. and L. D. Meyer. 1963. "The Effects of Various Rates of Surface Mulch on Infiltration and Erosion." *Soil Science Society of America Journal* 29:84–85.

McCullough, Sarah A. and Bryan A. Endress. 2012. "Do Postfire Mulching Treatments Affect Plant Community Recovery in California Coastal Sage Scrub Lands?" *Environmental Management* 49(1):142–50.

McLauglin, R. A. and T. T. Brown. 2006. "Evaluation of Erosion Control Products with and without Added Polyacrylamide." *Journal of the American Water Resources Association* 42(3):675–84.

McLauglin, R. A., N. Rajbhandari, W. F. Hunt, D. E. Line, R. E. Sheffield, and N. M. White. 2001. "The Sediment and Erosion Control Research and Education Facility at North Carolina State University." in *Soil Erosion Research for the 21st Century, Proceedings of the International Symposium*. Honolulu, HI.

Megahan, Walter F., Monte Wilson, and Stephen B. Monsen. 2001. "Sediment Production from Granitic Cutslopes on Forest Roads in Idaho, USA." *Earth Surface Processes and Landforms* 26(2):153–63.

Meshesha, Derege Tsegaye, Atsushi Tsunekawa, Mitsuru Tsubo, Nigussie Haregeweyn, and Firew Tegegne. 2016. "Evaluation of Kinetic Energy and Erosivity Potential of Simulated Rainfall Using Laser Precipitation Monitor." *Catena* 137:237–43.

Meyer, L. D. 1965. "Simulation of Rainfall for Soil Erosion Research." *Transactions of the ASABE* 8(1):63–65.

Meyer, L. D. 1988. "Rainfall Simulators for Soil Conservation Research." Pp. 75–95 in *Soil Erosion Research Methods*, edited by R. Lal. Ankeny, Iowa: Soil and Water Conservation Society.

Meyer, L. D. and W. C. Harmon. 1979. "Multiple - Intensity Rainfall Simulator for Erosion Research on Row Sideslopes." *Transactions of the ASABE* 22(1):100–103.

Meyer, L. D., W. H. Wischmeier, and G. R. Foster. 1970. "Mulch Rates Required for Erosion Control on Steep Slopes." *Soil Science Society of America Journal* 34:928–30.

Miller, W. P. 1987. "A Solenoid-Operated, Variable Intensity Rainfall Simulator." *Soil Science Society of America Journal* 51(3):832–34.

Ming-Han, L., C. L. Harlow, and M. Jett. 2003. "Comparison of Field and Laboratory Experiment Test Results for Erosion Control Products." in *ASAE Annual International Meeting*. St.

Joseph, MI.

Moore, I. D., M. C. Hirschi, and B. J. Barfield. 1983. “Kentucky Rainfall Simulator.” *Transactions of the ASABE* 26(4):1085–89.

Morgan, R. and J. Rickson. 1988. “Soil Erosion Control: Importance of Geomorphological Information.” Pp. 51–60 in *Geomorphology in Environmental Planning*, edited by J. M. Hooke. Chichester: Wiley.

Mutchler, C. K. and L. F. Hermsmeier. 1965. “A Review of Rainfall Simulators.” *Transactions of the ASABE* 8(1):67–68.

Mutchler, C. K., C. E. Murphree, and K. C. McGregor. 1994. “Laboratory and Field Plots for Erosion Research.” Pp. 11–37 in *Soil Erosion Research Methods*, edited by R. Lal. Ankeny, Iowa: Soil and Water Conservation Society.

National Cooperative Highway Research Program, (NCHRP). 1980. “Erosion Control During Highway Construction - Research Report.”

Novotny, V. 2003. *Water Quality: Diffuse Pollution and Watershed Management*. New York, New York: John Wiley & Sons, Inc.

Paige, G. B., J. J. Stone, J. R. Smith, and J. R. Kennedy. 2003. “The Walnut Gulch Rainfall Simulator: A Computer-Controlled Variable Intensity Rainfall Simulator.” *Transactions of the ASAE* 20(1):25–31.

Pall, R., W. T. Dickinson, D. Beals, and R. McGirr. 1983. “Development and Calibration of a Rainfall Simulator.” *Canadian Agricultural Engineering* 25:181–87.

Pearce, R. A., G. W. Frasier, M. J. Trlica, W. C. Leininger, J. D. Stednick, and J. L. Smith. 1998. “Sediment Filtration in a Montane Riparian Zone Under Simulated Rainfall.” *Journal of Range Management* 51(3):309–14.

Pitt, Robert, Shirley Clark, and Donald Lake. 2007. *Construction Site Erosion and Sediment Controls*. Lancaster, Pennsylvania: DEStech Publications, Inc.

Prats, Sérgio Alegre, Maruxa Cortizo Malvar, Diana Catarina Simões Vieira, Lee MacDonald, and Jan Jacob Keizer. 2016. "Effectiveness of Hydromulching to Reduce Runoff and Erosion in a Recently Burnt Pine Plantation in Central Portugal." *Land Degradation and Development* 27(5):1319–33.

Rade, Lennart and Bertil Westergren. 1990. *Beta Mathematics Handbook*. 2nd ed. Boca Raton: CRC Press.

Regmi, T. P. and A. L. Thompson. 2000. "Rainfall Simulator for Laboratory Studies." *Applied Engineering in Agriculture* 16(6):641–47.

Ricks, M., M. Horne, B. Faulkner, W. Zech, X. Fang, W. Donald, and M. Perez. 2019. "Design of a Pressurized Rainfall Simulator for Evaluating Performance of Erosion Control Practices." *Water* 11 (11)(Rainfall Erosivity in Soil Erosion Processes):2386.

Ricks, Matthew D., Wesley T. Wilson, Wesley C. Zech, Xing Fang, and Wesley N. Donald. 2020. "Evaluation of Hydromulches as an Erosion Control Measure Using Laboratory-Scale Experiments." *Water (Switzerland)* 12(2):1–17.

Rickson, R. J. 1995. "Simulated Vegetation and Geotextiles." Pp. 95–131 in *Slope Stabilization and Erosion Control: A Bioengineering Approach*, edited by R. Morgan and R. Rickson. London: Spon.

Risse, M. and B. Faucette. 2001. "Compost Utilization for Erosion Control." *University of Georgia Cooperative Extension Service Bulletin 1200*.

Robichaud, P. R., S. A. Lewis, J. W. Wagenbrenner, L. E. Ashmun, and R. E. Brown. 2013. "Post-Fire Mulching for Runoff and Erosion Mitigation Part I: Effectiveness at Reducing Hillslope

Erosion Rates." *Catena* 105:75–92.

Scholl, Bryan N., Greg Holt, and Chris Thornton. 2012. "Screening Study of Select Cotton-Based Hydromulch Blends Produced Using the Cross-Linked Biofiber Process." *Journal of Cotton Science* 16(4):249–54.

Scholl, Bryan N., Greg Holt, Chris Thornton, and Sara Duke. 2013. "Hydromulch Blends Using Agricultural Byproducts: Performance Implications of Cotton Quantity." *Journal of Cotton Science* 17(4):302–8.

Service, National Resource Conservation. n.d. "Ephemeral Gullies and Rills - Definitions." Retrieved October 27, 2020 (https://www.google.com/url?sa=t&rct=j&q=&esrc=s&source=web&cd=&ved=2ahUKEwjR-q6gkNbsAhVLc98KHd3LDoEQFjAPegQIARAC&url=https%3A%2F%2Fwww.nrcs.usda.gov%2FInternet%2FFSE_DOCUMENTS%2Fnrcs142p2_023211.doc&usg=AOvVaw2Wc7EgLqv9sXpZ5W4xfhfN).

Sharpley, A. N. and P. Kleinman. 2003. "Effect of Rainfall Simulator and Plot Scale on Overland Flow and Phosphorus Transport." *Journal of Environmental Quality* 32:2172–79.

Shelton, C. H., R. D. Bernuth, and S. P. Rajbhandari. 1985. "A Continuous - Application Rainfall Simulator." *Transactions of the ASABE* 28(4):1115–19.

Shoemaker, A. L. 2009. "Evaluation of Anionic Polyacrylamide as an Erosion Control Measure Using Intermediate-Scale Experimental Procedures." Auburn University.

Shoemaker, A. L., W. C. Zech, and T. P. Clement. 2012. "Laboratory-Scale Evaluation of Anionic Polyacrylamide as an Erosion and Sediment Control Measure on Steep-Sloped Construction Sites." *Transactions of the ASABE* 55(3):809–20.

Singer, M. T., Y. Matsuda, and J. Blackard. 1981. "Effect of Mulch Rate on Soil Loss by Raindrop Splash." *Soil Science Society of America Journal* 45:107–10.

Sprague, C. Joel and James E. Sprague. 2012. “Large-Scale Performance Testing of Erosion Control Products.” in *GeoAmericas 2012*. Lima, Peru.

Sutherland, R. A. 1998. “Rolled Erosion Control Systems for Hillslope Surface Protection: A Critical Review, Synthesis and Analysis of Available Data. I. Background and Formative Years.” *Land Degredation and Development 9* 465–86.

Sutherland, R. A. and A. D. Ziegler. 2006. “Hillslope Runoff and Erosion as Affected by Rolled Erosion Control Systems: A Field Study.” *Hydrological Processes* 20:2839–55.

Swanson, N. P. 1965. “Rotating-Boom Rainfall Simulator.” *Transactions of the ASABE* 8(1):71–72.

Thomas, N. P. and S. A. El Swaify. 1989. “Construction and Calibration of a Rainfall Simulator.” *Journal of Agriculture and Engineering Research* 43(1):1–9.

Turgeon, A. J. 2002. “Turfgrass Management.” in *Turfgrass Management*. Upper Saddle River, New Jersey: Prentice Hall.

Tyner, J. S., D. C. Yoder, B. J. Chomicki, and A. Tyagi. 2011. “A Review of Construction Site Best Management Practices for Erosion Control.” *Transactions of the ASABE* 54(2):441–50.

United States Enviromental Protection Agency, (US EPA). 1997. *Innovative Uses of Compost: Erosion Control, Turf Remediation and Landscaping*. Washington D.C.

United States Environmental Protection Agency, (US EPA). 2000. *2000 National Water Quality Inventory*. Washington D.C.

United States Environmental Protection Agency, (US EPA). 2005a. *Stormwater Phase II Final Rule: An Overview*. Washington D.C.

United States Environmental Protection Agency, (US EPA). 2005b. *Stormwater Phase II Final Rule: Construction Site Runoff Control Minimum Control Measure*. Washington D.C.

United States Environmental Protection Agency, (US EPA). n.d. “Clean Water Act Section 502: General Definitions.” Retrieved December 19, 2019 (https://www.epa.gov/cwa-404/clean-water-act-section-502-general-definitions).

University, Northeast Region Certified Crop Adviser-Cornell. 2010. “Competency Area 5: Soil Conservation AEM.” Retrieved October 27, 2020 (https://nrcca.cals.cornell.edu/soil/CA5/CA0541.1-2.php).

Vaughn, Steven F., James A. Kenar, Frederick C. Felker, Mark A. Berhow, Steven C. Cermak, Roque L. Evangelista, George F. Fanta, Robert W. Behle, and Edward Lee. 2013. “Evaluation of Alternatives to Guar Gum as Tackifiers for Hydromulch and as Clumping Agents for Biodegradable Cat Litter.” *Industrial Crops and Products* 43(1):798–801.

Weggel, J. R. and R. Rustom. 1992. “Soil Erosion by Rainfall and Runoff—State of the Art.” *Geotextiles and Geomembranes* 11:551–72.

Wilson, W. T. 2010. “Evaluation of Hydromulches as an Erosion Control Measure Using Intermediate-Scale Experiments.” Master Thesis, Department of Civil Engineering, Auburn University.

Xiao, M., L. N. Reddi, and J. Howard. 2010. “Erosion Control on Roadside Embankment Using Compost.” *Applied Engineering in Agriculture* 26(1):97–106.

Zech, W. C., J. L. Halverson, and T. P. Clement. 2007. “Development of a Silt Fence Tieback Design Methodology for Highway Construction Installations.” *Journal of the Transportation Research Board Transportation Research Record* 2011:21–28.

8 APPENDICES

8.1 APPENDIX A – TURBIDITY AND TSS PROCESSING PROCEDURES

TURBIDITY AND TSS PROCESSING PROCEDURES

Test Note: *These water quality testing procedures conduct Turbidity and TSS sampling simultaneously to maintain work efficiency and reduce dilution errors.*

Storage Note:Refrigerate water samples for a maximum of 72 hrs. until testing.

TSS Analysis Preparation

Step 1: Prepare glassware, deionized water, filtering apparatus, scales, turbidimeter, and vacuum pump.

Step 2: Prepare and label the required crinkle dishes and place filter membranes on each dish using clean tweezers. Do not use fingers.

Step 3: Prewash filter membranes by placing the filter disc on the filter holder of the filter apparatus with the wrinkled side upward, gridded side down. Attach the top funnel portion of the magnetic filter holder. Apply 10 mL of deionized water and provide suction to filter through membrane. Remove washed filter and place on corresponding crinkle dish. Repeat for all membranes.

Step 4: Place washed membranes in the oven at 103°C for one hour. Remove crinkle dishes and membranes from the drying oven and place in a desiccator and allow to cool to room temperature.

Step 5: Weigh the crinkle dish and filter using an analytical balance. Record weight to the nearest 0.0001 g.

Turbidity Analysis

Step 6: Confirm or recalibrate turbidimeter using standard samples.

Step 7: Vigorously shake the sample bottle to thoroughly mix all sediment in the solution.


Step 8: Transfer sample to 1,000 mL beaker, insert stir bar and place on magnetic stirrer and mix until solution is uniform throughout. Mix continuously through steps 9 though 14.

Step 9: Set the pipette set at 7.5 mL volume and fill turbidity sample cell to the line with 15 mL of solution. Cap the cell.

Step 10: Place the cell into the turbidimeter with the white arrow on the cell facing the black arrow on the unit. Take a turbidity reading on the undiluted sample. If the turbidimeter over ranges, proceed to Step 5.

Step 11: If the sample over ranges: dilute the sample 1:2 by mixing 100 mL of original solution with 100 mL of deionized water in a beaker and mix.

Step 12: Pipette the 1:2 diluted sample into a sample cell. Read the turbidity. If the sample over ranges, repeat step 11-12 until a reading is taken. Record the measured turbidity value and the dilution factor. The dilution factor is calculated as $F = 2^x$, where x is the number of 1:2 dilutions performed (example for 3 dilutions, F = 8).

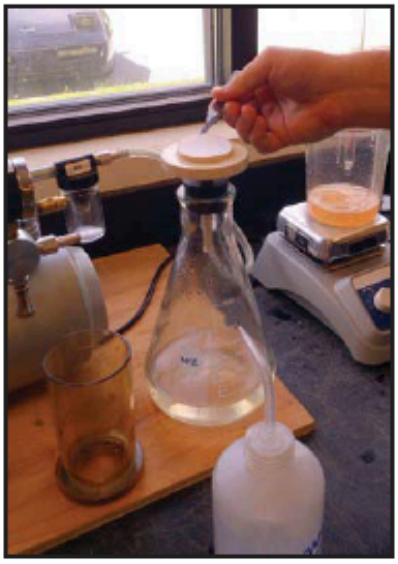

TSS Analysis

Step 13: Use tweezers to place the corresponding filter membrane on the filtering apparatus.

Step 14: Pipette 25 mL of diluted solution and place in apparatus.

Step 15: Filter sample through membrane using the vacuum pump. Rinse the filtrate on the filter with three 10 mL portions of deionized water.

Step 16: Slowly release the vacuum on the filtering apparatus. Gently remove the filter disc using the tweezers.

Step 17: Place the filter disc on its corresponding crinkle dish.

Step 18: Place membranes in the oven at 103˚C for one hour. Remove crinkle dishes and membranes from the drying oven and place in a desiccator and allow to cool to room temperature.

Step 19: Weigh the crinkle dish and filter using an analytical balance. Record weight to the nearest 0.0001 g.

8.2 APPENDIX B – HYDROMULCH DATASHEETS

Profile
Solutions for your Environment

EcoSolutions® EcoFibre® Plus Tackifier

Hydraulic Mulch — Wood with Tack

GREEN DESIGN ENGINEERING™
EARTH-FRIENDLY SOLUTIONS FOR SUSTAINABLE RESULTS™

Description

EcoSolutions® EcoFibre® Plus Tackifier is a fully biodegradable, Hydraulic Mulch (HM) composed of 100% recycled Thermally Refined™ virgin wood fibers and wetting agents (including high-viscosity colloidal polysaccharides). The HM is phytosanitized, free from plastic netting, and upon application forms an intimate bond with the soil surface to create a porous, absorbent and flexible erosion resistant blanket that allows for rapid germination and accelerated plant growth.

Recommended Applications

- Erosion control and revegetation for moderate slopes (≤2H:1V)
- Rough graded slopes
- Enhancement of vegetation establishment

Technical Data

Physical Properties*	Test Method	Units	Tested Value
Mass/Unit Area	ASTM D6566	g/m^2 (oz/yd^2)	≥ 336 (9.9)
Water Holding Capacity	ASTM D7367	%	≥ 1,200
Material Color	Observed	n/a	Green
Performance Properties*	**Test Method**	**Units**	**Tested Value**
Cover Factor[1]	Large Scale[2]	n/a	≤ 0.25
Percent Effectiveness[3]	Large Scale[2]	%	≥ 75
Functional Longevity[4]	ASTM D5338	months	≤ 3
Environmental Properties*	**Test Method**	**Units**	**Tested Value**
Ecotoxicity	EPA 2021.0	%	48-hr LC_{50} > 100%
Biodegradability	ASTM D5338	n/a	Yes
Product Composition			**Typical Value**
Thermally Processed Wood Fibers[5]			97%
Wetting Agent–Including high-viscosity colloidal polysaccharides			3%

* When uniformly applied at a rate of 3000 pounds per acre (3400 kilograms/hectare) under laboratory conditions. 1. Cover Factor is calculated as soil loss ratio of treated surface versus an untreated control surface. 2. Large scale testing conducted at Utah Water Research Laboratory. For specific testing information please contact a Profile technical service representative at 800-508-8681 or +1-847-215-3464. 3. % Effectiveness = One minus Cover Factor multiplied by 100%. 4. Functional Longevity is the estimated time period, based upon ASTM D5338 testing and field observations, that a material can be anticipated to provide erosion control and agronomic benefits as influenced by composition, as well as site-specific conditions, including but not limited to – temperature, moisture, light conditions, soils, biological activity, vegetative establishment and other environmental factors. 5. Heated within a pressurized vessel to a temperature greater than 360 degrees Fahrenheit (193 degrees Celsius) for 5 minutes at a pressure greater than 50 psi (345 kPa) in order to be Thermally Refined™/Processed and to achieve phyto-sanitization.

Packaging Data

Properties	Test Method	Units	Nominal Value
Bag Weight	Scale	kg (lb)	22.7 (50)
Bags per Pallet	Observed	#	40

UV and weather-resistant plastic bags. Pallets are weather-proof stretch wrapped with UV resistant pallet cover.

Profile Products
750 Lake Cook Road, Ste. 440
Buffalo Grove, IL 60089
800-508-8681 or +1-847-215-3464
www.profileproducts.com

Soil Cover® Wood with Tack

Hydraulic Mulch — Wood with Tack

Profile — Solutions for your Environment™

GREEN DESIGN ENGINEERING™ — EARTH-FRIENDLY SOLUTIONS FOR SUSTAINABLE RESULTS™

Description

SoilCover® Wood with Tack is a fully biodegradable, Hydraulic Mulch (HM) composed of 100% recycled Thermally Refined™ virgin wood fibers and wetting agents (including high-viscosity colloidal polysaccharides). The HM is phytosanitized, free from plastic netting, and upon application forms an intimate bond with the soil surface to create a porous, absorbent and flexible erosion resistant blanket that allows for rapid germination and accelerated plant growth.

Recommended Applications

- Erosion control and revegetation for moderate slopes (≤2H:1V)
- Rough graded slopes
- Enhancement of vegetation establishment

Technical Data

Physical Properties*	Test Method	Units	Tested Value
Mass/Unit Area	ASTM D6566	g/m^2 (oz/yd^2)	≥ 336 (9.9)
Water Holding Capacity	ASTM D7367	%	≥ 1,200
Material Color	Observed	n/a	Green
Performance Properties*	**Test Method**	**Units**	**Tested Value**
Cover Factor[1]	Large Scale[2]	n/a	≤ 0.25
Percent Effectiveness[3]	Large Scale[2]	%	≥ 75
Functional Longevity[4]	ASTM D5338	months	≤ 3
Environmental Properties*	**Test Method**	**Units**	**Tested Value**
Ecotoxicity	EPA 2021.0	%	48-hr LC_{50} > 100%
Biodegradability	ASTM D5338	n/a	Yes
Product Composition			**Typical Value**
Thermally Processed Wood Fibers[5]			97%
Wetting Agent–Including high-viscosity colloidal polysaccharides			3%

* When uniformly applied at a rate of 3000 pounds per acre (3400 kilograms/hectare) under laboratory conditions. 1. Cover Factor is calculated as soil loss ratio of treated surface versus an untreated control surface. 2. Large scale testing conducted at Utah Water Research Laboratory. For specific testing information please contact a Profile technical service representative at 800-508-8681 or +1-847-215-3464. 3. % Effectiveness = One minus Cover Factor multiplied by 100%. 4. Functional Longevity is the estimated time period, based upon ASTM D5338 testing and field observations, that a material can be anticipated to provide erosion control and agronomic benefits as influenced by composition, as well as site-specific conditions, including; but not limited to – temperature, moisture, light conditions, soils, biological activity, vegetative establishment and other environmental factors. 5. Heated within a pressurized vessel to a temperature greater than 360 degrees Fahrenheit (193 degrees Celsius) for 5 minutes at a pressure greater than 50 psi (345 kPa) in order to be Thermally Refined™/Processed and to achieve phyto-sanitization.

Packaging Data

Properties	Test Method	Units	Nominal Value
Bag Weight	Scale	kg (lb)	22.7 (50)
Bags per Pallet	Observed	#	40

UV and weather-resistant plastic bags. Pallets are weather-proof stretch wrapped with UV resistant pallet cover.

Profile Products
750 Lake Cook Road, Ste. 440
Buffalo Grove, IL 60089
800-508-8681 or +1-847-215-3464
www.profileproducts.com

Terra-Wood™ with Tacking Agent 3®

Hydraulic Mulch — Wood with Tack

Solutions for your Environment™

GREEN DESIGN ENGINEERING™
EARTH-FRIENDLY SOLUTIONS FOR SUSTAINABLE RESULTS™

Description

Terra-Wood™ with Tacking Agent 3® is a fully biodegradable, Hydraulic Mulch (HM) composed of 100% recycled Thermally Refined™ virgin wood fibers and wetting agents (including high-viscosity colloidal polysaccharides). The HM is phytosanitized, free from plastic netting, and upon application forms an intimate bond with the soil surface to create a porous, absorbent and flexible erosion resistant blanket that allows for rapid germination and accelerated plant growth.

Recommended Applications

- Erosion control and revegetation for moderate slopes (≤2H:1V)
- Rough graded slopes
- Enhancement of vegetation establishment

Technical Data

Physical Properties*	Test Method	Units	Tested Value
Mass/Unit Area	ASTM D6566	g/m^2 (oz/yd^2)	≥ 336 (9.9)
Water Holding Capacity	ASTM D7367	%	≥ 1,200
Material Color	Observed	n/a	Green
Performance Properties*	**Test Method**	**Units**	**Tested Value**
Cover Factor[1]	Large Scale[2]	n/a	≤ 0.25
Percent Effectiveness[3]	Large Scale[2]	%	≥ 75
Functional Longevity[4]	ASTM D5338	months	≤ 3
Environmental Properties*	**Test Method**	**Units**	**Tested Value**
Ecotoxicity	EPA 2021.0	%	48-hr LC_{50} > 100%
Biodegradability	ASTM D5338	n/a	Yes
Product Composition			**Typical Value**
Thermally Processed Wood Fibers[5]			97%
Wetting Agent–Including high-viscosity colloidal polysaccharides			3%

* When uniformly applied at a rate of 3000 pounds per acre (3400 kilograms/hectare) under laboratory conditions. 1. Cover Factor is calculated as soil loss ratio of treated surface versus an untreated control surface. 2. Large scale testing conducted at Utah Water Research Laboratory. For specific testing information please contact a Profile technical service representative at 800-508-8681 or +1-847-215-3464. 3. % Effectiveness = One minus Cover Factor multiplied by 100%. 4. Functional Longevity is the estimated time period, based upon ASTM D5338 testing and field observations, that a material can be anticipated to provide erosion control and agronomic benefits as influenced by composition, as well as site-specific conditions, including, but not limited to – temperature, moisture, light conditions, soils, biological activity, vegetative establishment and other environmental factors. 5. Heated within a pressurized vessel to a temperature greater than 360 degrees Fahrenheit (183 degrees Celsius) for 5 minutes at a pressure greater than 50 psi (345 kPa) in order to be Thermally Refined™/Processed and to achieve phyto-sanitization.

Packaging Data

Properties	Test Method	Units	Nominal Value
Bag Weight	Scale	kg (lb)	22.7 (50)
Bags per Pallet	Observed	#	40

UV and weather-resistant plastic bags. Pallets are weather-proof stretch wrapped with UV resistant pallet cover.

Profile Products
750 Lake Cook Road, Ste. 440
Buffalo Grove, IL 60089
800-508-8681 or +1-847-215-3464
www.profileproducts.com